Exploration of New Methods Involved for the Synthesis of PET Tracers

Guillaume P. L. Marie

A Thesis Submitted for The Degree of Doctor of Philosophy

At

Cardiff University

2014

Declaration

This work has not previously been accepted in substance for any degree and is not being concurrently for candidature for any degree.

Signed ..... (Guillaume P L Marie)
Date.....

Statement 1

This thesis is the result of my own investigations, except where otherwise stated. Other sources are acknowledged by footnotes giving explicit references. A bibliography is appended.

Signed ..... (Guillaume P L Marie)
Date.....

Statement 2

I hereby give consent for my thesis, if accepted, to be available for photocopying and for interlibrary loan, and for the title and summary to be made available to outside organisations.

Signed ..... (Guillaume P L Marie)
Date.....

Abstract

This work describes the development and the optimisation of microfluidic radiolabelling by using an Eckert & Ziegler device remotely controlled by a computer to perform the multistep synthesis of [^{18}F]-fluoro-2-deoxy-D-glucose ([^{18}F]-FDG). This device was then modified to control the fluidic transfers *via* flow of nitrogen and vacuum with the aid of a new one-way cassette system by using different concentrations of water for the Kryptofix solution. A new route was also explored to perform florbetaben ([^{18}F]-BAY94-9172), a potent Alzheimer's disease PET tracer.

Chapter 1 is an overview of positron emission tomography techniques to synthesise tracers.

Chapter 2 is a brief introduction of the PETIC centre (Wales), where the fluoride-18 was delivered to produce [^{18}F]-FDG.

Chapter 3 describes the reaction of the $[K^{+}\subset 2.2.2]^{18}F^{-}$ complex on mannose triflate and the variety of products formed. The Eckert & Ziegler platform was furnished with a cassette module and a microfluidic tubing to perform the radiolabelling fluorination of mannose triflate to the tetraacetate [^{18}F]-deoxy-D-glucose and [^{18}F]-FDG.

Chapter 4 is focused on the modifications on the Eckert & Ziegler modules by using 1-way cassettes to limit the use of mechanical valves. [^{18}F]-FDG was synthesised *via* a semi-automated procedure by limiting the number of modules present in the hot cell.

Chapter 5 is an investigation for the preparation of several triethylene glycol derivatives following the syntheses of Kryptofix [2.2.2]. The use of triethylene glycol chain will be essential for the synthesis of the Florbetaben precursor.

The Chapter 6 is the exploration of a new synthetic route leading to the precursor of florbetaben.

Acknowledgements

I would like to thank my supervisor Professor Dr Thomas Wirth for his support and wisdom throughout my studies at Cardiff University.

I would like to thank the company Eckert & Ziegler for their financial support and Dr Giovanni Imperato and Dr Dominic Franck for their advices.

Many thanks to Mr Adam Dabkowski, Dr Peter Llewelyn, Dr Katrin Probst for their help and guidelines for using radioactivity.

I would also like to thank Dr Mart, Kevin, Kate, Julien, Piotr, Matthew, Richard, Alastair, Elisabetta, Dr Brown, Sarah, Dr Faraldos, Oscar, Tom, Stacy, Steven, Virginie, Cyril, Dr. Nowicka for making my days enjoyable.

I must also acknowledge all the analytical and technical staff especially Dr Rob Jenkins, Robin, Gaz, Steve for their help.

Abbreviations and acronyms

∅	diameter
$[K^+ \subset 2.2.2]^{18}F^-$	Kryptofix [2.2.2]/potassium cation complex with [^{18}F]-fluoride ion
Ac	acetyl
AD	Alzheimer's disease
APCI	atmospheric pressure chemical ionisation
aq	aqueous
Ar	aromatic
BMI(OTf)	1-butyl-3-methylimidazolium trifluoromethanesulfonate
BMS	borane dimethyl sulfide complex
b.p.	boiling point
Bn	benzyl
Boc	*tert*-butoxycarbonyl
br	broad
Bq	Becquerel
cat.	catalytic
Ci	curie
d	day(s)
d	doublet
dd	double doublet
DIBAL	diisobutylaluminium hydride
DMA	*N*,*N*-dimethylacetamide
DMAP	4-dimethylaminopyridine
DMF	dimethylformamide
DMSO	dimethylsulfoxide
dps	decay per second
e.g.	*exempli gratia*
E&Z	Eckert and Ziegler (German company, Berlin)
EFS	2-(2-nitro-1[H]-imidazol-1-yl)-*N*-(2,2,3,3,3-pentafluoropropyl)-acetamide
equiv	equivalent(s)
Et	ethyl
ETFE	ethylene tetrafluoroethylene
Eu. Ph.	European pharmacopeia

FDG	fluorodeoxyglucose
g	gram
GBq	gigabecquerel
Δ	heat
h	hour(s)
HPLC	high performance liquid chromatography
Hz	hertz
^{i}Pr	isopropyl
IR	infra-red
J	coupling constant
K[2.2.2]	kryptofix® [2.2.2] or (4,7,13,16,21,24-hexaoxa-1,10-diazabicyclo[8.8.8]-hexacosane)
keV	kilo electron volt
L	ligand
lit.	literature
m	multiplet
M	molar
MBq	mega Becquerel
mCi	millicurie
Me	methyl
MHz	megahertz
MRI	magnetic resonance imaging
MPa	megapascal
µL	microliter(s)
µL/s	microliter(s) per second
µmol	micromole(s)
mCi	millicurie
mL	milliliter(s)
mmol	millimole(s)
m.p.	melting point
Ms	methane sulfonyl
nca	no-carrier-added
N	nitrogen
NMR	nuclear magnetic resonance
OAc	acetate
OTf	triflate

p	page
p	*para*
P_4tBu	N-[[tert-butyl- imino-bis[tris(dimethylamino) phosphoranylideneamino]phosphoranyl]- imino-bis(dimethylamino)phosphoranyl]-N-methylmethanamine
PE	petroleum ether
PET	positron emission tomography
Ph	phenyl
Pr	propyl
PMT	photomultiplier tubes
PP	polypropylene
PTFE	polytetrafluoroethylene
QC	quality control
QMA	quaternary methyl ammonium
RCY	radiochemical yield
r.t.	room temperature
s	singlet
SA	specific radioactivity
S_N2	2nd order nucleophilic
S_NAr	nucleophilic aromatic substitution
SPE	solid phase extraction
SPECT	single-positron emission tomography
t	triplet
$t_{1/2}$	half-life time
TBAF	tetra-*n*-butylammonium fluoride
TBS	*tert*-butyldimethylsilyl
TEA	triethylamine
Tf	triflyl
THF	tetrahydrofuran
TLC	thin layer chromatography
TMS	trimethylsilyl
TPX®	polymethylpentene (PMP) characteristics
Ts	*p*-toluenesulfonyl
UV	ultra-violet
v/v	volume for volume
w/w	weight for weight

Chapter 1: Introduction

1 General overview

Marginalised in the past, clinical diagnosis received over recent decades a huge interest. It has been growing with the development of combined techniques to improve disease detection, early treatment response and therapy monitoring. The fusion between usual anatomical techniques like X-ray (CT) or magnetic resonance imaging (MRI)[1], associated with high sensitive molecular imaging techniques such as single-photon emission tomography (SPECT) or positron emission tomography (PET) offered an essential method for biomedical research and clinical diagnosis. The fused PET-CT method is specially used for cancer patient management, in particularly for oncology, cardiology and neuropsychiatry.[2-4]

1.1 **Tracer principle**

The Chemistry Nobel prize winner in 1943, George Charles de Hevesy[5, 6] performed studies on the diffusion of radioactive elements in metabolic processes. Using bean plants he studied the absorption of radioactive molecules at low-concentrations. Radioactive sites were located with accuracy and precision using a Geiger counter. This was offering a new non-invasive diagnostic method which was able to analyse the emission of γ-rays with high sensitivity.[3, 7] This technique avoided the use of excessive doses of radioactive agents and so the potential toxicity risk for the metabolism.

The use of radioactive molecules as markers or tracers of biological non-radioactive processes of a metabolism is the foundation of SPEC and PET imaging.

The design of new tracers, in this case radiotracers or radiopharmaceuticals, and technologic improvements have developed better sensitivity and better specificity for PET images.[3, 8] Two types of imaging tracers are commonly synthetised: inorganic chemicals with radioactive metals and coordinated ligand(s), or organic compounds, which are small molecules almost similar to the biological active molecule with a radioactive atom. Today, a large variety of labeled molecules[9, 10] are routinely produced to detect biological modification within the metabolism, to predict or follow the progression of diseases and for the discovery of new drugs.[11-13]

1.2 **Positron Emission Tomography**

To obtain a high-resolution picture of the distribution of a tracer molecule within a body, the PET method is using the physical properties of positrons combined with an efficient and selective

detection of antiparallel γ-rays.[3, 13, 14] Radioactive proton-rich nuclei decay to more stable atoms by converting a proton to a neutron.[2, 8, 15] The new nature of this element induced the release of three entities: a positron (β^+), the emission of a neutrino (ν) and loss of one electron (e^- or β^-). The emitted positron annihilates immediately after collision with an electron present in its environment, producing two diametrically opposed γ-rays of 511 keV each (see Figure 1).

$$ {}^{A}_{Z}X \rightarrow {}_{Z-1}{}^{A}Y + {}^{0}_{1}\beta^{+} + \nu + e^{-} $$

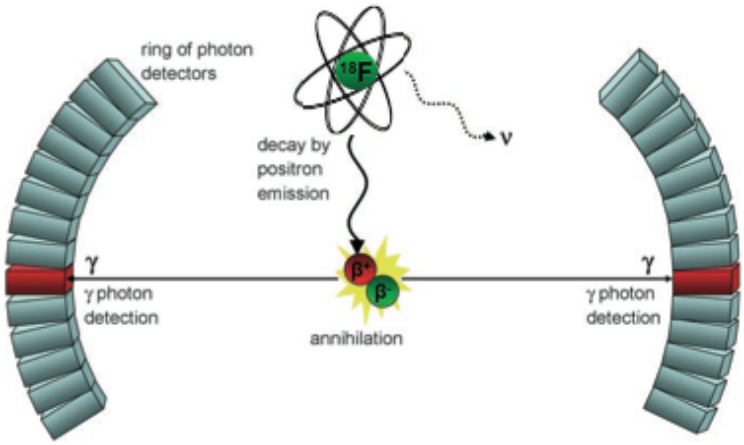

Figure 1: Illustration of annihilation process with the formation of two anti-parallel quanta (γ) identified simultaneously by two γ-cameras (present in red) parts of the ring scanner.[9]

The γ-camera also known as Anger scintillation camera, named from its inventor Hal Anger[16], can be described as a multitude of very small detectors. Usually forming a circle around the body or the object, PET cameras are designed to detect the paired photons generated from the same annihilation event. Starting from the closest of the annihilation, the main parts of these detectors are the collimator, a large area of scintillation crystal and an array of photomultiplier tubes (PMT).[7, 8, 17]

The received gamma rays, which are not visible to the eye, are converted into flashes of light by the scintillation crystal, usually made of (sodium iodide with thallium doping) (NaI(Tl)) or bismuth germinate (BGO). Face to the crystal, the collimator also known as the parallel-hole collimator consists in a lead plate full of small holes parallel to each other. Only photons travelling along the hole axis will pass into the scintillation crystal, the others (oblique angles) will be absorbed by the collimator. Acting as an efficient filter only 0.1% of the gamma rays will reach the scintillation crystals, which means 99.9% of emitted photons will not be treated. At the rear of the crystal, the light is transformed into electronic pulses by the PMTs and amplified (factor of 10^7) to offer a reliable current able to be treated by a computer. Signals are then analysed and (x;y) coordinates are generated

to give a 2 D image. The energy received by the crystal will determine the coordinate z and will then provide 3D PET images.

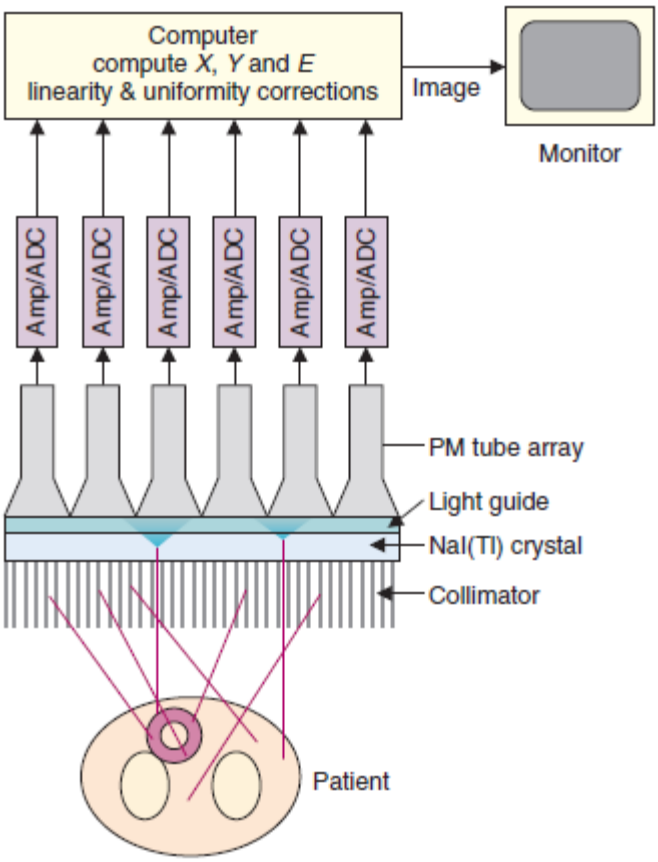

Figure 2: Schematic components and basic principles of a PET camera.

Generally combined with a CT scanner, fused PET-CT images offer the advantages of the two techniques (see Figure 3). The CT pictures are appreciated for their morphological details and PET images for the detection of low-level radiotracers inside the subject.

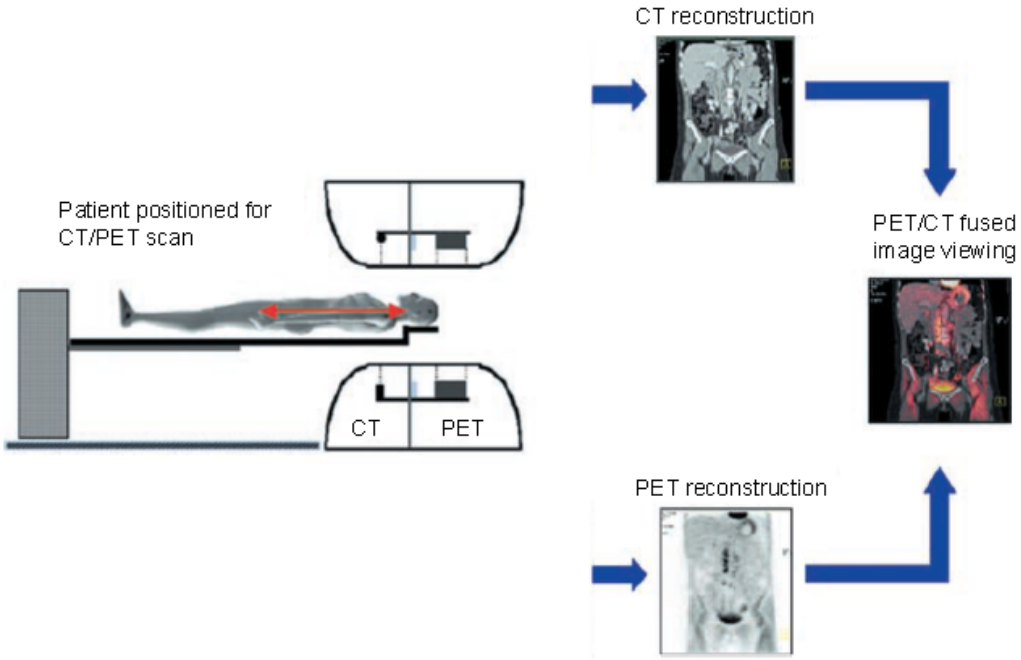

Figure 3: A standard PET-CT acquisition for a patient.[7]

1.3 PET radionuclides

Usually chosen for suitable physical properties, PET nuclei possess a long enough half-life ($t_{½}$) to encompass the synthesis of the tracer and the biologic process studied (see Table 1). The desired $t_{½}$ ranged from 20 minutes to 7 days. Another important factor is its decay mode. The radioisotope must decay completely or nearly by emission of positrons (β^{+}). This is to avoid other nuclear reactions able to generate equivalent energy γ-rays and contaminate the calculation to determinate the source of the annihilation event.

Table 1: Characteristics and production reaction of the most common PET radioisotope.[3, 9, 18]

Nuclide	Half-life [min]	Maximum energy [MeV]	Decay mode [%]	Nuclear reaction[a]	Decay product
$^{11}_{6}C$	20	0.97	β^+ [100]	$^{14}N(p,\alpha)^{11}C$	^{11}B
$^{13}_{7}N$	10	1.20	β^+ [100]	$^{16}O(p,\alpha)^{13}N$	^{13}C
$^{15}_{8}O$	2	1.74	β^+ [100]	$^{15}N(d,n)^{15}O$	^{15}N
$^{18}_{9}F$	110	0.64	β^+ [97]	$^{20}Ne(d,\alpha)^{18}F$ $^{18}O(p,n)^{18}F$	^{18}O
$^{68}_{31}Ga$	68	1.90	β^+ [89] EC[c] [11]	$^{68}Ge - {}^{68}Ga$ generator[b]	^{68}Zn

a) nuclear reactions will be explain in Section 1.4; b) production of ^{68}Ga: $^{69}Ga(p,2n)^{68}Ge$, generator: $^{68}Ge\left(t_{1/2} = 271\ d\right) \rightarrow {}^{68}Ga$; c) electron capture

The ^{11}C and ^{18}F nuclides are by far the most used isotopes for PET labeling. Despite a short half-life (20 min), carbon-11 offers an incredible advantage, the possibility of synthesising radiotracers identical to the non-radioactive analog, such as replacement of a carbon-12 by a carbon-11. However fluorine-18 is the positron-emitting isotope of choice for several reasons. Its long half-life (see Table 1) allows multistep radiosynthesis and the transport of doses to other clinical sites for all day patients. By emitting the lowest energy of all nuclei previously mentioned, it offers high spatial resolution for PET imaging. Hence the most routinely produced PET tracer used over the world is [^{18}F]-fluoro-2-deoxy-D-glucose also named [^{18}F]-FDG **1**.

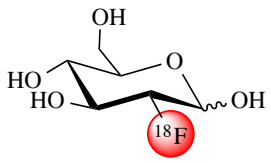

1

1.4 **Production of nuclides**

In nuclear medicine the most frequent way to produce nuclides is the cyclotron, an accelerator of particles (see Figure 4). The production of radionuclides demands a high frequency electric field applied to an ion beam, generated *via* the source present at the middle of the machine. The electrical field increases the energy of the particles in raising their celerity through two electrodes named "dees". It forms excited particles with reasonable high energy (around 20 MeV) able to perform the

desired reaction in practical yield. The magnetic field, perpendicular to the electrical one, leads particles to travel in spiral orbits. This acceleration chamber is continuously under high vacuum (around 10^{-5} and 10^{-7} mm of Hg) to accelerate effectively the ions. When the level of energy is reached, the particles exit the chamber and are deflected into the target. The bombardment of the particles to the atoms of the target provides the energised desired nuclei.[19]

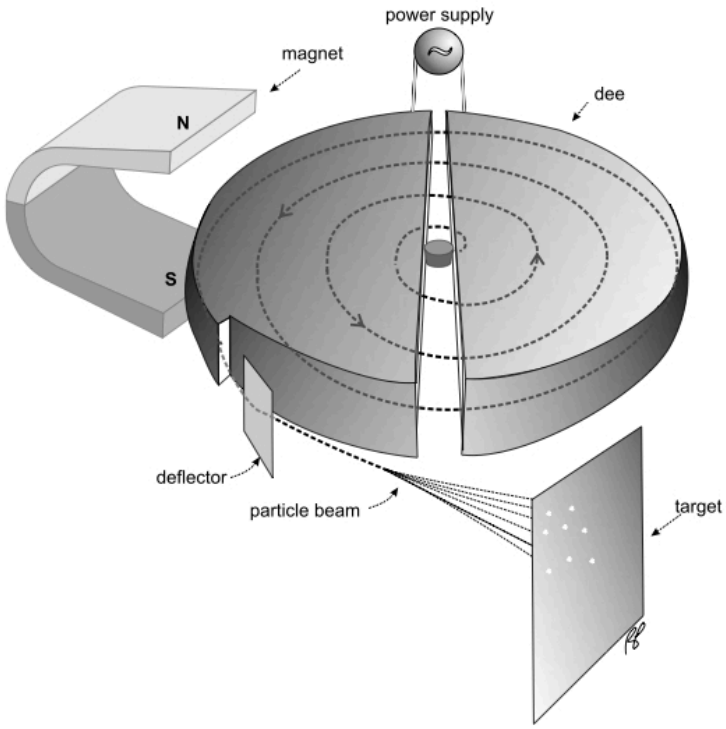

Figure 4: Illustration of a cyclotron accelerating particles with electro-magnetic fields to offer energised atoms, used for PET images.[20]

This allows the reactions previously mentioned (see Table 1) to be explained further. For example if an [^{20}Ne] atom is irradiated with a deuteron beam (one proton and one neutron) to produce a nucleus of [^{18}F] with the emission of an alpha particle ($^{4}_{2}$He), the reaction is written $^{20}\mathrm{Ne}(\mathrm{d},\alpha)^{18}\mathrm{F}$. This method forms [^{18}F]-F_2 gas for electrophilic fluorination. Similarly, if [^{18}O] nucleus is bombarded with a proton to form [^{18}F] atom and neutron, the nuclear reaction can be abbreviated $^{18}\mathrm{O}(\mathrm{p},\mathrm{n})^{18}\mathrm{F}$. With this reaction, electrophilic fluorine ([^{18}F]-F_2) and nucleophilic fluoride ([^{18}F]-F^-) can be respectively produced using a gas or liquid target.

1.5 Notion of specific activity

The specific activity (SA) is defined as the amount of radioactivity (MBq, mCi) per unit mass of a radionuclide or a labeled tracer (g). Low SA occurred with the presence of "cold" isotopes of the radioactive atoms (carrier-added). The formation of non-radioactive tracers competes with the radioactive ones and provides lower RCY. This deteriorates the PET signal-noise ratio by saturating the binding sites of the reactive tracer and causing by sizeable mass, pharmacological and toxic risks for the patient.[21] The SA reaches its maximum value when the labeled atoms in the sample are free of its isotopes (carrier-free). The SA can be calculated by using the physical properties of the radionuclide, such as the number of atoms of the radioactive element (N) divided by the corresponding half-life ($t_{1/2}$), and by Avogadro's number (N_A) to convert grams to moles (Equation 1).[17, 22]

$$\mathbf{SA\ (MBq/mol)} = \frac{\mathbf{\ln 2}}{\mathbf{t_{1/2}}} \cdot \frac{\mathbf{N}}{\mathbf{N_A}} \qquad \text{Equation 1}$$

For a same number of atoms (N), SA is the highest for the element having the shortest half-life. Therefore [^{15}O] has the highest theoretical specific activity with a half-life of 2 min (see Table 1).

1.6 Radiolabelling with [^{18}F]

In spite of a definite interest for [^{18}F]-labeling, fluorine atoms are rarely present in molecules with biological activity. Therefore the effect of the fluoro-substituent on the organism has to be studied to offer at least similar activity than the non-fluorous parent molecule.[23] Atoms generally substituted by fluorine atoms are hydrogen or hydroxyl moieties and their protected derivatives. The replacement by fluorine leads to a modification of the electron density of the molecule due to the strong electronegativity of the fluorine atom (4.0, 2.1 for hydrogen and 3.5 for oxygen in Pauling scale). However steric parameters of the biotracer are almost unchanged, indeed van der Waal's radii of fluorine, hydrogen and oxygen are 1.35, 1.20 and 1.52 Å respectively. Recent studies have shown some benefits by the incorporation of fluorine atom in biologically active drugs[24, 25] by improving their safety and efficiency for the patient.[23] Indeed fluorine substitution can influence the distribution, the selectivity to the receptors and extend drug metabolism.

1.6.1 Electrophilic [^{18}F]

Electrophilic [^{18}F] can generally be produced by two different nuclear reactions $^{20}Ne(d,\alpha)^{18}F$ and $^{18}O(p,n)^{18}F$ with a preference for the latter.[26] Electrophilic fluorinations proceed with the use of a carrier, for example $^{19}F_2$ gas, which, when mixed with ^{18}F (see Scheme 1) forms the radioactive [^{18}F]-F_2 used for the reaction.

$$^{18}F \quad + \quad ^{19}F_2 \longrightarrow \quad ^{18}F-^{19}F \quad + \quad ^{19}F$$

Scheme 1: Preparation of the diatomic molecule $^{18}F-^{19}F$.

Due to the presence of one radiolabelled atom the theoretical radiochemical yield can reach a maximum of 50%. The powerful oxidizing activity of the difluorine gives an unspecific labeling leading to a mixture of products. This makes this method difficult to use for a routinely large-scale production. Mild and more selective reagents were developed such as [^{18}F]-acetyl hypofluorite[27] or [^{18}F]-xenon difluoride[28] and, more recently, *N*-fluorobenzenesulfonimide[29, 30] and selectfluor®[31, 32] leading to a large range of electrophilic reactions with fluorine-18. One of the first reported synthetic route of [^{18}F]-FDG **1** was proposed by Ido and co-workers[33] in 1978. The synthesis was carried out with the electrophilic specie [^{18}F]-F_2; 6 years later the reaction was improved by the use of [^{18}F]-acetyl hypofluorite (see Scheme 2).[34]

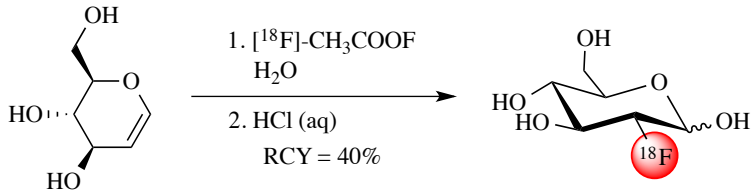

2 **1**

Scheme 2: Preparation of [^{18}F]-FDG **1** *via* electrophilic ^{18}F fluorination using [^{18}F]-acetyl hypofluorite.

Other clinically used PET tracers still rely on electrophilic [^{18}F]-fluorination for example by addition to allylic moiety. [^{18}F]-EFS or [^{18}F]-2-(2-nitro-1[H]-imidazol-1-yl)-*N*-(2,2,3,3,3-pentafluoropropyl)-acetamide **4**, used to detect tissue hypoxia, is obtained in 17% radiochemical yield[35] as shown in Scheme 3.

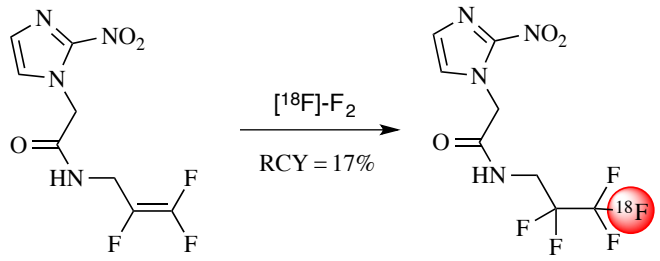

3 **4**

Scheme 3: Electrophilic [^{18}F]-fluoro labeling of **3** to [^{18}F]-EFS **4**.

Another known routinely produced PET tracer, 6-[^{18}F]-fluoro-L-DOPA **6**, can probe cerebral dopamine metabolism for the diagnosis of Parkinson's disease. The fluorination by electrophilic carrier ([^{18}F]-F_2 or [^{18}F]-AcOF) is achieved by initial incorporation of protecting groups and leaving group, here the trimethylstannyl precursor **5**. This approach limits the presence of labile hydrogen and so, increases the selectivity of the radiolabelling. The tracer **6** was provided in a reasonable radiochemical yield (a maximum of 25%) after HPLC purification (see scheme 4).[36]

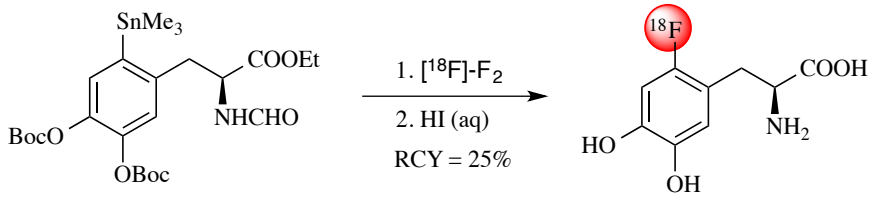

5 **6**

Scheme 4: [^{18}F]-fluoro labeling of [^{18}F]-fluoro-L-DOPA **6** by direct electrophilic substitution.

Labeling a molecule with [^{18}F]-F_2 has a huge drawback. Electrophilic aromatic substitution has a maximum value of SA of about 0.6 to 16 GBq/µmol[37] whereas no-carrier-added nucleophilic pathway has a theoretical SA of 6.3 x 10^4 GBq/µmol.[38]

1.6.2 Nucleophilic [$^{18}F^-$]

Carbon-fluorine bond formations can be effectively performed by direct nucleophilic substitution of an aliphatic carbon or unsaturated system like aryl groups following a S_NAr-mechanism. Owing to the highest electronegativity, the [^{18}F]-fluoride ion is very sensitive to hydrogen bonding and can be easily solvated by protic solvent such as water or alcohols due to the basic properties of the anion. To increase the nucleophilicity, the fluoride-18 must be under anhydrous

conditions and exposed *via* the coordination of the potassium cation by a cryptand (bicyclic aminopolyether), or associated with an ammonium salt (see Section 1.7.2).

As electrophilic pathway, precursors should not own labile hydrogens to avoid side reactions within the incorporation of fluoride-18.

Nucleophilic aliphatic substitution

The [^{18}F]-Florbetaben or [^{18}F]-BAY94-9172 (**8**) is a promising PET imaging tracer delineating the presence of β-amyloid (Aβ) plaques in the brain, which are a significant factor associated with the development of Alzheimer's disease (AD). The labeling was performed at 120 °C to provide after deprotection and semi-preparative HPLC purification the desired tracer **8** in 30% decay-corrected yield for a total synthesis of 90 min. The radiochemical purity was reported to be excellent (>99%).[39-41]

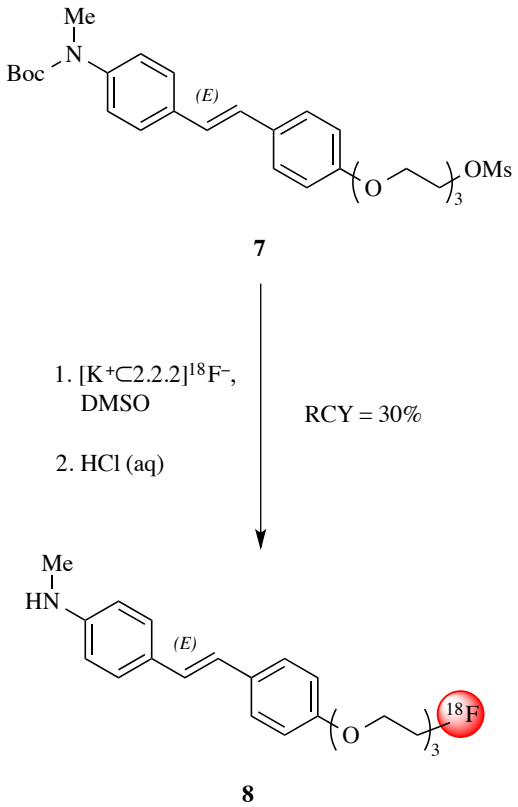

Scheme 5: Radiosynthetic route for [^{18}F]-Florbetaben **8** by S_N2 mechanism.

Nucleophilic aromatic substitution

Following the literature, nucleophilic aromatic substitution with fluorine-19 was developed 63 years ago by Burnett *et al*.[42] More interest emerged with the growth of fluorine-18 labeling. Several reactions were performed with activation of arenes by electron-withdrawing moieties, in *ortho* or *para* position, associated with a leaving group (LG). These reactions include the Balz-Schiemann reaction, the Wallach reaction and reactions with standard leaving group for S_NAr ($–NO_2$, $–Me_3N^+$, halogen).[43]

Achieved under harsh conditions and poor efficiency, functionalised substrates offered low radiochemical yield and new strategies have appeared by using hypervalent iodine compounds and/or using new devices (see section 1.7.2).

1.7 Preparation of fluorine-18 for S_N2 reaction following the example of [^{18}F]-FDG 1

The routine production of clinical PET tracers requires a high degree of reproducibility. The presence of impurities in consumables or in aqueous [^{18}F]-fluoride solution has a detrimental effect on the radiolabeling. However, automation and standardisation have optimised the conditions such as time reaction (between 20 and 30 min) and RCY (≈60%, activity corrected, almost double than manual procedure).[44]

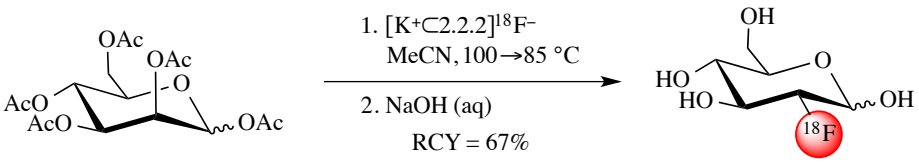

9 **1**

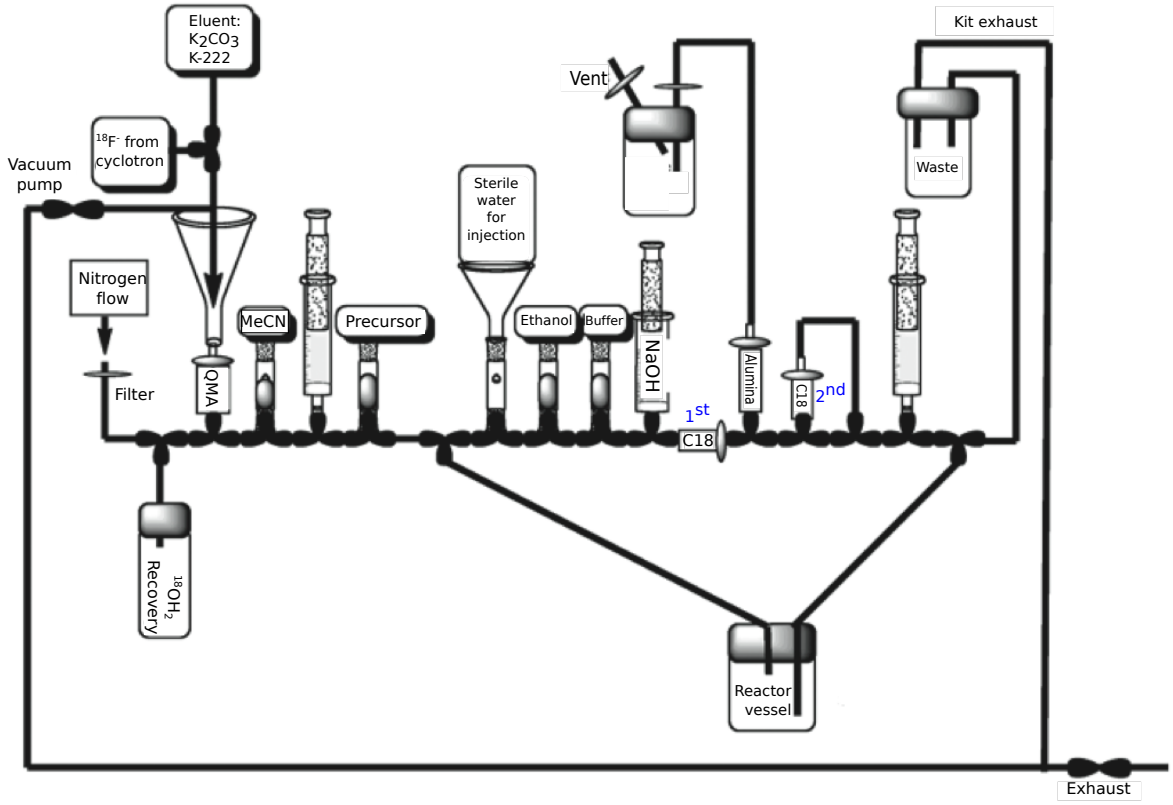

Figure 5: Nucleophilic nca pathway for [^{18}F]-FDG **1** performed by a General Electric (GE) medical system: TracerLab MX_{FDG}, a single-use cassette synthesiser.

TracerLab platform is the most used synthesiser over the world for routine [^{18}F]-FDG production. This example will illustrate the different steps for a direct radiofluorination synthesis, accompanied with progress achieved in the literature.

1.7.1 Step 1: Trapping and elution

After irradiation of [^{18}O]-water by protons in the cyclotron, the aqueous [^{18}F]-fluoride solution is transferred to the synthesiser unit or module present inside the PET laboratory. The fluoride-18 is separated from the [^{18}O]-water by an anion exchange cartridge (preconditioned with $NaHCO_3$, 8.4%, 5 mL)[45] and by using a pressure of helium or nitrogen gas. Trapped by a Sep Pak QMA light cartridge (Waters, USA) with quaternary ammonium chloride at the edge (see Figure 5); [^{18}F]-fluoride is eluted using 0.6 to 1 mL of a solution of acetonitrile/water (50/50 or more recently 4/96, v/v). It contains weak base associated with cryptand (K_2CO_3 or $KHCO_3$ and Kryptofix [2.2.2]), or tetrabutylammonium salt such as Bu_4NHCO_3 or Et_4NHCO_3[46].

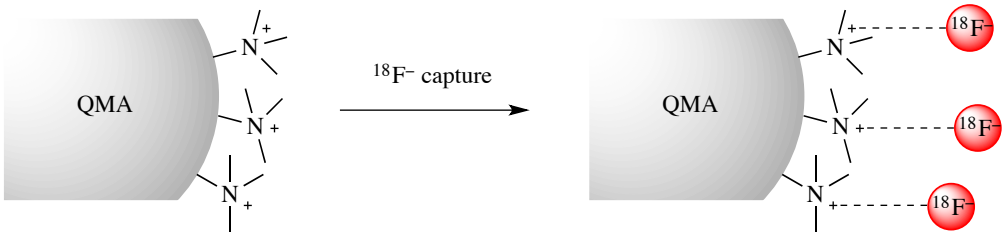

Figure 6: Conventional trapping of [^{18}F]-fluoride by Sep Pak QMA light cartridge[47].

1.7.2 Step 2: Azeotropic drying

The evaporation of the solvents is commonly carried out by a succession of three dry acetonitrile vials, at around 95 °C in the reactor vessel under reduced pressure and nitrogen or helium flow.[10] Within the evaporation process (8.5 minutes), TracerLab procedure involves 240 µL of acetonitrile (3 x 80 µL).

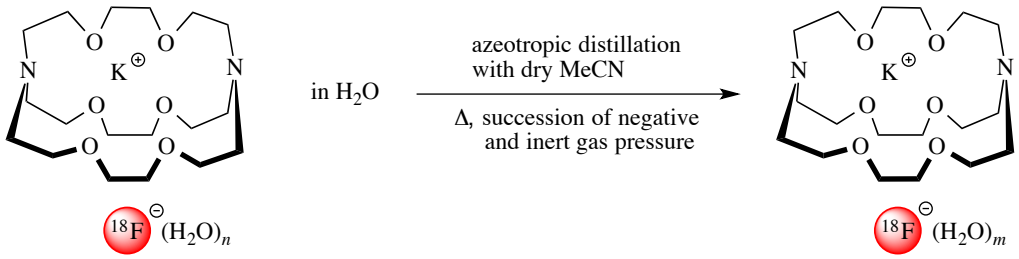

Scheme 6: Distilled Kryptofix [2.2.2]/potassium cation complex with "naked" [^{18}F]-fluoride ion for nucleophilic reaction; $m << n$.[22]

Even if more vigorous conditions may accelerate the drying process, higher temperature or too strong negative and positive pressure will provoke an uncontrolled splattering of solvents and will be accompanied with a loss of activity. This iterative azeotropic distillation looses more than 30% (activity corrected) of the radioactivity present in the vessel. Different alternatives and studies were performed over the last 20 years to limit the loss of radioactivity and to improve the time-consuming process.[48]

The use of low water concentration,[49] (96/4, v/v, MeCN/water) solution to elute the fluoride-18 may dry the $[K^+\subset 2.2.2]^{18}F^-$ complex after one distillation with a loss of activity of less than 4%. Other alternatives were described such as anhydrous $[K^+\subset 2.2.2]OH^-$ or strong organic bases such as phosphazene base (P_4tBu)[50, 51] in dry acetonitrile. Electrochemical separations associated with microfluidic apparatus are able to catch the [^{18}F]-fluoride on an electrode. After washing out the water

with acetonitrile, fluoride-18 is considered dried and directly conditioned for the labeling without azeotropic distillation.[52, 53]

Another strategy using hypervalent iodine and microreactor has been developed leading to a [^{18}F]-labelling of unreactive iodonium salt[54] or [^{18}F]-labelling with a low concentration of water (<0.3% v/v) and without cryptand/base complex. Reactions led to a reasonable RCY (see Scheme 8).

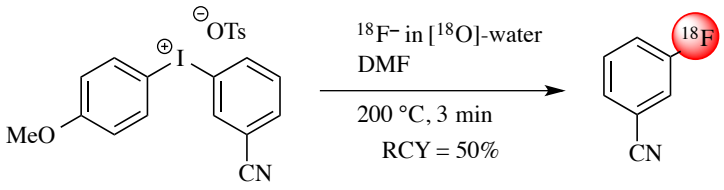

10 **11**

Scheme 7: Radiofluorination of diaryliodonium tosylates salt in DMF/[^{18}O]-water (72/28, v/v).

Lee *et al.*[55] recently reported the influence of the radiochemical yield per amount of precursor for another common PET tracer, the [^{18}F]-fluorothymidine also named [^{18}F]-FLT. For similar radiolabelling conditions half of precursor leads to a significant drop of incorporation of fluorine-18 (for 20 and 10 mg of precursor, the RCY is: 90 and 50%, respectively). The Chromafix® PS-HCO_3 and QMA cartridges, ion exchange columns are usually washed with strong bases such as OH^- or KCO_3^-. These anions might involve side reactions such as elimination and hydroxylation to the precursor and leading to multiple separation steps.[56] The use of inert anions such as $^-$OTf or $^-$OMs, owing to weak nucleophilic properties, doesn't interfere with [^{18}F]-fluoride labeling and carries out [^{18}F]-incorporation independently to the amount of precursor.

1.7.3 Step 3: Radiolabeling and deprotection

The incorporation of fluorine-18 usually takes place in aprotic and polar solvents like acetonitrile, DMSO or DMF at relatively high temperature in a sealed reactor or in a microfluidic system. The labeling by nucleophilic aromatic substitution can be performed at up to 200 °C instead of approximately 85-100 °C used for aliphatic substitution.

Alternative solvents have been described to be efficient for [^{18}F]-fluorination. Protic tertiary alcohols (*tert*-amyl alcohol, ^{t}BuOH) led to [^{18}F]-FDG **1** in up to 77% RCY.[56, 57]

The possibility of [^{18}F]-fluorination in the presence of traces of water was elaborated 13 years ago by using an ionic liquid, 1-butyl-3-methylimidazolium trifluoromethanesulfonate (BMI(OTf)), to form the labeled FDG **1** in 59% RCY.[58]

1.7.4 Step 4: Deprotection/hydrolysis

The cleavage of the four acetyl moieties of 2-[^{18}F]-fluoro-1,3,4,6-tetra-*O*-acetyl-D-glucose ([^{18}F]-TAG) is performed under basic or acid conditions. In contrast to the acidic hydrolysis ($HCl_{(aq)}$, 1 N, 120 °C, 5 minutes), basic deprotection occurs almost instantaneously under mild conditions ($NaOH_{(aq)}$, 2 N, 40 °C). Another basic method is performed by the TracerLab MX_{FDG} (see Figure 5). The deprotection occurs with 800 µL of 2 N NaOH at room temperature through the first tC18 Sep Pak cartridge (Waters). Both tC18 columns were conditioned with 3 mL of ethanol and 22 mL of water within the synthesis. The tC18 resin holds back all nonpolar molecules such as [^{18}F]-TAG or Kryptofix [2.2.2] and polar substances are eluted through the resin with water (10 mL) such as [^{18}F]-FDG **1**.

1.7.5 Step 5: Purification

For the basic deprotection at 40 °C, three cartridges are used before to collect [^{18}F]-FDG **1**. The first cartridge is based on ion-exchange resin (SCX, Grace or IC-H, Alltech), which neutralises the pH of the solution to physiological pH. Then neutral alumina column (Waters) removes the unreacted fluorine-18 and finally tC18 Sep Pak cartridge removes the nonpolar molecules.

For TracerLab process the ion-exchange cartridge is replaced by tC18 Sep Pak column (2nd), to provide the solution at physiological pH. The mixture elutes through the neutral alumina column and a sterile filter (Millex-GS, 0.22 µm) to purify the [^{18}F]-FDG **1** solution.

Even if these solid phase extraction (SPE) methods using cartridges are reliable and easy implementable into the equipment, side products such as glucose or 2-chloro-2-deoxy-D-glucose remain inside the product vial. Only HPLC purification can proceed to a complete removal of impurities. The disadvantages of this technique are time consuming to perform purification step compare to SPE columns and the requirement of specific HPLC conditions for each PET probe.

1.7.6 Step 6: dispensing

The product vial is then diluted and divided in several smaller vials by a dispensing module, which is generally comparable to the size of the production synthesiser. One vial is analysed to check the purity of the reaction solution produced (quality control, QC). When confirmed, the [^{18}F]-FDG solution can be injected to patient.

1.8 **Automation and new methods**

Fully-automated or semi-automated synthesisers are the most used devices in the world for clinical productions of radiolabeled compounds and in academic researches. The RCY between the original methodology and automated version can almost double.[10, 59] It facilitates the innovations of new synthesis techniques already used in conventional chemistry (cold chemistry) to make the radiolabeling syntheses faster and more efficient with the desire to simplify and reduce the price of the synthesisers.

1.8.1 Automated apparatus for routine production of PET radiopharmaceuticals

Automated synthesis carries out basic operations as heating, cooling, injecting gas pressure, negative pressure, filtration, reagents transfer etc. The transfer of reagents is commonly performed by pressure gradients. The use of inert gas pressure and vacuum pump associated with multiple check valves (stopcocks) guide liquids inside modules. It can as well be completed by some motor-driven syringe pumps. Reactions take place in a vial or in channels, for microreactors. Controlled by a computer, the interface software generates in real time the common parameters useful of the radiolabelling such as pressure, level of radioactivity, empty or full vials, temperature etc (see Figure 7). The interface generally offers the possibility to manually interfere in the reaction in case of problems (not for the Synthera Interface).

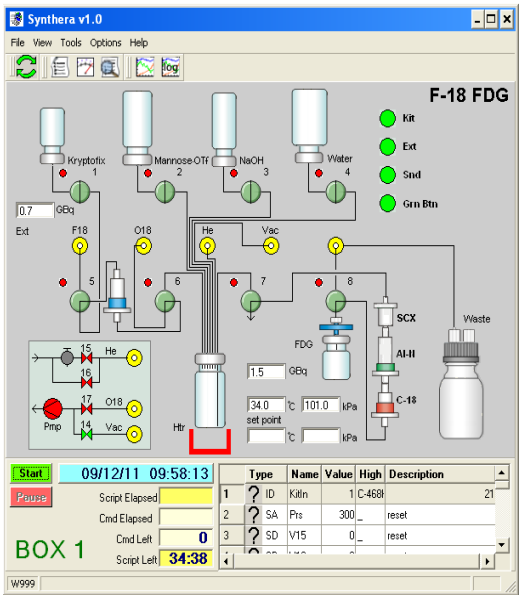

Figure 7: Interface software of Synthera [^{18}F]-FDG synthesiser (IBA, Belgium) used for routine production in the Cardiff PET centre.

Two categories of automated or semi-automated apparatus will be described: the cassette-based synthesisers and the modular system, with however an exception for modularLab system which combine both methods (Eckert & Ziegler, Germany).

The cassette-based systems (see Figure 8) are subject to sterile one-use consumables (cassette, reagents etc.) to comply with the GMP regulations and reproducibility from run to run. However, it is generally limited to two reactions. Recently, new type of cassette-based synthesiser has been developed to achieve the synthesis of different PET tracers with the same apparatus and the possibility to realise 3 chemical reactions in one cassette.[60]

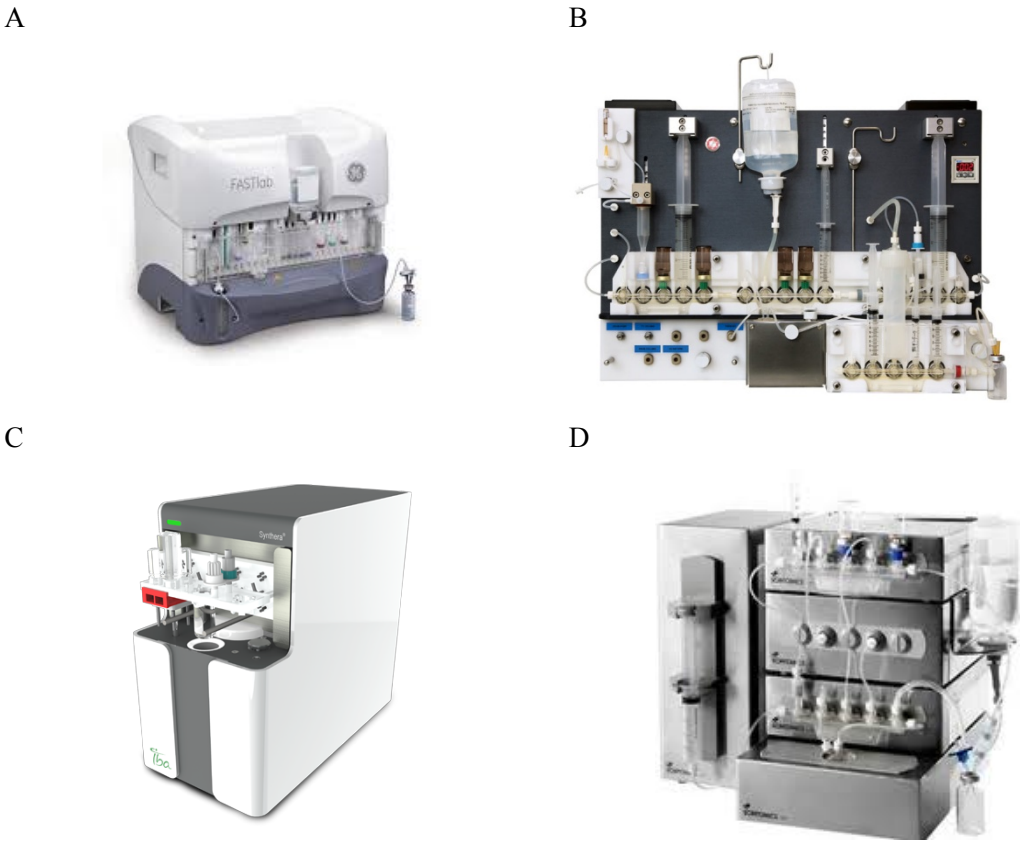

Figure 8: the most widespread cassette-based automated modules: A) Fastlab, GE Health Care; B) NEPTIS synthesiser, Ora; C) Synthera, IBA cyclotrons solutions; D) GRP module, SCINTOMICS.[60]

Modular automated systems generally need more space inside the hot cell but offer flexibility by allowing a large range of chemical operations with radionuclides. The complexity of multi-stage syntheses is to avoid the contamination with other solvents or accumulate impurities from stage to

stage and not to loose chemicals or radioactivity inside the large surface of tubing used in such devices (see Figure 9).

Figure 9: ModularLab standard (Eckert & Ziegler, Germany).

1.8.2 New techniques for [^{18}F]-radiolabelling

The field of microreactor devices and capillary loop system for radiolabelling has grown over the last decades mainly with the apparition of new materials (polymers)[61, 62] and the reduction of quantity of tracer needed per dose for chemical or biochemical assays. The miniaturisation of microfluidic systems is ideal to control small amount of reagents and can lead to portable devices to enable radiosynthesis remote from the production site.[63, 64]

Reducing space between molecules allows a rapid homogeneous mixing (in the order of microseconds) compare to batch mixing (the order of seconds or longer). The temperature distribution is considerably improved in microfluidic systems by high surface to volume ratio. The flow of the solutions can be perfectly controlled by syringe pumps. All these factors can influence yield and selectivity of reactions in a shorter time which is convenient for short life nuclides.[61]

In 2005, Lee and co-workers described a multistep synthesis of [^{18}F]-FDG in a microfluidic device[65] inspiring the development of automated radiolabelling processes on the microscale.[66] The synthesis of other PET tracers[63, 67-70] carried on with an interest for aromatic nucleophilic substitution (see Figure 10).

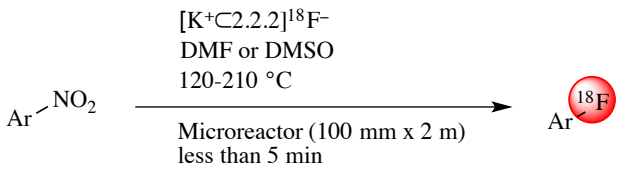

Scheme 8: Radiolabelling for aryl groups activated in *ortho*, *meta* or *para* position by an electron withdrawing group.[71]

The use of microreactors or hypervalent iodine (III) were not the only improvements. Several chelated metals were investigated such as Ni[72], Al([73]), Pd[74] and Cu[75, 76] as a co-catalyst to perform fluorination with fluorine-18 in practical yield.

Promising techniques with a particularity were also recently reported for radiolabelling. A compact and semi-automated synthesis platform[77] was designed to perform reaction under high pressure (up to 1.4 MPa) in a sealed reactor vessel. The advantages of such condition are the shorter reaction times, the enhancement of radiochemical yields and the use of volatile species such as reagents and precursors. The tight reaction system also avoids the loss of radioactive reagent over the labeling process by maintaining each chemical inside the vessel. The second apparatus[78] was provided with stepper motors, which were able to remove tubing from the reaction vial and so limited the contamination of reagents over the different steps of the radiolabelling. The syntheses occurred in a pressurised reactor vessel (up to 1 MPa) where, removed tubing was replaced with a stopper prior to reaction conditions such as heating or flow of nitrogen to avoid loss of radioactivity.

Chapter 2: PETIC centre and aims

2 PETIC centre and aims

With an aging worldwide population and a life span tending to increase, Alzheimer's disease (AD) and cancer have become two of the most important public healthcare problems over the world. Many governmental projects have been in charge of studying and diagnosing these diseases.[79]

Cardiff (Wales, UK) has not been an exception. Operational in 2010, the PET centre (PETIC[80]) has performed the routine production of [^{18}F]-FDG for clinical diagnoses and studies. New synthetic methods have also been processed for [^{18}F]-FLT and for different radioactive nuclei such as the [^{89}Zr] production and purification. A large range of PET isotopes (^{11}C, ^{13}N, ^{15}O, ^{18}F, ^{124}I, ^{64}Cu) have been produced onsite and can be directly delivered to the three hot cells (Gravatom Engineering Systems Ltd, UK) located in the research laboratory (see Figure 10).

The dose calibrator probe inside the hot cell is linked to the digital reading placed outside the hot cell. This permits an instant radioactivity measurement of several different radionuclides with accuracy and constancy.[20] Before use, each instrument are checked and calibrated.

A B

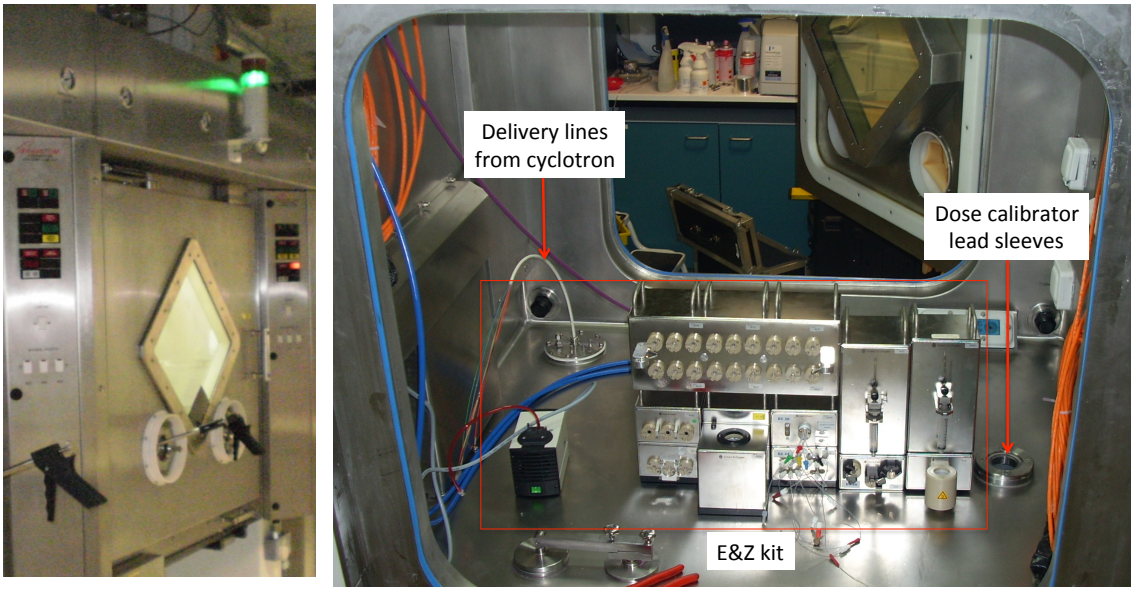

C

Figure 10: A) The hot cell in PETIC research laboratory, furnished with tongs and windows at each side of the cell to respectively manipulate goods inside and visually follow the reaction process. B) The inside of the hot cell with the Eckert & Ziegler kit next to the dose calibrator lead sleeves and the delivery lines. C) Digital reading of the dose calibrator instrument located outside the hot cell (CRC®-25PET, Capintec Inc., USA).

The aim of this work was to setup and explore different methods for [^{18}F]-FDG production using the E&Z platform in this new environment. Most of the synthetic routes for PET tracers are 20 years old (25 years old for FDG[59]). The development of new techniques already known in non-radioactive chemistry was the first objective, such as using microfluidic syntheses. Another aspect was the achievement of a more compact synthesis unit to restrict the exposure of the electronic devices to radiation.

The development of a potassium salt soluble in anhydrous solvents was investigated to reduce the time consumed by the azeotropic distillation for radiopharmaceutical syntheses.

Then we were focused on the development of mono or bis-protected triethylene glycol derivatives *via* the synthetic routes leading to K[2.2.2].

The last perspective was the optimisation of a new synthetic route of the precursor **7** leading to the florbetaben **8** (see Scheme 9), a phase 3 study PET probe for Alzheimer disease (Bayer company, Germany).[41]

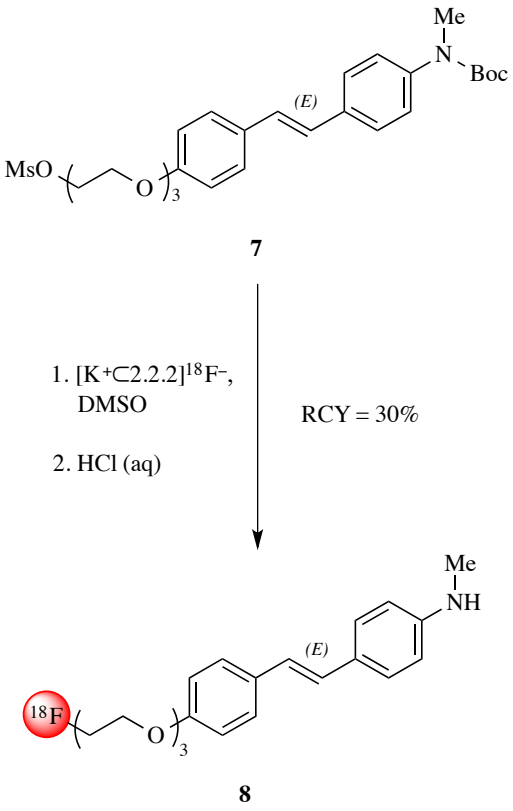

Scheme 9: Radiolabelling to [^{18}F]-Florbetaben **8** *via* S_N2 mechanism.

Chapter 3: Fully-automated syntheses for direct nucleophilic [^{18}F]-fluorination

3 Fully-automated syntheses for direct nucleophilic [^{18}F]-fluorination

3.1 Incorporation of fluoride-19 to mannose triflate 9

As previously discussed in Chapter 1, the most frequent route for synthesising [^{18}F]-FDG is the no-carrier-added fluorination of 1,3,4,6-tetra-*O*-acetyl-2-trifluormethanesulfonyl-β-D-mannopyranose **9**. The procedure involves the presence of a phase transfer agent such as the 4,7,13,16,21,24-hexaoxa-1,10-diazabicyclo[8.8.8]hexacosane also named Kryptofix [2.2.2]. Associated with [$^{18/19}$F]-fluoride and a weak base (K_2CO_3 or $KHCO_3$), the $[K^+\subset 2.2.2]^{18/19}F^-$ complex allows the [$^{18/19}$F]-fluorination, as reported by Hamacher and co-workers.[59]

More recently, Brown and co-workers depicted the chemical yield of this reaction and identified side products and their ratio (see Scheme 10).[81]

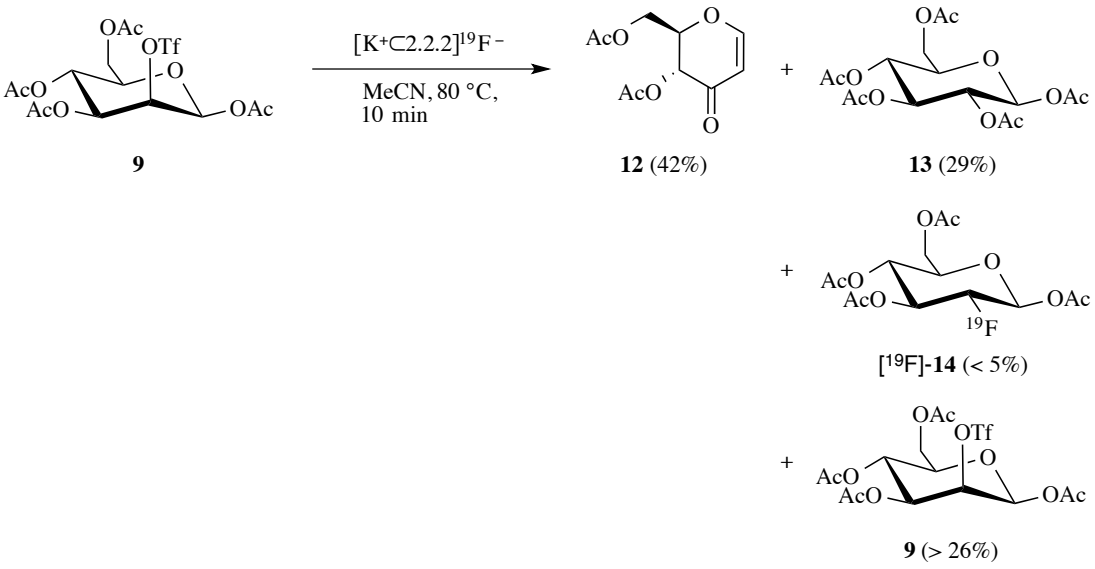

9

12 (42%)

13 (29%)

[^{19}F]-**14** (< 5%)

9 (> 26%)

Scheme 10: Characterisation of products formed by reacting a "naked" fluoride salt with mannose triflate **9**.

Brown *et al.* pointed out the extremely low conversion (< 5%) to the fluorinated [^{19}F]-deoxy-glucose **14**; and the predominant formations of side products such as the enone **12** (42%) and the pentaacetate β-D-glucose **13** (29%) with some unreacted tetra-*O*-acetyl-2-*O*-trifluoromethanesulfonyl D-mannose **9** (> 26%). After hydrolysis under basic or acidic conditions of [^{19}F]-**14**, [^{19}F]-FDG **1** is usually obtained in quantitave yield.[59, 81]

As mentioned in Section 1.7, the radiochemical yield is around 60% (decay corrected) for the [^{18}F]-FDG synthesis by using an automated synthesiser. The significant difference between chemical yield (< 5%) and RCY (≈60%) are mainly due to the amount of fluoride used for the fluorination. On one hand the preparation of [^{19}F]-FDG is achieved with a fluoride source (KF, TBAF…) approximately or exactly equivalent to the mannose triflate **9**. On the other hand [^{18}F]-fluoride is produced in picomole scale (Equation 2) whereas the mannose triflate **9** is present in μmole scale (25 mg, 52 μmol).

$$n = \frac{A}{N_A} \cdot \frac{t_{1/2}}{\ln(2)} \qquad \text{Equation 2}$$

The number of moles of the radioactive element can be calculated by using the radioactivity of the sample in Becquerel (A), the Avogadro's number (N_A) and the half time of the radioactive atom (s). For example for 100 GBq of [^{18}F]-fluoride the number of mole for [^{18}F] is 1 nanomol. The amount of radioactivity used for each experiment in this work (entries 1 to 39) is 50 times less radioactive.

The RCY (%) is the quotient between the radioactivity delivered by the cyclotron (A_0, in mCi) and the amount of radioactivity of the pure radiolabeled product collected at the end of the experiment (A_{exp} in mCi). Because of [^{18}F] decays (half of the radioactivity is consumed after 110 minutes), the latter value must be adjusted (A_t in mCi) to be able to compare with the initial activity (A_0) as shown in Equation 3.

$$RCY = \frac{A_t}{A_0} \cdot 100 = \frac{A_{exp}.e^{-0.0063\,.\,t}}{A_0} \cdot 100 \qquad \text{Equation 3}$$

The 0.0063 coefficient is the quotient between ln(2) and the half time (min) of the radioactive nucleus. The t parameter is the time spent in minutes between the measurement of the activity received from the cyclotron and the measurement of the vial product by using a dose calibrator.

Along this work the notion of RCY was not used due to the analysis of a product mixture mixing [^{18}F]-fluoride and fluorinated [^{18}F]-deoxy-glucose **1** or **14**. The term radiochemical conversion was preferred. Radiochemical conversion (%) is the ratio of these fluorinated [^{18}F]-deoxy sugars (**1** and **14**) inside the mixture. It was monitored by radio-TLC.

3.2 Investigation of the Hamacher method

The [^{19}F]-fluorination of tetraacetylated D-mannose **9** occurred in batch-mode following the work of Hamacher *et al.*[59] (see Scheme 11). The reaction was performed with 25 mg (52 μmol, 19 times less than Hamacher) of mannose triflate **9** and was monitored by TLC analysis.

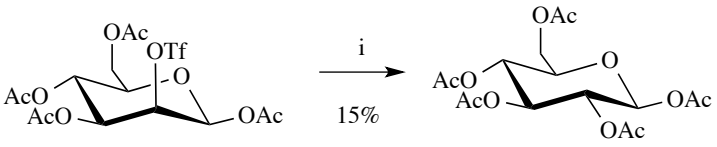

9 **13**

i. K^{19}F (1 equiv), K[2.2.2] (1.2 equiv), K_2CO_3 (0.15 equiv), CH_3CN, reflux, 20 min.

Scheme 11: Pentaacetate glucose formation from mannose triflate **9** using fluorination agent.

The product mixture was analysed by ^{1}H and ^{19}F NMR spectroscopy at the end of the process. A sample of pentaacetylated glucose **13** present in the laboratory was used to identify this molecule in the crude product mixture. The ^{19}F NMR did not confirm the presence of the desired [^{19}F]-deoxy-glucose **14**.

The reaction was then transferred to microfluidic conditions, so they can be compared with the batch process. Using PC remote syringes and Peltier reactor module from the Eckert & Ziegler platform (see Figure 12), the microfluidic fluorination of mannose triflate **9** was performed in a capillary loop tubing linked to two syringes. The PEEK loop (Vici, Switzerland) was a 3 m long tubing shaped as a double helix with an internal diameter of 0.5 mm (total volume 589 μL) forming a cylinder of 30 mm of diameter. One syringe was filled with mannose triflate in MeCN (3 mL) (blue) and the other one (red) was filled with a fluorinated agent (TBAF) soluble in organic solvent (MeCN, 3 mL). The software (ModularLab) was configured to proceed the reaction with an overall flow rate of 14 μL/s (7 μL/s each syringe, minimum speed). Mixed with a T-mixer, the combined solutions were heated at different temperatures (70, 85 and 95 °C). The different conditions afforded the same product mixture: elimination product **12** and the protected β-glucose **13**, inseparable by flash chromatography.

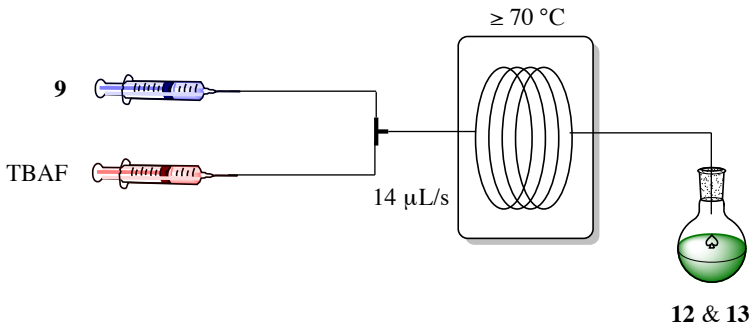

Scheme 12: Microfluidic reaction with mannose triflate **9** and TBAF in MeCN.

To identify the possible presence of the deoxy-glucose **14**, the crude mixture was monitored by ^{19}F NMR. Unfortunately no relevant peaks were observed. The reaction conditions (**9**: 25 mg, 52 µmol) might not be suitable for the detection of the [^{19}F]-product **14** by NMR spectroscopy. However, for an equivalent amount of starting material **9**, [^{18}F]-fluorination can be analysed by radio-TLC (Canberra, Belgium) and radio-HPLC (agilent system, Germany).

3.3 Generalities about radio-detection

The detection of radiolabelled substances is generally performed by radio-HPLC and radio-TLC. The high performance liquid chromatography (HPLC) is one of the most widely used analytical techniques. The addition of a radio-detector allows the analysis of radioactive samples. The sensitivity of this detector is higher than the usual UV and refractive index detectors. The full setup is controlled *via* specific software (in PETIC, Laura software). The analysis of the mixture of the [^{18}F]-FDG reaction was performed with a phenomenex column (Resex, RHM-Monosaccharide H^+) in 30 minutes. The other method, radio-TLC, has the advantage to be fast (5 minutes). It is the same principle than thin layer chromatography (TLC), a drop (≈5 µL) of the radioactive crude mixture is applied on the bottom edge of a silica gel plate. The TLC plate is then placed inside a developing chamber with solvent mobile phase. For [^{18}F]-FDG, the mixture of solvents used was 5% (v/v) of distilled water (millipore, USA) in acetonitrile. After complete development of the chromatogram, the plate is placed on the rack as shown in Figure 11. The computer, with the control of Laura software, moves the probe (NaI crystal) along the plate and detects the spots of radioactivity. In these conditions (5% distilled water in acetonitrile), the free [^{18}F]-fluoride stays on the bottom edge of the TLC plate and [^{18}F]-FDG **1** and the protected [^{18}F]-deoxy-glucose **14**

migrate. The use of the second method (radio-TLC) was preferred to the first one (radio-HPLC) due to its convenient time consuming (5 minutes).

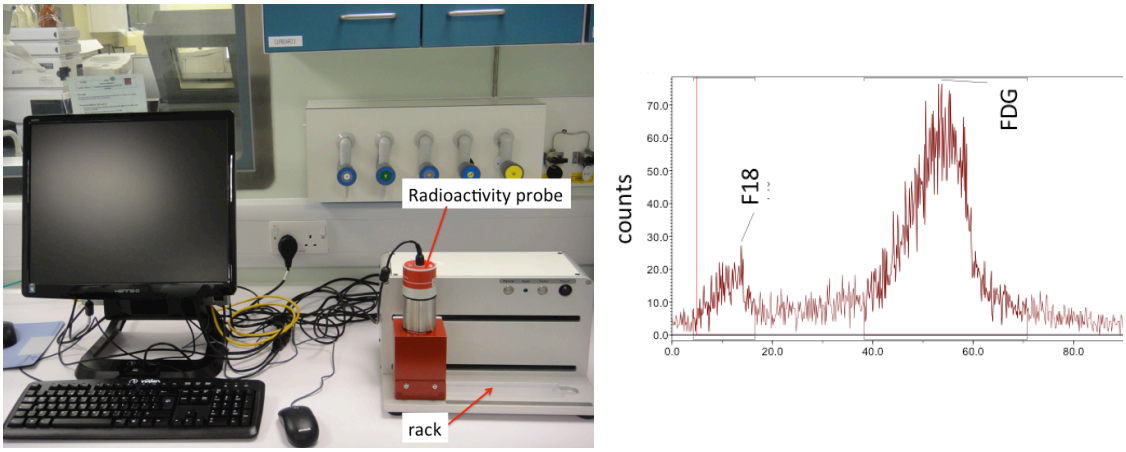

Figure 11: Radio-TLC apparatus (left picture) and radio-TLC chromatogram (right picture).

3.4 E&Z platform performed for [^{18}F]-fluorination of mannose triflate 9

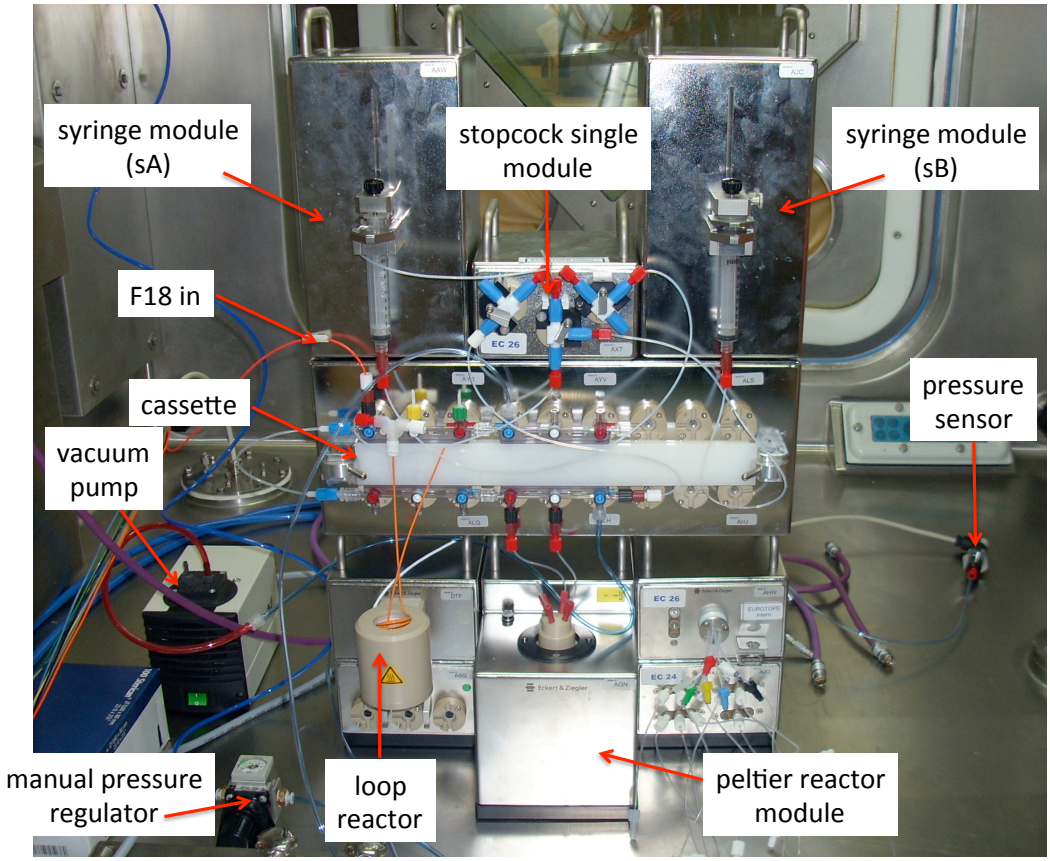

Figure 12: The first setup used for the tetraacetate [^{18}F]-deoxy-glucose **14** synthesis.

The synthesiser was setup in a shielded hot cell as shown in Figure 12. The entire reaction process was controlled outside the cell by a computer with ModularLab software.

This interface is able to control all actions: heating, cooling, turn valves etc. It is an automated or manual programing system with interactive scheme of the devices (see Figure 13). The modules are daisy-chained together with connections to the source of inert gas (nitrogen) and to the power supplier placed outside the hot cell. Daisy-chaining minimises the number of cables passing through the hot cell to link the power supply. The two sensors (see Figure 12 and Scheme 13) monitored the pressure (bar) and radioactivity (no units) in

real time. The main part of the platform was the Peltier reactor module, which allows temperature control to 150 °C and water cooling. Connections for liquid and gas transfers were allowed by tubing constructed out of polytetrafluoroethylene (PTFE). The loop reactor was designed to heat double helix capillary loop system (length = 3 m, Ø = 0.5 mm,), which forms a cylinder of 30 mm of diameter. Each [^{18}F]-fluorination reaction was using 25 mg of mannose triflate (52 µmol) in dry acetonitrile (1.1 to 2 mL).

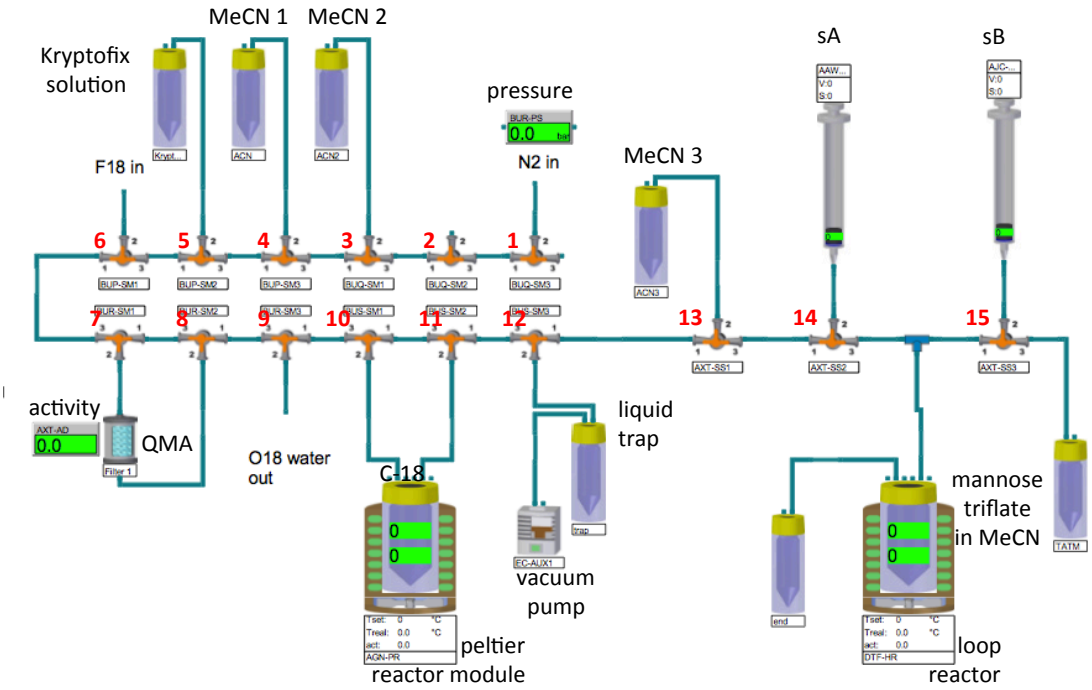

Scheme 13: ModularLab control panel developed for protected [^{18}F]-deoxy-glucose **14** using a twelve 3-way valves cassette.

The reaction process commenced with the elution of the aqueous [^{18}F]-fluoride to the synthesiser. The radioactive solution was transferred from the cyclotron (cyclone® 18/9, IBA, Belgium) to the intersection 6 (see Scheme 13) *via* the [^{18}F]-line present inside the hot cell.

The valves 6, 7, 8 and 9 were configured by ModularLab software to allow the aqueous [^{18}F] to pass through the QMA cartridge. The cartridge was loaded with the [^{18}F]-fluoride and the [^{18}O]-water was collected into a waste vial (O18 water, intersection 9). Dried with a flow of nitrogen, the [^{18}F]-fluoride was then eluted into the reactor vial from the cartridge by using a Kryptofix solution (ABX, Germany) containing K_2CO_3 (4.2 mg, 30.4 µmol) and Kryptofix [2.2.2] (22.6 mg, 60.0 µmol) in 600 µL of water/MeCN (50/50 v/v). The liquid transfer into the 5 mL V-shape reactor vial (Alltech, Grace Discovery Sciences,

USA) was allowed by the negative pressure performed by the vacuum pump (see Scheme 13).

The drying process was first carried out at 90 °C with both positive and reduced pressure within 2 minutes. The simultaneous use of negative and nitrogen flow allowed the acceleration of vapor removal over the evaporation steps.

The azeotropic drying sequence was carried out with acetonitrile (2 x 1 mL). The acetonitrile (1 mL) was transferred to the heated reactor vessel (55 °C) *via* the vacuum pump. The Peltier reactor heated the mixture at 95 °C under reduced pressure and flow of nitrogen. This sequence was repeated once to remove residual traces of water. The whole azeotropic sequence was achieved over 4 minutes.

The Peltier module was cooled to 35 °C. The 2 mL of acetonitrile (MeCN 3) were drawn by syringe A (sA) and injected to the reactor vial. The $[K^{+}\subset 2.2.2]^{18}F^{-}$ solution was then contained in sA. The mannose triflate **9** dissolved in dry acetonitrile (2 mL) was transferred inside syringe B (sB). The mixing of the two solutions was performed with a T-mixer (PTFE) at 14 µL/s as overall flow rate.

The radiolabelling reaction took place in a PEEK loop (double helix, length: 3 m, ∅: 0.5 mm) in continuous flow at 80 °C. Only a small amount of radioactivity was recovered (< 30%, entries 1 to 3, Table 2).

Table 2: Radiolabelling proceeded in a 3 m PEEK loop tubing.

Entry	Activity received (GBq)	Process time (min)	Recovery of activity, decay-corrected (%)
1	1.5	34	19
2	1.5	30	27
3	1.5	30	23

The experiment 1 was longer (34 instead of 30 minutes) due to a problem of elution of the vial at the intersection 3 (MeCN 1, Scheme 13). The vial was replaced and the reaction occurred normally. The three reactions (experiment 1 to 3) were performed by the same method described above Table 2.

A part of the loss of radioactivity was detected for the synthesis 3. The vacuum trap (liquid trap, Scheme 13) was placed in the sleeve of the dose calibrator to detect online the presence of radioactivity inside this one. Within the azeotropic sequence, the dose calibrator detected 27 MBq after the evaporation of the first vial of acetonitrile at 90 °C under reduced

pressure. The value increased to 147 MBq after evaporation of the second vial of acetonitrile under the same conditions.

Table 3: Azeotropic distillation performed at 90 °C instead of 95 °C.

Entry	Activity received (GBq)	Process time (min)	Recovery of activity, decay-corrected (%)
4	1.8	34	30
5	1.5	30	37

The reactions 4 and 5 (Table 3) were performed with a different azeotropic distillation process. The acetonitrile (2 x 1 mL) injected to the reactor vessel was evaporated at 55 °C for 30 seconds and then at 90 °C (instead of 95 °C) over 90 seconds. No presence of activity was detected inside the vacuum trap. The recovery of activity was collected up to 37%. However after the azeotropic distillation was achieved, the $[K^{+}\subset 2.2.2]^{18}F^{-}$ complex was not dry and solvents were still inside the reactor vessel. So water residuals might be present in the reactor vial, which can decrease the efficiency of the [^{18}F]-fluorination. Higher temperature (>90 °C) should be used to complete the evaporation of solvents inside the reactor vessel.

The experiment 4 was stopped step by step to check the efficiency of each process, which can explain the delay of 4 minutes compared to the reaction 5.

The reactor vial was still radioactive after elution of the $[K^{+}\subset 2.2.2]^{18}F^{-}$ complex by syringe A. At the experiment 4, 50 % (decay-corrected) of the initial radioactivity was present in the reactor vial. The cassette was highly radioactive at the end of the synthesis. Some drops of the reaction mixture remained inside the cassette. In order to rinse the cassette, the modularLab program was modified to perform the synthesis of [^{18}F]-FDG **1** by adding the NaOH solution (1 M, 1 mL) and 3 mL of distilled water.

3.5 E&Z synthesiser configured for [^{18}F]-FDG 1 synthesis

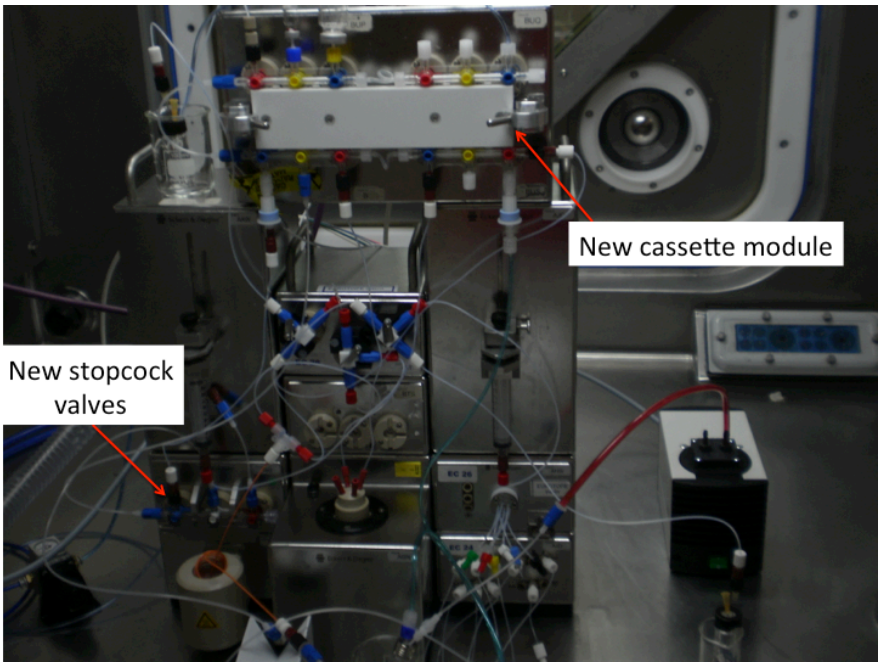

Figure 13: New configuration of the modules with the new shortened cassette module.

This method integrated the new cassette module (12 mechanical valves instead of 18) and the addition of a three 3-way valves module (see Figure 13). The addition of this latter module (see Scheme 14) was required to transfer automatically the reaction mixture inside the loop (radiolabelling process) to the reactor vial for the hydrolysis step. The deprotection step was accomplished in the reactor vial with a solution of NaOH. The organisation of the modules was modified due to the addition of these new modules.

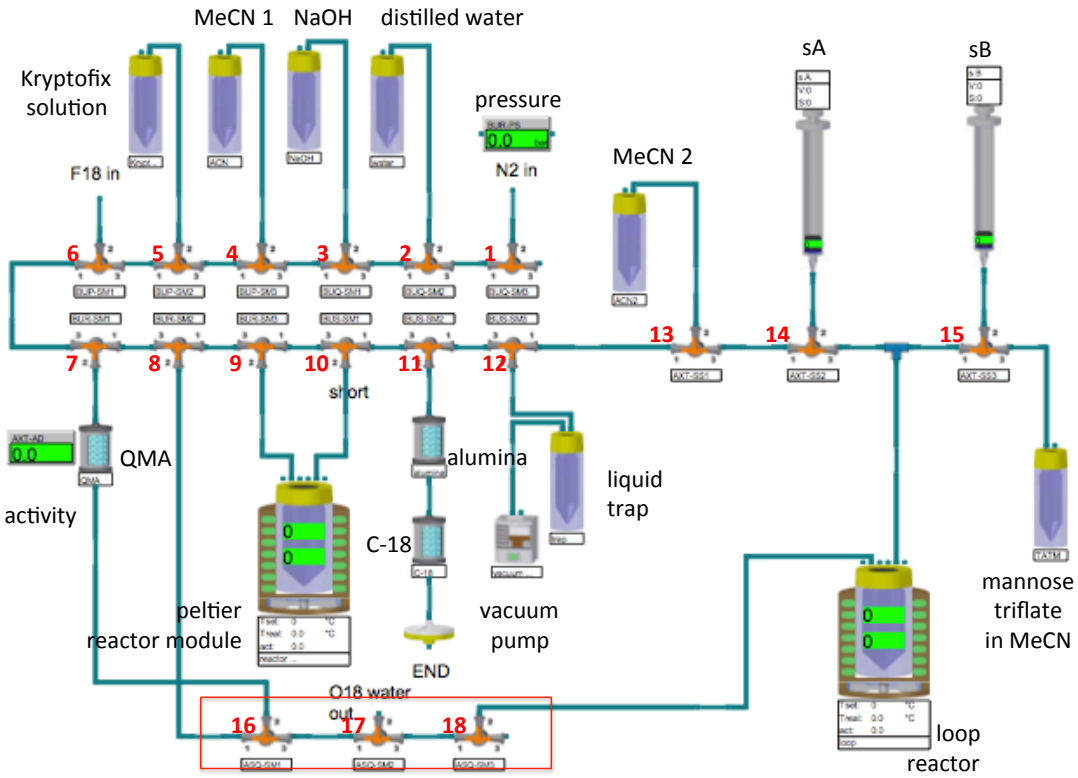

Scheme 14: Configuration of the E&Z platform used for the radiosynthesis of [^{18}F]-FDG **1.**

After the loading of the QMA cartridge with [^{18}F]-fluoride, the cartridge was dried under nitrogen pressure for 80 seconds.

The Kryptofix solution (ABX) was eluted through the QMA cartridge and then to the reactor vial under reduced pressure at room temperature. The $[K^{+}\subset 2.2.2]^{18}F^{-}$ complex was heated at 70 °C for 50 seconds and for an additional 70 seconds under pressure of nitrogen.

The azeotropic solution was performed with one vial of acetonitrile (1 mL, see MeCN 1, Scheme 14) at 55 °C under negative pressure. The reactor vial was heated to 95 °C for 50 seconds under reduced pressure and nitrogen flow and for an additional 20 seconds under nitrogen.

The reagent mixtures were more concentrated; the volume of solvent was 0.5 mL less than the experiments 1 to 5 (2 mL). The $[K^{+}\subset 2.2.2]^{18}F^{-}$ complex heated at 39 °C was transferred into syringe A *via* 1.5 mL of dry acetonitrile present at the intersection 13. Syringe B withdrew the mannose triflate solution dissolved in 1.5 mL of dry acetonitrile.

The solutions were driven to the T-mixer. The resulting mixed solution was then eluted to the loop tubing to achieve the [^{18}F]-fluorination. The reaction was carried out at 85 °C instead of 80 °C (reactions 1 to 5) and collected in the reactor vial. The vacuum line was opened within this sequence to ventilate the reactor vial.

The deprotection step occurred at 50 °C for 50 seconds prior to the elution of NaOH (1 M, 1 mL, ABX) in the reactor vessel under reduced pressure.

After the addition of 3 mL of distilled water (3 mL) into the Peltier module, the reaction mixture was collected inside sA. The solution was then injected through the 2 cartridges (alumina & C-18, see Section 1.7.5) for purification. The purified mixture was collected in the product vial.

Table 4: Study of the recovery of activity for [^{18}F]-FDG preparation.

Entry	Activity received (GBq)	Process time (min)	Recovery of activity, decay-corrected (%)
6	3.0	38	10
7	2.4	34	18
8	1.5	36	14

The process time for the experiment 6 was longer than the experiment 7 and 8 due to a mistake on modularLab at the elution of the reaction mixture in the loop to the reactor vial. To complete the synthesis of [^{18}F]-FDG **1**, the deprotection step and elution to the product vial was performed manually. The deprotection step for the reaction 8 proceeded in 100 seconds instead of 50 seconds.

The recovery was low for each reaction (below 20 %, Table 4). Following the reaction 8, 10% (decay-corrected) of the initial radioactivity was trapped by the alumina cartridge. The alumina cartridge generally used to trap the [^{18}F]-fluoride indicated the presence of unreacted fluoride-18 in the reaction mixture.

The alumina and C-18 cartridges were removed for the experiments (9 to 11). The PEEK tubing connecting the several modules were shortened and the reactor vial was replaced by a 7 mL PEEK flat vial. The larger capacity of the vial (7 instead of 5 mL), its material (PEEK instead of glass) and its shape (flat instead of V-shape) improved the recovery of the radioactivity (see Table 5) by containing the splashes inside the reactor vial.

Table 5: Study of the recovery of activity after achievement of the [^{18}F]-FDG preparation in a flat PEEK reactor vial.

Entry	Activity received (GBq)	Process time (min)	Recovery of activity, decay-corrected (%)
9	1.1	30	68
10	1.85	33	52
11	1.1	30	64

3.6 Segmented flow in capillary tubing

To our knowledge no radiolabelling by using segmented flow has been described in literature. The strength of segmented or biphasic system in a micro-channel is a rapid and efficient mixing comparing to continuous flow. The droplets immiscible with its neighbour phases (liquid/liquid or liquid/gas), generate an internal vortex for both phases due to a difference of viscosity and surface tension (see Figure 14).[82, 83] The drops containing the reagents react faster and more efficiently due to their small volume.

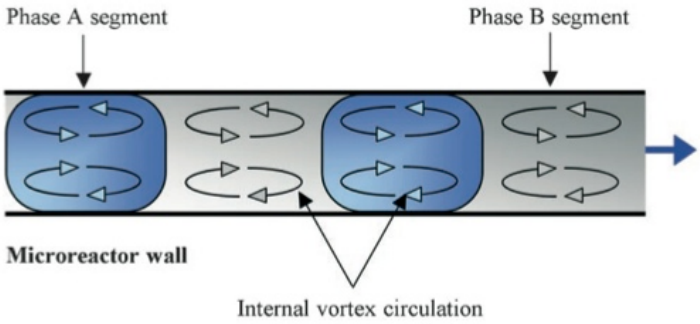

Figure 14: Schematic mixing phenomenon involved in microfluidic segmented flow.[82]

3.7 Formation of the [^{18}F]-deoxy-glucose 14 by using ionic liquids for the segmented flow procedure

A series of 15 reactions was performed to obtain a percentage of conversion of the [^{18}F]-deoxy-fluoride **14** superior to 0%. The maximum temperatures used for the drying process and the azeotropic distillation increased by at least 20 °C. The sequence time for these processes was also longer to enhance the removal of solvents and to obtain better conversion.

As mentioned in the Section 1.7.3, the use of an ionic liquid such as BMI(OTf) can perform in batch the [^{18}F]-fluorination with presence of water in reasonable RCY (lit.[58] 59%). Two attempts were performed by using 300 µL of the ionic liquid (see Table 6).

Table 6: Radiolabelling achieved with the presence of an ionic liquid by using segmented technique.

Entry	Activity received (GBq)	Process time (min)	Recovery of activity, decay-corrected (%)	Radiochemical conversion (%)
12	3.3	38	69	5
13	1.3	30	—	54

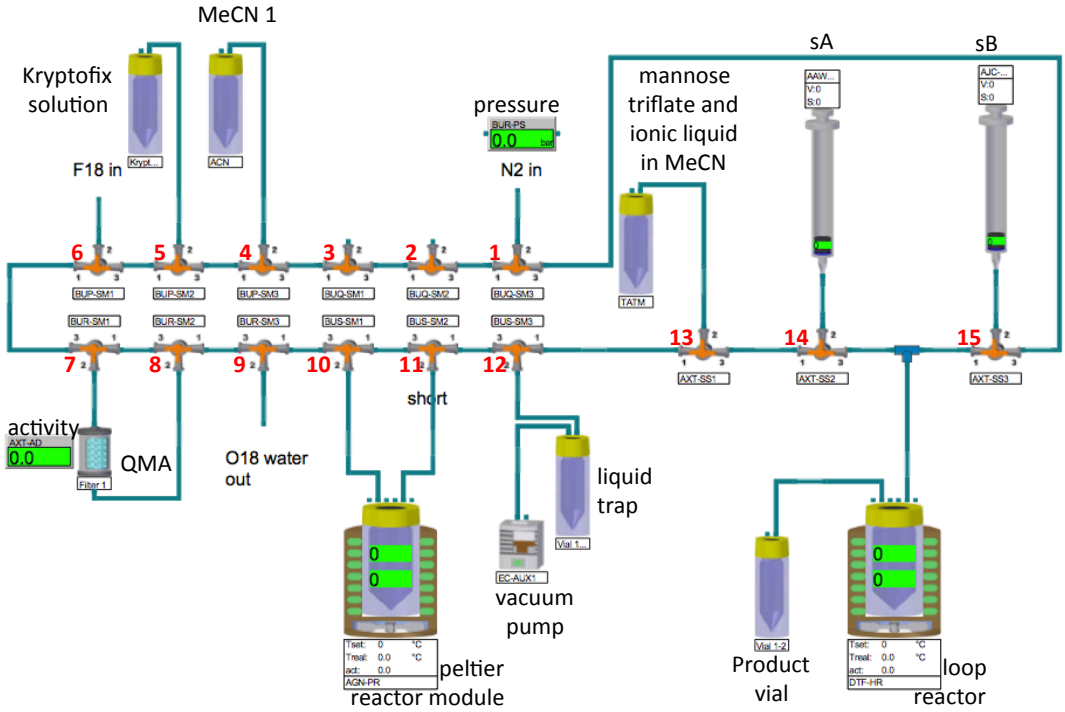

Scheme 15: Radiolabeling of mannose triflate 9 in the presence of ionic liquid.

The aqueous [^{18}F]-fluoride from the cyclotron was transported to the QMA cartridge where the [^{18}F]-fluoride was trapped. The cartridge was dried for 50 seconds over a nitrogen flow.

The commercial Kryptofix solution (ABX) was eluted into the reactor vial under reduced pressure. The elution carried on for an additional 1 minute under reduced pressure and flow of nitrogen.

The evaporation of the solvents performed with an azeotropic distillation (1 mL of acetonitrile) occured with a maximum of temperature of 120 °C for approximatly 6 minutes under vacuum and nitrogen stream.

The mannose triflate with the ionic liquid (300 µL, 1.6 µmol) in acetonitrile (1.5 mL) was added into the heated reactor vial (43 °C) by using syringe A. The solution was then withdrawn to syringe A and syringe B filled with the nitrogen gas.

The segmented flow was performed *via* the simultaneous addition of the substrates to the loop at 14 µL/s overall flow rate. The [^{18}F]-incorporation for the experiment 12 was carried out at 95 °C.

The recovery of activity for this experiment (see Table 6) was obtained in 69% but the incorporation of [^{18}F] was very low (5%). This percentage of incorporation was improved for the experiment 13 (54%) by increasing the maximum temperature over the solvent evaporation step (125 instead of 120 °C) and by decreasing the temperature of the segmented-based reaction from 95 °C to 85 °C. This enhancement of [^{18}F]-incorporation was not fully understood. But the temperature (125 °C) established for the removal of solvents might perform a better [^{18}F]-fluorination even without the ionic liquid. The choice was made to find better conditions to remove the water present in the commercial Kryptofix solution and to not use an ionic liquid, which is also toxic.[84]

3.8 New configuration system of [^{18}F]-fluorination of mannose triflate 9 performed in segmented flow.

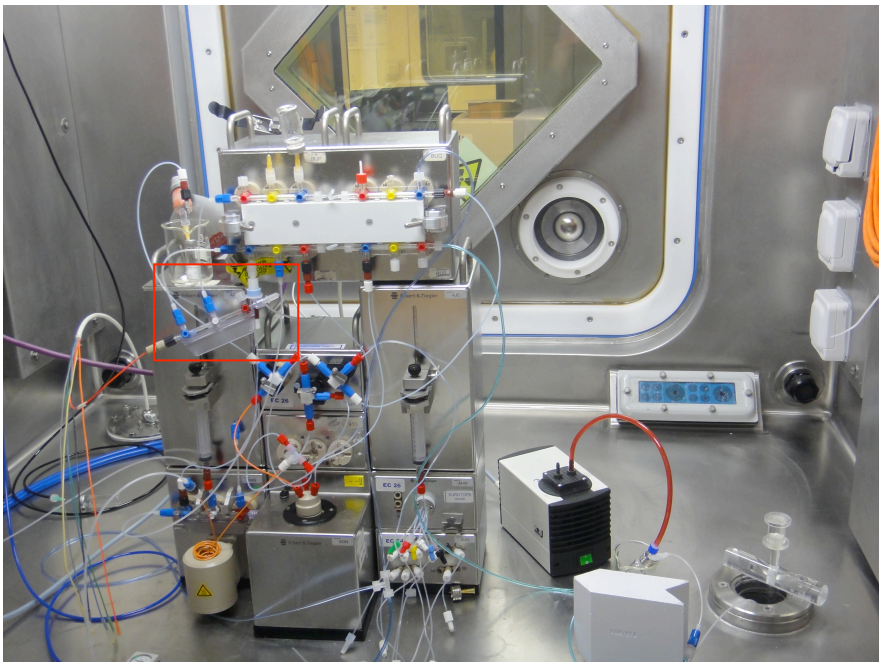

Figure 15: New line connections for the segmented flow method.

The good recovery of activity with high radiochemical conversion was the main issue for each attempt. Under reduced and nitrogen pressure, a high temperature (>110 °C) will transport the radioactivity away from the reactor vial with the withdrawing of the solvent vapor. At low temperature (<90 °C) under reduced and nitrogen pressure, the presence of water might remain inside the reactor vial and the [^{18}F]-fluorination will not occur as described in Section 1.7.2.

The possible presence of water inside the cassette for the elution of $[K^+\subset 2.2.2]^{18}F^-$ complex with the mannose triflate solution might be a source of contamination. This water might remain from the solvent evaporation steps by condensing inside the cassette. Syringe A (intersection 14 in Scheme 16) was hence connected directly to the reactor vessel, which should minimise the presence of water inside the reaction mixture.

The mannose triflate **9** usually provided by Sigma-Aldrich in a vial was purchased from ABX, in a sealed vial routinely used by PET centres.

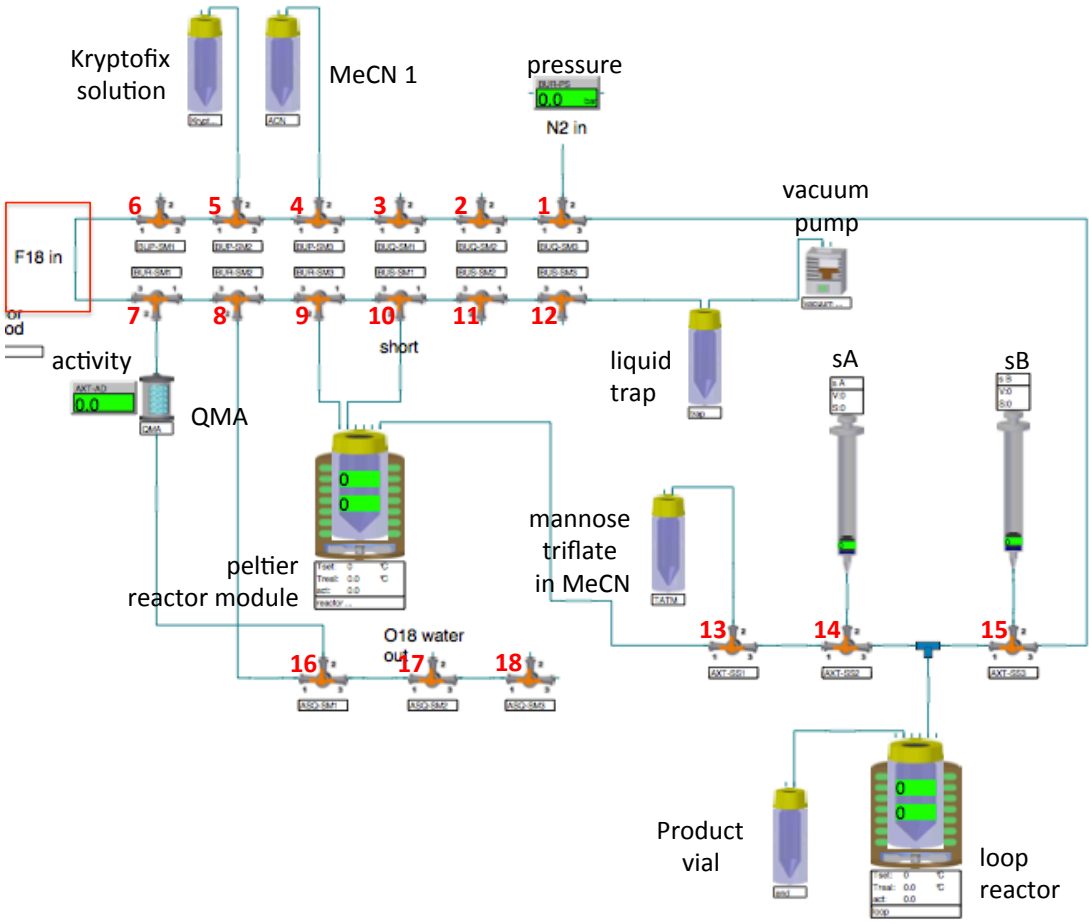

Scheme 16: New configuration of the segmented flow procedure for the formation of [^{18}F]-deoxy glucose **14**.

Following similar steps than the reactions achieved previously (see Section 3.7), the drying process occurred with an increasement of 10 °C of the temperature. A single azeotropic drying sequence was achieved. The solvent removal commenced at 120 °C under reduced pressure over 50 seconds and for an additional 70 seconds under reduced pressure and nitrogen flow. The addition of the dry acetonitrile (MeCN, valve 4) into the reactor vessel heated to 80 °C was performed under reduced pressure. The reaction mixture was heated to 110 °C for 80 seconds and for an additional 1 minute at 130 °C under reduced pressure. The evaporation process carried on over 80 seconds at 130 °C under reduced and nitrogen pressure.

The mannose triflate solution (1.5 mL) was injected into the heated reaction mixture (43 °C) *via* syringe A. The combined solution was then withdrawn by the same syringe (A). The syringe B was filled with nitrogen gas.

Table 7: Radiolabelling synthesis using segmented flow in loop tubing.

Entry	Activity received (GBq)	Process time (min)	Recovery of activity, decay-corrected (%)	Radiochemical conversion (%)	Loop tubing
14	1.2	35	40	54	3 m
15	1.2	102	21	74	2 x 3 m
16	1.2	36	27	62	5 m

The segmented flow applied for the radiolabeling process of the experiment 14 was performed at 100 °C with an overall flow rate of 14 µL/s. The recovery of activity was obtained in 40% with an [^{18}F]-incorporation of 54% (see Table 7). It was the best incorporation obtained with such recovery of activity (40%).

The concentration to dryness of the [K^+⊂2.2.2]$^{18}F^-$ complex for the reaction 15 was performed in identical conditions than the experiment 14. The [^{18}F]-labeling was performed in 2 identical loops (length =3 m, ∅ = 0.5 mm, each). The first loop was heated in the loop reactor at 100 °C and the second was heated in a water bath at 75 °C. Comparing to the reaction 14, the [^{18}F]-incorporation was better (74% vs 54%) but the recovery of activity was lower (21% vs 74%) (see Table 7).

A longer and smaller PEEK capillary tubing (length = 5 m, Ø = 0.01 mm) was used for the radiolabelling of mannose triflate **9** (see Table 7). The reaction was performed at 100 °C at 14 µL/s. The results obtained for the experiment 156 (see Table 7) were comparable to those performed with two loops (15, Table 7).

3.9 **Conclusion**

An automated radiolabeling synthesis was setup to perform the [^{18}F]-fluorination of mannose triflate **9** in a continuous or segmented microfluidic strategy. The recovery of activity in this Chapter was low and showed the difficulties of these techniques. However the development of a segmented flow method allowed the synthesis of the tetraacetylated [^{18}F]-deoxy-D-glucose **14**. The achievement of the [^{18}F]-fluorination in small size tubing was abandoned but the desire to produce [^{18}F]-FDG **1** in a compact synthesiser was promoted.

Chapter 4: Synthetic routes to radiopharmaceuticals using fluidic devices

4 Synthetic routes to radiopharmaceuticals using fluidic devices

4.1 Compact E&Z platform using tee luers

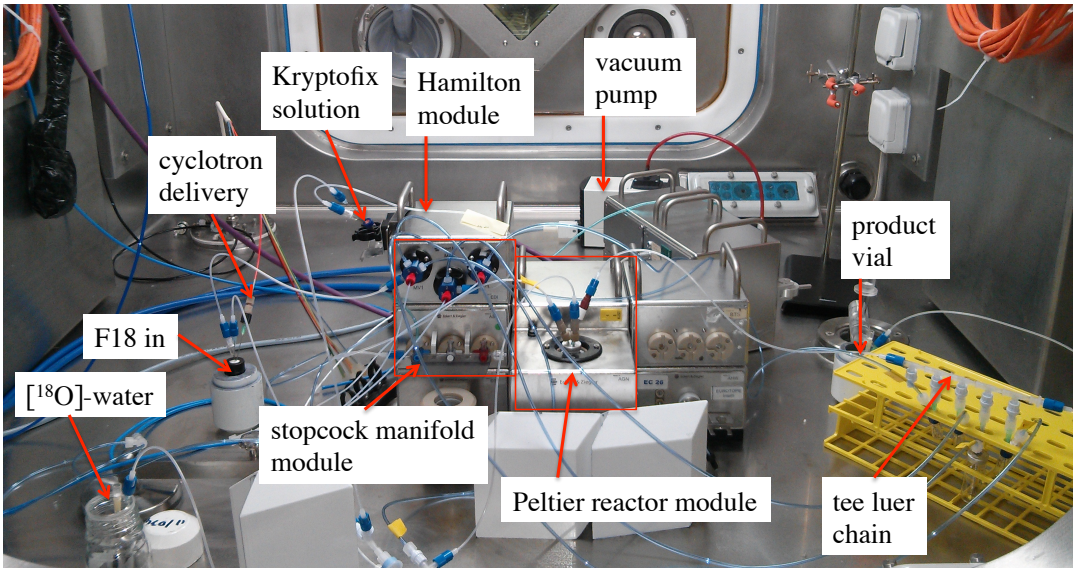

Figure 16: The configuration of E&Z modular platform for [^{18}F]-FDG **1** production.

In collaboration with the Eckert & Ziegler company, we decided to study the substitution of the cassette and its modules by luer adapters (connectors) (see Figure 16 and Figure 17) to perform a compact synthesiser. The exposure of radioactivity to electric devices can possibly damage them over time. All previously used modules contain electronic circuit broads. It was suggested to keep the number of modules inside the hot cell to a minimum. Two modules could already be outside the hot cell: the vacuum pump and the nitrogen gas controller (Hamilton device). The first attempt commenced with the use of tee luers (internal volume = 0.35 mL), which fit together and form a chain (see Figure 16). The setup required a reactor vessel (5 mL flat bottom glass vial) for performing the different steps of the synthesis. The use of such flat reactor vial is the same than the ones provided by TracerLab MX_{FDG} and Synthera (see Figure 6 and 7, respectively) for [^{18}F]-FDG **1** production.

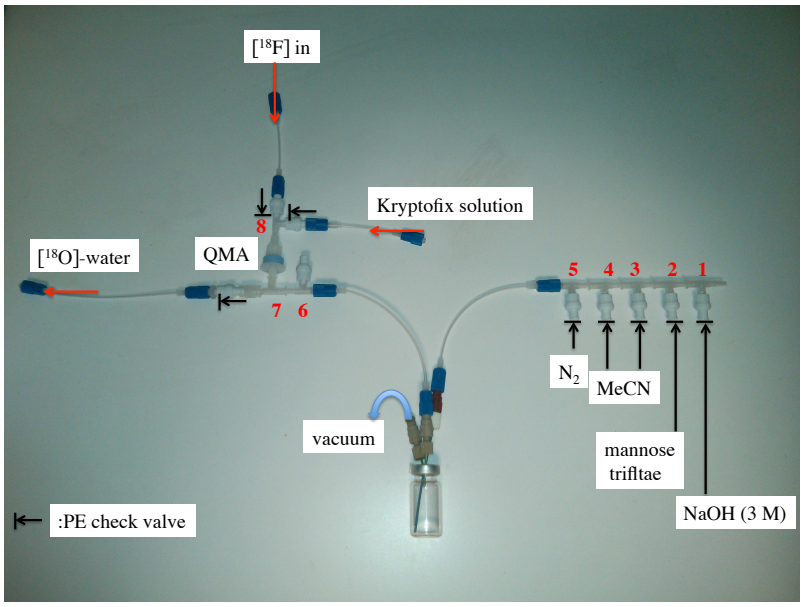

Figure 17: Picture of the setup using luers for [^{18}F]-FDG **1** synthesis.

Once all reagents were placed, the liquid transfers were performed by using the Hamilton module and a vacuum pump (see Figure 16). The full control of liquid transfers required the use of check valves. These connectors were constructed out of polyethylene (PE). They prevent backflow under positive pressure permitting gases and liquids to flow through it only in one direction (see Figure 17, the way of black arrows and Scheme 17, green arrow). Furthermore a reduced pressure can also afford the movement of liquids or gases as shown in Scheme 17.

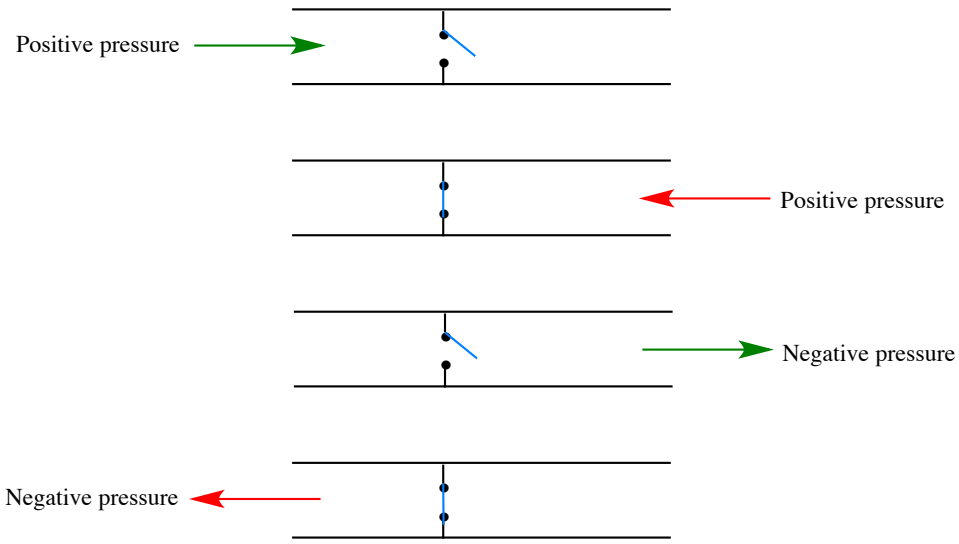

Scheme 17: Illustration of the check valve working as a door system (red arrow the valve is closed, green arrow the valve is open).

Liquid directions were controlled by *vacuo* and nitrogen pressure or nitrogen/nitrogen pressure. For each liquid transfer, a positive pressure of nitrogen (1.5 bar) was added into the desired vial to push the solution through the system to reach its destination. For example, at the intersection 8 (see Figure 17) the aqueous [^{18}F]-fluoride from the "F18 in" vial was pushed straight to the QMA cartridge *via* a pressure of nitrogen applied on the top of this vial. The horizontal check valve, at the intersection 8, restricted the access of the aqueous [^{18}F]. Therefore, this mixture did not contaminate the Kryptofix solution. The [^{18}O]-water passed through the QMA cartridge and the [^{18}F]-fluoride was trapped by this one.

The applied pressure of nitrogen delivered at the crossing 6 allowed the [^{18}O]-water to flow to the [^{18}O]-water vial. The reactor vessel was hence not contaminated by this water. The QMA cartridge was then dried under pressure of nitrogen. The horizontal check valves positioned at the intersection 7 did not allow the backflow of the [^{18}O]-water to the reactor vial under reduced pressure.

The Kryptofix solution was transported to the QMA cartridge to form the $[K^{+}\subset 2.2.2]^{18}F^{-}$ complex and eluted into the reactor vial. This achievement was controlled by using simultaneously nitrogen and vacuum pressure. The nitrogen and vacuum flow were directly applied from the Kryptofix solution vial and the reactor vial, respectively.

The challenge of this technique was to avoid the transfer of the other reagents within the use of the vacuum pump. Indeed, an applied reduced pressure from the reactor vessel performed the transport of the solutions present in the intersections 4 and 3 (see Scheme 17). A stream of nitrogen was required at the intersection 5 to neutralise the effect of the vacuum. The solutions in position 1 and 2 were not affected due to the proximity with the ventilated product vial, which weakened the vacuum.

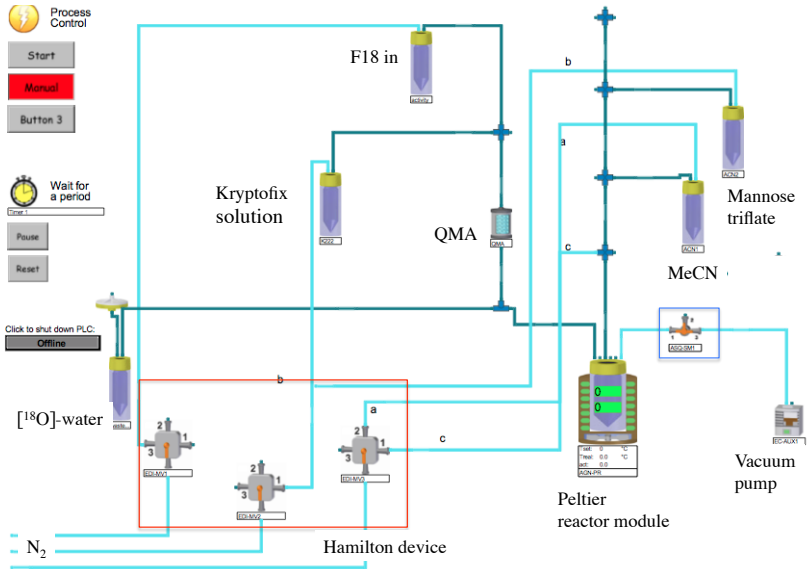

Figure 18: First configuration of fluidic transfers with one mechanical valve.

The reaction occurred with the [^{18}F]-incorporation of mannose triflate **9** to form the protected [^{18}F]-deoxy-glucose **14**. To elute the reaction mixture from the reactor vessel to the product vial, a positive pressure of nitrogen was added. A mechanical valve (blue square in Figure 18) was added to close or open the line connected to the vacuum pump. The advantage was the enhancement of the drying process under nitrogen pressure to the ventilated reactor vial. The $[K^+ \subset 2.2.2]^{18}F^-$ complex was dried at 95 °C within 270 seconds. The azeotropic distillation was achieved with 1 mL of acetonitrile at 95 °C for 5 minutes. The radiolabeling was performed at 90 °C over the same time (5 minutes). The recovery was better than the experiments achieved in the Section 3.8 but the percentage of incorporation was relatively low (36%, Section 3.8: up to 72%). This result can be explained by the lower temperatures used for the whole process (up to 95 °C), comparing to the 130 °C as maximum temperature for the experiments of the Section 3.8.

Table 8: First reaction achieved with three modules.

Entry	Activity received (GBq)	Process time (min)	Recovery of activity, decay-corrected (%)	Radiochemical conversion (%)
17	1.5	36	67	36

The major drawback of this approach was the inner diameter of the tee luers (∅ = 3 mm). Its relatively large diameter led to small droplets being lost inside the tubing. Another issue was the exposure of the PE check valves to acetonitrile which damaged them over time.

4.2 Reducing internal volume of the fluidic devices and new check valves

To obtain more efficient liquid transfers, E&Z provided more suitable consumables (see Figure 19). The first one was a 1-way cassette also named cube constructed out of polymethylpentene (TPX®, blue square), with an inner diameter of 0.9 mm and composed of five inputs/outputs. Each entry/exit was screwed with an adapter thread to luer female constructed out of polypropylene (PP) and a plastic join placed between both to avoid leaks. Solvent resistant, PP check valves were fitted to solve the problem of blockage and allow their reuse. Some of the tee luers were replaced by a low pressure Tefzel® tee which has a smaller dead volume (2.9 µL instead of 0.35 mL). For the first complete [^{18}F]-FDG **1** synthesis with induced fluidic transfers, the 3 M solution of NaOH (3 mL) was injected manually inside the reactor vessel for the hydrolysis step.

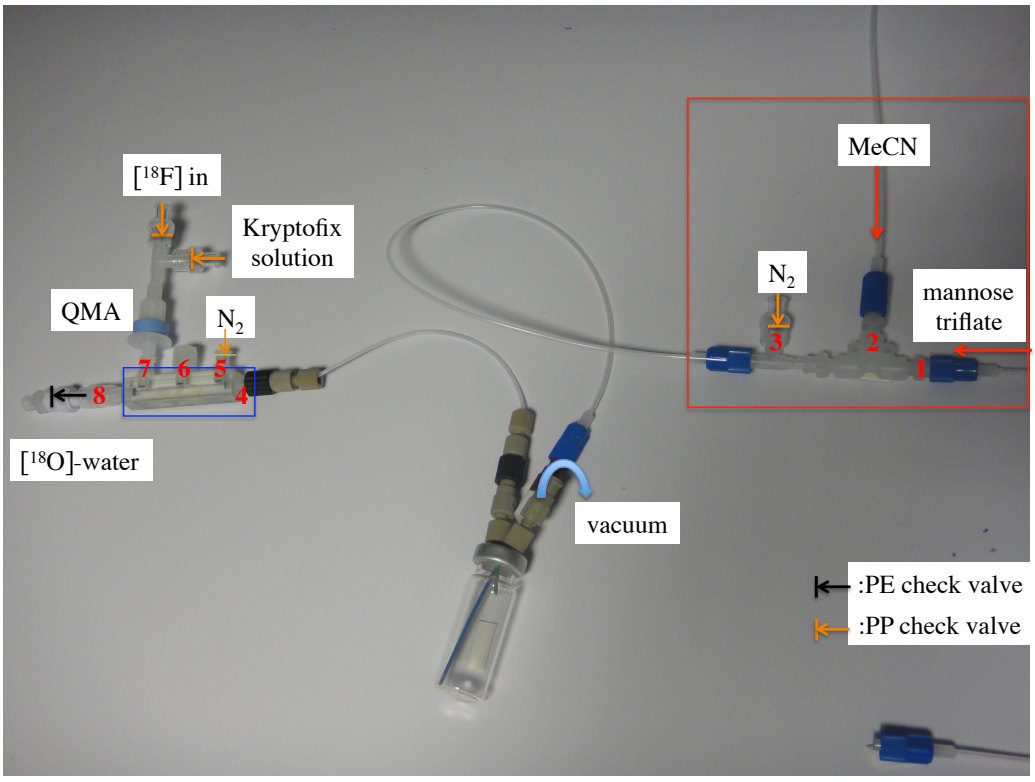

Figure 19: First try of radilabelling using fluidic components without valves.

The QMA cartridge was placed to the input 7 (see Figure 19) to ease the removal of [^{18}O]-water to the intersection 8. Nitrogen pressure was applied into the "F18 in" vial and at the input 5 to perform an efficient removal of water to the [^{18}O]-water waste vial. The transport of the $[K^+\subset 2.2.2]^{18}F^-$ complex to the reactor vial was performed by simultaneous nitrogen pressure, applied into the Kryptofix solution, and a reduced pressure used into the

reactor vial. The whole pressure of nitrogen was reduced to 1 bar (1.5 bar in Section 4.1) and a syringe filter (0.22 μm, Miller GV) was added to weaken the pressure of nitrogen applied into the Kryptofix vial to control the transfer of $[K^{+}\subset 2.2.2]^{18}F^{-}$ complex. Similar to the Section 4.1, nitrogen pressure was also added at the intersection 3 (see Figure 19) to avoid the elution of reagents such as mannose triflate solution and dry acetonitrile (outputs 1 and 2, Figure 19).

The temperature of each step was increased to improve the incorporation of [^{18}F]-fluoride. Therefore the removal solvents were evaporated for 10 minutes at 110 °C as maximum temperature. The labeling of mannose triflate was performed at 100 °C for 5 minutes. Both processes were under consecutive flow of nitrogen and reduced pressure or both. Afterwards the deprotection step was achieved at 40 °C for 1 minute.

Table 9: Experiment was performed with a 1-way cassette

entry	activity received (GBq)	process time (min)	recovery of activity, decay-corrected (%)	Radiochemical conversion (%)
18	1.5	109[a]	85	19
19	0.9	32	44	91

a) measurement of radioactivity.

The aim of this experiment was focused on the efficiency of the recovery of activity by monitoring the amount of activity present after the deprotection step under usual labeling conditions. The measurement was performed after the radioactivity decayed to a quarter of the initial value for safety concerns. The reactor vial was then introduced to the sleeve of the dose calibrator with the aid of long tweezers. The measurement of the radioactivity was also preformed for the cube, which presented traces of radioactivity. The cube seemed to be suitable for fluidic transfers and for not becoming contaminated with radioactivity.

The high recovery of activity (85%, see Table 9) led to the complete synthesis of [^{18}F]-FDG **1** with deprotection step (NaOH, 3 M, 5 mL). At the end of the process, the crude mixture was driven to the product vial (see Figure 21) to determine the radioactivity present inside the vial.

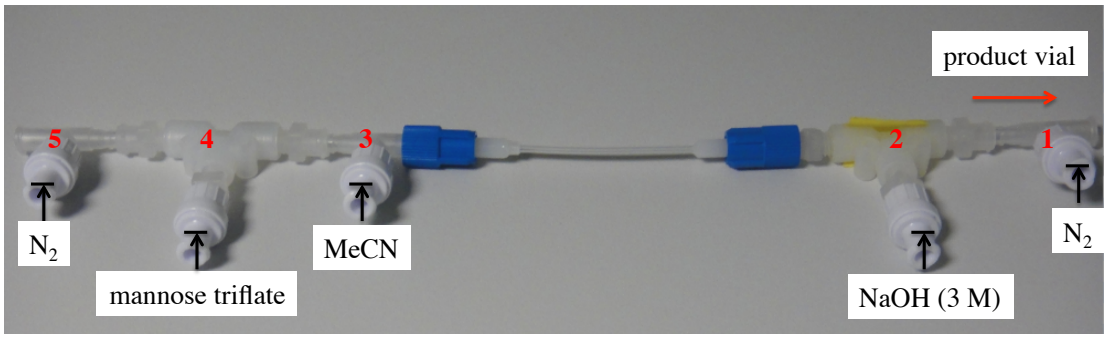

Figure 20: two Tefzel® tees used for [^{18}F]-FDG synthesis.

The setup was again minimised by the association of the two Tefzel® tees. This method provided the [^{18}F]-FDG **1** in 91% conversion (see Table 9). The quite low recovery of activity (44%) was explained with the presence of drops in the luer tees after transfer of the reaction mixture to the product vial and with the aqueous solution of NaOH and inside the IC-H cartridge (up to 35%, decay corrected).

The nitrogen flows at the edges of the two tees (input 1 and 5, Figure 20) were necessary to perform the synthesis. The nitrogen pressure (intersection 1, Figure 20) was used to guide fluidic transfers of reagents to the reactor vial and the second (intersection 5) to neutralise the negative pressure provided by the vacuum pump.

The next method limited again the number of luer tees by using only two of them. One on the top of the QMA cartridge and the other one connected to a low pressure Tefzel® cross (see Figure 21). Check valve for the reactor vial were placed to the reactor vial to improve the confinement of this vial.

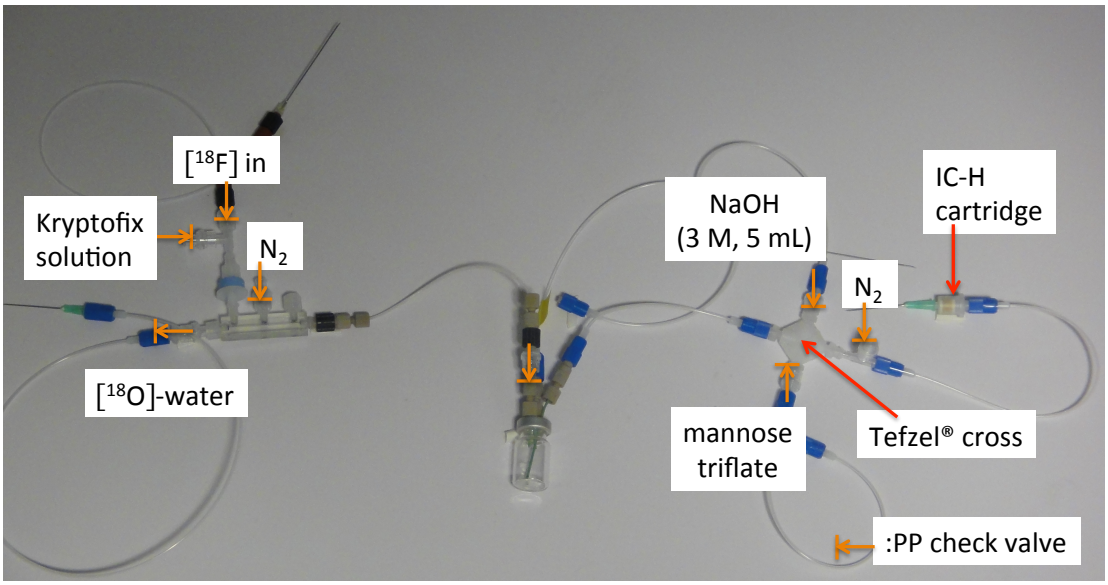

Figure 21: Reliable control of fluid sequences by using a Tefzel® cross.

The recovery of activity was again the parameter to focus on. Therefore no acetonitrile was used for the azeotropic distillation. The drying process still took 10 minutes at 110 °C as maximum temperature. Unfortunately the radioactivity present in the product vial was low (37% (see Table 10) instead of 85% in Table 9).

Table 10: Reaction achieved with a Tefzel® cross.

entry	activity received (GBq)	process time (min)	recovery of activity, decay-corrected (%)	Radiochemical conversion (%)
20	1.4	26	37	74

The residual radioactivity was mainly located in the IC-H cartridge (21%, ion exchange cartridge) and in the vacuum trap (vacu-guard 150, Whatman, UK). For this latter no value can be provided due to the size of the vacuum trap being larger than the sleeve of the dose calibrator. Nevertheless the removal of activity was observed with the activity sensor present inside the Peltier reactor module. The sensor was not calibrated and had no unit. However, the multiple reaction runs allowed the detection of an important loss of radioactivity when the sensor decreased by one unit. Before the addition of the solution of mannose triflate in acetonitrile (0.6 mL), the instrument indicated 15. After a series of vacuum and nitrogen flow at reasonable temperature (between 90 and 110 °C), the level dropped to 13-12 over the labeling process.

To sum up, the loss of radioactivity did not happen, or just a little, within the drying process but over the [^{18}F]-incorporation. A new procedure of labeling must be found to simultaneously minimise the loss of activity and enhance the percentage of [^{18}F]-incorporation. The check valve placed on the top of the reactor did not allow the transport of liquid from the reactor vial to the cube on the Peltier reactor module (see Figure 23) and so loss of radioactivity was avoided in this path.

4.3 Development of a semi-automated fluidic transfer by using two cubes

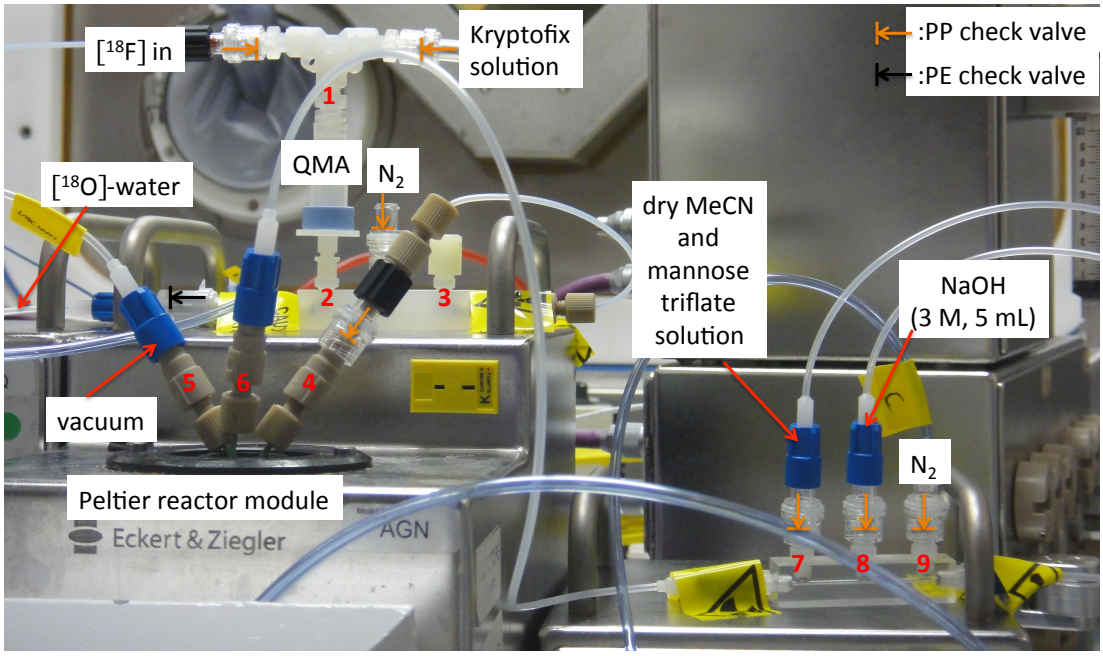

Figure 22: ModularLab platform for [^{18}F]-FDG synthesis using two plastic cubes.

The Tefzel® tee replaced the tee luer at the intersection 1 (see Figure 22) for the reasons mentioned previously (section 4.1 and 4.2). Under the QMA cartridge, the new cube constructed out of polypropylene (PP) with similar dimensions than the cube located at the right (TPX®, inputs 7 to 9). The program operating the synthesis was the same as in the previous setup (Section 4.2).

Table 11: Radiolabelling synthesis performed in a polypropylene vial.

entry	activity received (GBq)	process time (min)	recovery of activity, decay-corrected (%)	Radiochemical conversion (%)
21	1.2	29	20	26

However the glass vial was replaced by a flat bottom plastic vial (PP, 5 mL). The desired [^{18}F]-FDG **1** was obtained in 26% conversion (see Table 11). The difficulty was to reach the required temperature with plastic vial than glass vial due to a bad thermal conduction of the polypropylene. Plastic vial did still have some advantages. Its price (cheaper than glass vial) and had less affinity with fluoride ions. So removing the radioactivity with a minimum of solvent was easier (30 Bq left). A smaller flat bottom plastic vial (PP, 2.5 mL) was also used but the percentage of conversion was lower (6%). No explanation was found. The efficiency of the drying and radiolabelling in a small volume should provide better conversion.

An estimation of the amount of radioactivity present in each major part of the synthesiser, able to enter in the sleeve of the dose calibrator, was monitored (see Table 12). The delivery of the [^{18}F]-fluoride from the cyclotron into a vial instead of a straight delivery to the system was the reason of the first loss of activity (2.6%). The analyses were achieved without the precursor (mannose triflate **9**) and the ion exchange cartridge but with the same amount of solvents. Therefore 1 mL of dry acetonitrile (labeling process), 4 mL of NaOH (3 M) (hydrolysis) and 4 mL of water (washing reactor vial) were used to recover the activity inside the product vial. To obtain relevant results, flat bottom glass vial was chosen instead of a plastic one for their better thermal conduction.

Table 12: Investigation of the repartition of radioactivity.

location	recovery of activity, decay-corrected (%)
[^{18}F]-vial (from cyclotron)	100 (633 MBq)
QMA cartridge	96
product vial	42
QMA cartridge (after elution)	0.8
[^{18}F]-vial (after transfer)	2.6
reactor vial (glass, 5 mL)	4.8
vacuum pipe	0.4
[^{18}F]-waste vial	≈ 0
cube (PP) (end of synthesis)	0.6

The radioactivity of the QMA cartridge was determined before and after the elution of the captured [^{18}F]-fluoride. All the others parts were monitored at the end of the procedure.

In total only 51% of the radioactivity initially present inside the [^{18}F]-vial were found, which means 49% were lost inside the vacuum trap.

Therefore the majority of the solvents were evaporated at 95 °C as maximum temperature instead of 110 °C (see Section 4.2). However the drying process was performed in 11 minutes instead of 10 minutes (see Section 4.2) in the 5 mL plastic vial (PP). The nitrogen applied into the reactor vial over the drying process was introduced on the top of the vial (see Figure 22, intersection 9) and not by the longest tubing present in this one (see Figure 21). This modification allowed the reduction of the splattering over the drying process.

A mechanical valve was added between the reactor vial and the cube having the reagents such as mannose triflate solution and NaOH solution (see Figure 23). The objective was to heat the reactor vial, at the end of the azeotropic distillation, at 100 °C under reduced pressure only. As mentioned in Sections 4.1 and 4.2 the use of reduced pressure was always associated with a pressure of nitrogen to avoid the uncontrolled flow of the reagents to the system. The volume of the mannose triflate solution was reduced to 1.2 mL (instead of 1.5 mL) to minimise the loss of radioactivity by the evaporation of the acetonitrile solvent over the radiolabelling (97 °C for 5 minutes under negative pressure and nitrogen pressure).

Table 13: Procedures with nitrogen pipe connected directly to the reactor vial.

Entry	Activity received (GBq)	Process time (min)	Recovery of activity, decay-corrected (%)	Radiochemical conversion (%)
22	1.1	32	59	20
23	1.0	27	57	32

The low conversion (see Table 13) of the experiment 22 was explained by a loss of the mannose triflate solution within its transfer into the reactor vial. The reaction 23 was performed with no significant problems. The achievement at lower temperature for drying and labeling sequences in the plastic reactor vial (PP) performed reasonable recovery (59 and 57%) but low conversion (20 and 32%). Therefore maximum temperatures, for drying and labeling steps, were increased by around 10 degrees.

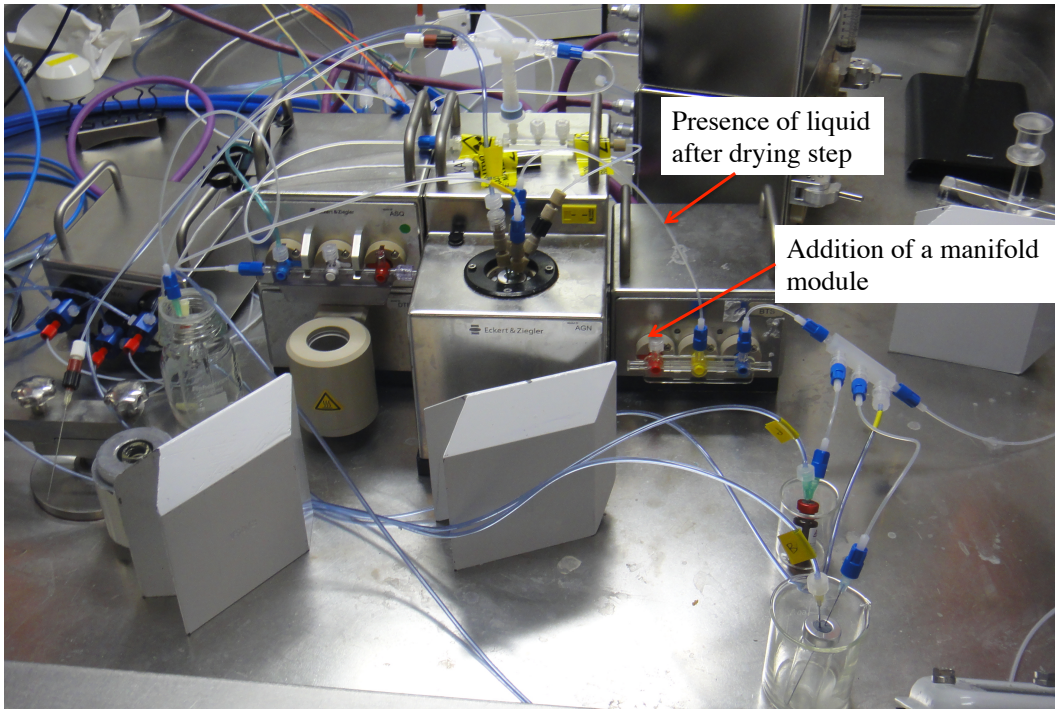

Figure 23: Final configuration for the production of [^{18}F]-FDG using the E&Z platform.

Table 14: Radiolabelling proceeded at 110 °C in 5 mL plastic vial.

Entry	Activity received (GBq)	Process time (min)	Recovery of activity, decay-corrected (%)	Radiochemical conversion (%)
24	1.2	28	35	72

Experiment 24 was focused on the loss of the radioactivity over the drying and radiolabelling process *via* the sensor present inside the Peltier module. After elution of $[K^+\subset 2.2.2]^{18}F^-$ complex, the activity collected inside the reactor was 11. Over the first part of the drying step (95 °C for 6 minutes) the value decreased to 8 due to the presence of liquid inside the tubing (see Figure 23). Then the dry acetonitrile (500 µL) used for the azeotropic distillation (110 °C for 5 minutes under consecutive nitrogen pressure and reduced pressure) rinsed this tubing and allowed the recovery of the initial value (11). The mannose triflate in 1.2 mL of dry acetonitrile was added into the reactor vial. The labeling process occurred at 105 °C as maximum temperature for 5 minutes under consecutive positive and negative pressure. The activity inside the reactor vessel decreased to 9. The deprotection step with a solution of NaOH (3 M, 4 mL) was performed at 55 °C for 1 minute with no change of radioactivity. The crude mixture was eluted through the IC-H cartridge and into the product vial. The IC-H cartridge trapped 21% of the radioactivity (decay corrected) and explained the low recovery of the activity (35%, Table 14). However in the product vial, 72% of the [^{18}F]-fluoride was incorporated to the mannose triflate **9** to form the desired [^{18}F]-FDG **1**. To avoid the trapping of the free [^{18}F]-fluoride by the IC-H cartridge, this one should react longer over the radiolabelling sequence.

Table 15: Reduction of the amount of MeCN for the azeotropic distillation and use of less water for the Kryptofix solution.

Entry	Activity received (GBq)	Process time (min)	Recovery of activity, decay-corrected (%)	Radiochemical conversion (%)
25	1.1	32	50	66
26	1.5	32	59	70
27	1.6	30	**59**	**79**
28[a]	0.9	29	54	**50**

a) radiosynthesis of [^{18}F]-FDG **1** without azeotropic distillation.

The experiments 25 to 28 were performed with a different Kryptofix solution. The concentration of water was reduced (17 instead of 50%, v/v). The solution was prepared with 4 mg of K_2CO_3 and 24 mg Kryptofix in dry acetonitrile (500 µL) and deionised water (100 µL). The drying process was performed in 7 minutes at 105 °C as maximum temperature under negative and positive pressure. The radiolabelling occurred with a 7 minute sequence heated at 105 °C. The deprotection step was achieved with a 3-minute sequence at 55 °C using a solution of NaOH (3 M, 4 mL). To obtain better recovery of activity 4 mL of distilled water was used to rinse the reactor vial and the IC-H cartridge. The recovery of activity was better than in the Table 13 with good radiochemical conversion (up to 79%, experiment 27). The difference of radiochemical conversion was achieved by shortening the time of the radiolabelling process for the experiment 25 (100 s). It was the same experiment for the reactions 26 and 27. The only explanation found was the use of the damaged Hamilton device, which leaked.

After replacement of the Hamilton device by a new one, a similar program was used but without the azeotropic distillation. The aim was to evaluate the efficiency of the drying process without the addition of dry acetonitrile. The experiment was performed in lower incorporation (50%, entry 28) than the reaction runs achieved in Table 15.

4.4 Two cube method with anhydrous Kryptofix solution.

4.4.1 Development of various anhydrous potassium salts to elute radioactivity from QMA cartridge

The presence of water in the Kryptofix solution is one of the main reasons of the time-consuming process of no-carrier-added [^{18}F]-fluoride incorporation. The azeotropic distillation generally requires a minimum time of 5 minutes.[10]

Attempts were carried out to understand the elution process in more detail. An aqueous solution of [^{18}F]-fluoride was eluted through a preconditioned QMA cartridge. The [^{18}F]-fluoride was trapped on the cartridge and the [^{18}O]-water was recovered in a beaker. Deionised water (1 mL) was manually injected through the cartridge by using a syringe. The activity sensor placed near the cartridge did not detect any change of radioactivity inside the ion exchange cartridge. After drying over airflow, a solution of Kryptofix [2.2.2] (24 mg, 63.7 µmol) dissolved in dry acetonitrile was added through the cartridge by using a syringe. The radioactivity inside the cartridge remained the same than before the transfer of the

Kryptofix mixture. A solution of K_2CO_3 (4 mg, 29 μmol) dissolved in 1 mL of deionised water was injected through the ion exchange cartridge. The [^{18}F]-fluoride ions were eluted from the cartridge into the beaker. The potassium carbonate salt is the active substrate able to remove the radioactive anions from the cartridge *via* anion exchanges ([^{18}F]-fluoride replaced by carbonate).

Therefore, several potassium salts dissolved in anhydrous solvents were investigated as replacement for the K_2CO_3 salt to elute the [^{18}F]-fluoride from the QMA cartridge (see Table 16).

The reactions took place in a plastic reactor vial and mannose triflate **9** was still dissolved in acetonitrile (1.1 mL).

Table 16: List of potassium salts used for fluoride-18 elution.

Entry	Salt	Solvent (μL)	elution of activity from the QMA cartridge
1	potassium sorbate	MeOH (825)	yes
2	potassium hexanoate	MeOH (825)	no
3	potassium acetate	MeOH (400)	partially
4	*trans*-4-hydroxy-L-proline potassium	MeOH (400)	no
5	K_2CO_3	MeOH (500)	yes

The potassium salts were prepared with the same method. Potassium hydride (30 wt % in dispersion oil) was added dropwise to a stirred solution of a carboxylic acid (1 g) in a dry solvent (diethylether) under an inert atmosphere. The resulting solid was filtered off and wash with 20 mL of petroleum ether (PE) and placed under vacuum overnight.

Dissolved in anhydrous methanol the potassium solutions (24 mg) were injected through a [^{18}F]-fluoride loaded QMA cartridge. The radioactivity sensor connected to the E&Z platform was placed near the cartridge to determine the level of radioactivity present inside the cartridge (see Scheme 18).

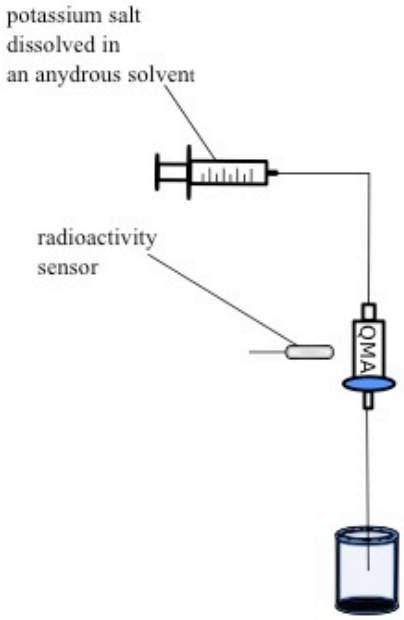

Scheme 18: Setup for elution of [^{18}F]-fluoride present in the QMA cartridge *via* potassium salts with radioactivity sensor connected to the E&Z kit.

Most of the synthesised salts did not remove the activity from the cartridge (see Table 16, entries 1 to 4). The sorbate salt (entry 1) was an exception. No explanation was provided but in comparison of the hexanoate and sorbate salts, the presence of a conjugated C–C double bonds system might allow the elution of the [^{18}F]-fluoride from the QMA cartridge. However sorbic acid and sorbate salts are toxic[85] so, it cannot be used for clinical studies.

The exploration of an anhydrous solvent able to dissolve the K_2CO_3 salt was investigated. Several dry solvents were used such as DMSO, DMF, ethanol, *i*-PrOH, 3-pentanol, triethylene glycol and methanol. The potassium carbonate salt was only soluble in methanol after 2 minutes in an ultrasonic bath.

The prepared Kryptofix solution (K[2.2.2] (24 mg, 63.7 μmol), K_2CO_3 (4 mg, 28.9 μmol) in anhydrous MeOH (600 μL)) passed through the [^{18}F]-loaded cartridge. The radioactivity was removed from the cartridge.

In conclusion, an anhydrous Kryptofix solution was used as an alternative to the commercial Kryptofix solution (ABX). Even if methanol is toxic, it can be removed at lower temperature (65 °C) than water and acetonitrile (100 and 82 °C, respectively).

4.4.2 Radiosynthesis in anhydrous Kryptofix solution

Table 17: Use of an anhydrous Kryptofix solution.

Entry	Activity received (GBq)	Process time (min)	Recovery of activity, decay-corrected (%)	Radiochemical conversion (%)
29	1.6	28	33	73
30	1.2	30	39	50
31	1.6	34	55	32

A new method was performed for the use of the anhydrous Kryptofix with a shorter drying process. The anhydrous Kryptofix solution (see Chapter 5) was prepared with K_2CO_3 (4 mg), K[2.2.2] (24 mg) and dry MeOH (600 µL). After elution of the Kryptofix solution, the $[K^+ \subset 2.2.2]^{18}F^-$ complex was flowed to the heated reactor vial (65 °C) with applied nitrogen pressure. That sequence was common to the three reactions (29 to 31). The drying process of the experiment 29 was performed at 105 °C for 160 seconds under nitrogen pressure and 220 seconds at 110 °C with both negative and positive pressure. The mannose triflate solution in dry acetonitrile (1 mL) was transferred in the heated reactor vessel (50 °C, reactions 29 to 30). The labeling process occurred at 105 °C under reduced pressure and nitrogen flow for 260 seconds. The basic solution of NaOH (3 M, 3 mL) was eluted to the reactor vial at 50 °C. The deprotection step was performed at 55 °C for 40 seconds. The reaction was eluted to the IC-H cartridge and then to the product vial (common step for reactions 29 to 31). The conversion to [^{18}F]-FDG **1** was high (73%) but the recovery of activity relatively low (33%). The radioactive sensor present inside the Peltier module detected a loss of activity over the radiolabelling sequence (15 to 8).

To obtain a better recovery of activity, the radiolabelling of reaction 30 was performed under milder conditions (95 instead of 110 °C) for a similar time (260 seconds). The drying process proceeded at the same temperature than in experiment 29 but over a longer period. The reactor vial was heated to 105 °C under nitrogen pressure for 180 seconds, and 160 seconds at 110 °C under consecutive negative and nitrogen pressure. The crude mixture in the product vial contained less [^{18}F]-FDG **1** (50% conversion) but the recovery of activity increased by 6% (39 instead of 33%).

The third experiment (31) proceeded with a drying step at 95 °C (160 seconds) and then at 105 °C (120 seconds) under negative pressure and nitrogen flow. The labeling process was similar than the reaction (29). The recovery was better (55 instead of 39%) but the labeling process was worse (32 instead of 50%). The 34-minute reaction time involved a leak

with the cube above the Peltier module after elution of the $[K^+\subset 2.2.2]^{18}F^-$ complex in the reactor vessel.

4.4.3 The anhydrous Kryptofix solution performed the formation of [^{18}F]-FDG **1** (see Radiosynthesis in anhydrous Kryptofix solution

Table 17). However the residual activity after elution of the Kryptofix solution was higher with MeOH than with a MeCN/water mixture (800 instead of 400 decay per seconds (dps)). It could be explained by the lower density of MeOH (d = 0.79) compared with water (d = 1). The dry Kryptofix solution might be transferred faster through the QMA cartridge than the aqueous mixture. The exchange between the carbonate anions and [^{18}F]-fluorides might not happen as much as in the aqueous Kryptofix solution leading to the loss of activity. The protocol using anhydrous Kryptofix solution stopped due to a possible nucleophilic attack of the methanol to the carbon of the mannose triflate **9** having the leaving group (—OTf).

4.5 Low concentration of water for Kryptofix solution

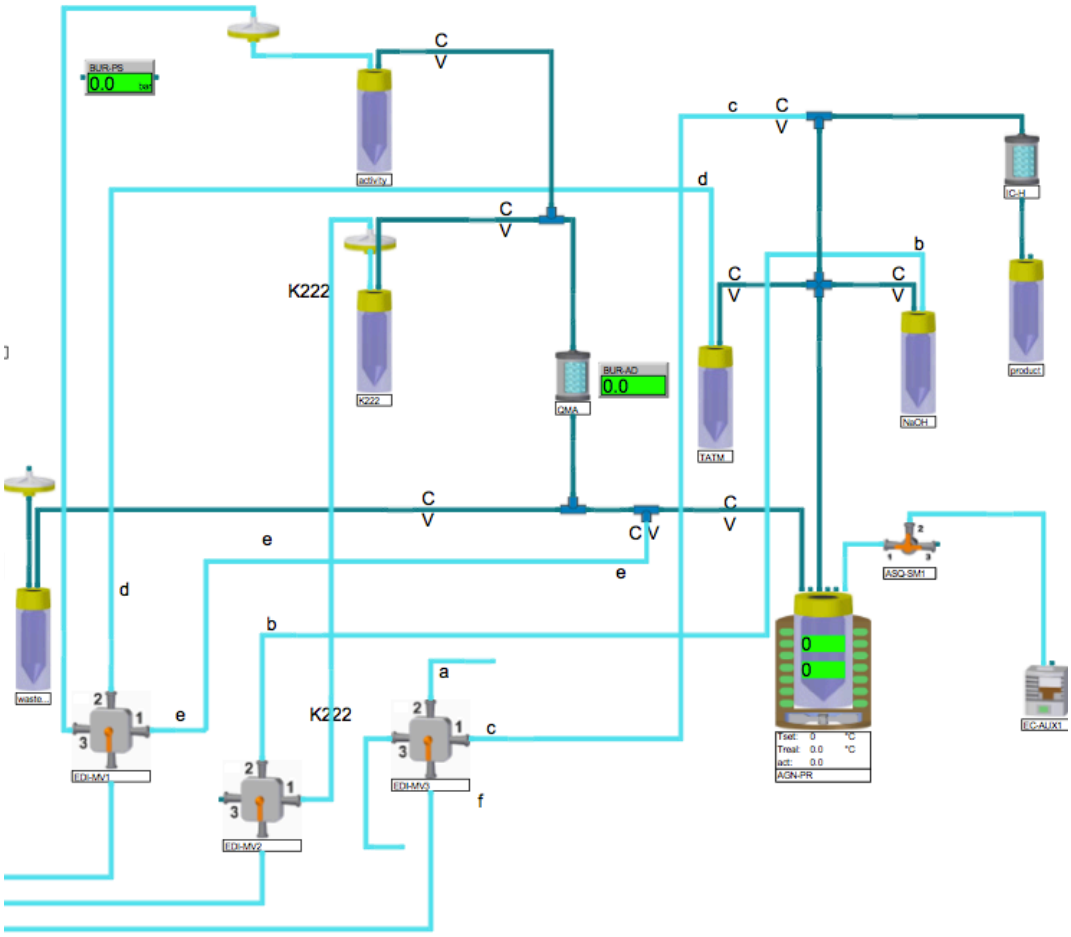

Figure 24: Semi-automated radiolabelling synthesis of [^{18}F]-FDG **1** by using low water concentration for Kryptofix solution.

The reactions of Table 18 were performed with 50 µL of distilled water and 450 µL of dry acetonitrile within the Kryptofix solution (in ABX solution: 300 µL of water, 300 µL of MeCN). The amount of the other reagents remained similar than in Section 4.4 (4 mg of K_2CO_3, 24 mg K[2.2.2]). The azeotropic distillation took place with 1 mL of dry acetonitrile.

Table 18: [^{18}F]-FDG synthesis prepared with 50 µL of water for the Kryptofix solution.

Entry	Activity received (GBq)	Process time (min)	Recovery of activity, decay-corrected (%)	Radiochemical conversion (%)
32	1.6	32	—	82

33	1.5	28	48	8
34	1.7	29	53	67
35	0.4	26	20	84
36	2.0	28	**56**	**77**
37	1.5	33	89	25

For experiment 32, the $[K^{+}\subset 2.2.2]^{18}F^{-}$ complex was transferred to the heated reactor vial (65 °C). The drying process started at 95 °C within 250 seconds under nitrogen flow. The azeotropic distillation occurred at 90 °C with the addition of 500 µL of dry acetonitrile under positive pressure for 15 seconds. The reaction mixture was heated to 105 °C under nitrogen pressure for 160 seconds. At 110 °C the vacuum was applied to the reaction mixture with nitrogen flow over 140 seconds.

The addition of the mannose triflate solution in 1 mL of acetonitrile was performed in the reactor vial heated to 50 °C. The labeling process started at 95 °C under nitrogen pressure for 160 seconds. The reactor vial was then heated to 105 °C for 140 seconds under nitrogen flow and reduced pressure.

At 55 °C, the aqueous solution of NaOH (3 M, 3 mL) was added to the reaction mixture. After 40 seconds, the reactor vial was emptied by transfer of the reaction mixture to the IC-H cartridge and then into the product vial (1 minute). A vial of 4 mL of deionised water replaced the empty vial of NaOH and water was transferred to the reactor vial to rinse this one and the IC-H cartridge (160 seconds).

The flows of nitrogen applied in position c and e (see Figure 24) within the hydrolysis, transported a part of the radioactivity to the vacuum trap. Therefore, the product vial was not monitored by the dose calibrator. Having a high conversion (82%) for the reaction 32, the next experiment (33) was followed the same protocol with the use of only one input of nitrogen pressure (c).

The reaction 35 afforded an unexpected low conversion (8%) but the new hydrolysis program using only one input of nitrogen pressure for the mixing was efficient. The radioactivity collected in the product vial was 48% (decay corrected). A loss of radioactivity was monitored in the Peltier reactor module over the radiolabelling process (24 to 17).

The experiment 36 was performed with the same method than the reaction 35. The results were rather different. The recovery of activity was relatively similar (53% for 36 and 48% for 35) but the incorporation was significantly different (67% for 36 and 8% for 35). No explanation was found. Nevertheless, the loss of activity over the labeling process was also noticed in the Peltier module for the reaction 36 (18 to 12).

The radiolabelling process for the reaction 37 commenced at 90 °C instead of 95 °C (reactions 34 to 36). The mannose triflate in acetonitrile (1 mL) was still transferred to the heated reactor vial (50 °C). The reactor vial was then heated to 90 °C for 1 minute under flow of nitrogen. The temperature increased by 5 °C for 100 seconds and by 10 degrees to 105 °C with both nitrogen flow and vacuum for an additional 100 seconds. Unfortunately two check valves leaked over the synthesis (F18 and mannose triflate). The conversion of [^{18}F-FDG] **1** in the product vial was monitored by radio-TLC (82%) but the recovery of activity was not analysed due to the leaks.

Reaction 38 was performed with a new program. In order to increase the conversion, the QMA cartridge was dried under nitrogen flow but also with 1 mL of acetonitrile.

The transfer of the aqueous [^{18}F]-fluoride present from the "F18 in" vial was performed under nitrogen flow for 1 minute. The pressure of nitrogen stopped and dry acetonitrile (1 mL) was added manually with a syringe into the "F18 in" vial. An additional 3 minutes of nitrogen flow was applied to the "F18 in" vial and at the intersection 3 (see Figure 21). The Kryptofix solution was eluted through the QMA cartridge to the reactor vessel heated to 65 °C for 30 seconds. The drying process started at 105 °C for 250 seconds under nitrogen pressure (intersection 3). The solution was cooled to 90 °C and 500 µL of acetonitrile were added for the azeotropic distillation (15 seconds). The reactor vial was heated to 110 °C for 160 seconds under reduced pressure and nitrogen flow. At the end of he drying process, the Peltier radioactive sensor detected a loss of activity of 4 units from the transfer of the $[K^+\subset 2.2.2]^{18}F^-$ complex into the reactor vial.

The radiolabelling process had also a loss of activity (2 units). This step commenced by heating the crude mixture at 90 °C for 1 minute under nitrogen flow and an additional 100 seconds at 95 °C. The labeling carried on at 105 °C for 100 seconds under vacuum and nitrogen pressure.

Cooled at 55 °C, the deprotection step carried out for 160 seconds by using NaOH solution (3 M, 3 mL) followed by distilled water (3 mL).

The radioactivity collected in the product vial was 59% and [^{18}F]-fluoride was incorporated to mannose triflate **9** in 77% conversion (Table 17, experiment 36).

The last reaction (37) had leaks with the cube connected to the reagents such as mannose triflate solution. Therefore the results (82% conversion, 25% recovery) cannot be compared with the experiments 35 and 36. Nevertheless, the drying and radiolabelling process provided loss of activity of 3 units.

The first reaction had no recovery because of the loss of the aqueous KOH solution with the radioactive reaction mixture within the vacuum trap. The pressure of nitrogen eluted the solution into the vacuum line and then to the trap.

The second attempt (33) had a similar program, except for the labeling process; only one check valve was placed differently. Instead of being attached to the TPX® cube, it was placed at the [^{18}O]-waste vial. The result was significantly lower.

The third experiment (34) had no obvious leaks or issues over the process. It offered a relatively good recovery of activity (53%) and practical [^{18}F]-incorporation (67%). By following the radio-detector inside the reactor module, the notable loss of activity was again recorded within the azeotropic distillation (2 at 70 to 95 °C and 2 more at 105 °C under vacuum).

Some changes were performed for the next experiment (35): a step at 80 °C for 1 minute was added to minimise the loss of activity and the QMA cartridge after [^{18}F]-trapping was washed with 1 mL of dry acetonitrile to remove the possible residual traces of [^{18}O]-water.

The recovery was increased and the [^{18}F]-incorporation also (56% and 77%, respectively, see Table 18).

The last experiment got a leak with the stopcock manifold over the synthesis, which explains the low recovery.

4.6 **Conclusion**

The intensive optimisation of the radiolabelling with 5 modules offered at the end (experiment 32 and 37) reasonable recovery (56%) and good [^{18}F]-incorporation (77%). The production of [^{18}F]-FDG was achieved with 5 modules instead of 8 for the microfluidic method (Chapter 3). Also the Hamilton device and the vacuum pump can be placed outside the hot cell. To our knowledge no synthesis of [^{18}F]-FDG **1** has been described was performed with only three mechanical valves. The efficiency of the cubes was crucial. They were not contaminated by the radioactivity and they can be produced by a workshop at different sizes and with any required number of inputs/outputs. The PP check valves were also important in the development of this technique. They blocked efficiently one direction under positive pressure and were resistant to acetonitrile.

Chapter 5: Exploration of cryptand [2.2.2] syntheses and polyethylene glycol derivatives

5 Exploration of cryptand [2.2.2] syntheses and polyethylene glycol derivatives

Described in chapter 1 as one of the pathways to perform the [^{18}F]-fluorination, Kryptofix [2.2.2] was used in this work for each radiolabelling process. This macro bicyclic phase transfer is generally synthesised over several days in low yields (see below). But there are commercial suppliers such as Merck Millipore (Germany), which sell this cryptand.

5.1 **Synthetic routes for Kryptofix [2.2.2]**

5.1.1 Multistep synthesis

The synthesis of Kryptofix [2.2.2] **20** was performed for the first time in 4 steps (see Scheme 19).[86, 87] The synthetic route was performed under high dilution conditions for several steps. The first cyclisation occurred in benzene (concentration of the diamine **15**: 0.045 M) by the nucleophilic reaction between the diamine **15** and the diacid chloride **16** (0.5 equiv, must be prepared[87]). The formed monocyclic aza-crown ether **17** was reduced by $LiAlH_4$ in THF (concentration of **16**: 0.1 M), to form the tetraoxadiamine macrocyclic compound **18** in 75% yield. Another equivalet of diacid chloride **16** was added to condense with the monocycle **17** in toluene (concentration: 9.10^{-3} M). Obtained in 45% yield, the bicyclic compound **18** was then reduced by borane agent (1 M in THF). The formed diamine borane derivative was then hydrolysed with HCl (6 M) under reflux to form the desired Kryptofix [2.2.2] in quantitative yield.

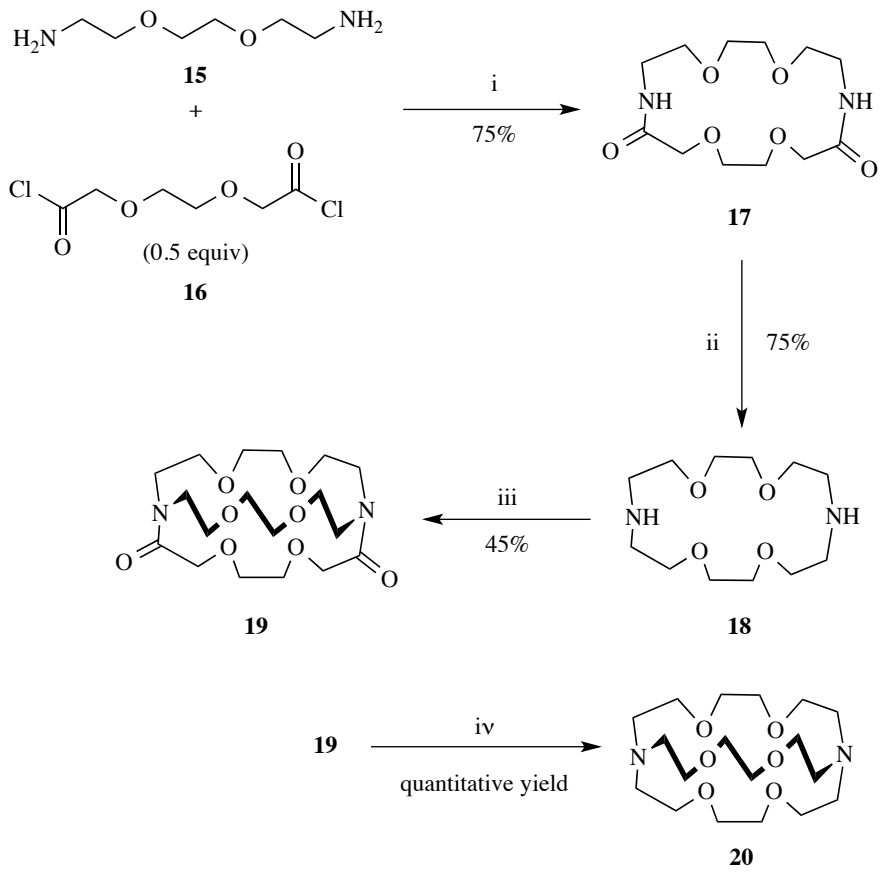

i. dry benzene, r.t., 8 h, 75%; **ii.** $LiAlH_4$ (6.7 equiv), dry THF, reflux, 24 h, 75%; **iii. 15** (1 equiv), TEA (2.2 equiv), dry toluene, r.t., 10 h, 45%; **iv.** step 1: BH_3•THF (4 equiv), dry THF, 0 °C→reflux, 2.5 h and step 2: HCl (6 M), reflux, quantitative yield.

Scheme 19: Multistep synthesis of Kryptofix [2.2.2] **20**.

This 4 step preparation provided the desired Kryptofix in 25% overall yield. The first optimisation was reported by Kulstad and Malmsten.[88] They provided the desired aza-crown ether **20** in one step as shown in Scheme 20.

5.1.2 One-step synthesis

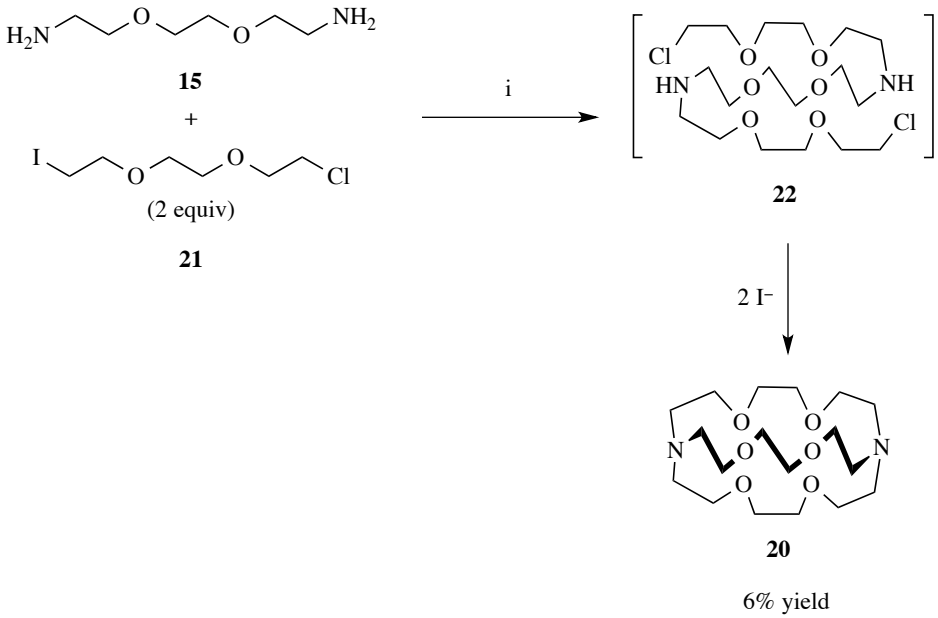

i. Na_2CO_3 (2 equiv), CH_3CN, reflux, 3 d, 6%.

Scheme 20: Direct synthesis of the bicyclic diaza-crown ether **20**.[88]

The nucleophilic attack of the diamine **15** to two equivalents of 1-chloro-2-(2-(2-iodoethoxy)ethoxy)ethane **21** (must be prepared[88]) formed the intermediate **21**. The halogen-halogen exchange permits the ring-closure and the formation of the Kryptofix [2.2.2] **20** in 6% yield. The driving force of the reaction is the presence of the iodide, a good leaving group (pka = –10 in water) and more reactive than the chlorine moiety (pka = –7 in water).

The same group (Kulstad and Malmsten) investigated under the same conditions the use of the 1,2-bis(2-iodoethoxy)ethane **23**. Kryptofix [2.2.2] **20** was not isolated, only the monocyclic 1,10-diaza-18-crown-6 was synthesised together with byproducts not described in the paper (see Scheme 21).[88]

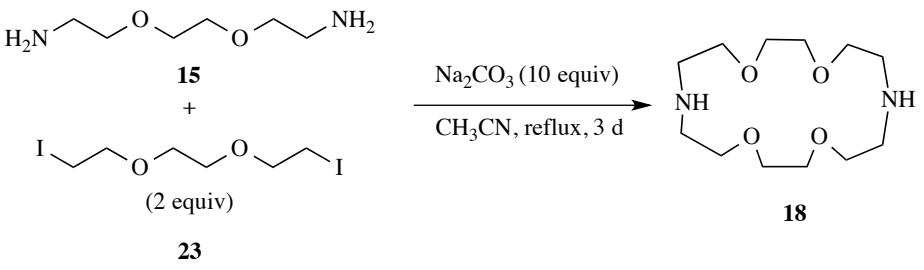

i. Na_2CO_3 (2 equiv), CH_3CN, reflux, 3 d, yield not mentioned.

Scheme 21: Monocyclic diaza-crown ether **18** formation from 1,2-bis(2-iodoethoxy)ethane **23.**[89]

A straightforward method for Kryptofix [2.2.2] **20** was reported by Krakowiak and co-workers 21 years ago.[90] The cryptand [2.2.2] was synthesised by using the ditosylate derivative of triethylene glycol and a large excess of a base (Na_2CO_3, 19 equiv) (see Scheme 22). The reaction mixture was refluxed for 6 days and then filtered at room temperature. The solid was dissolved in a stirred solution of dichloromethane. After filtration, the filtrate was concentrated and purified through an alumina column to remove the inorganic sodium salt coordinated by the ligand. The mixture was then chromatographed on silica gel column to isolate the final product **20** in 36% yield.

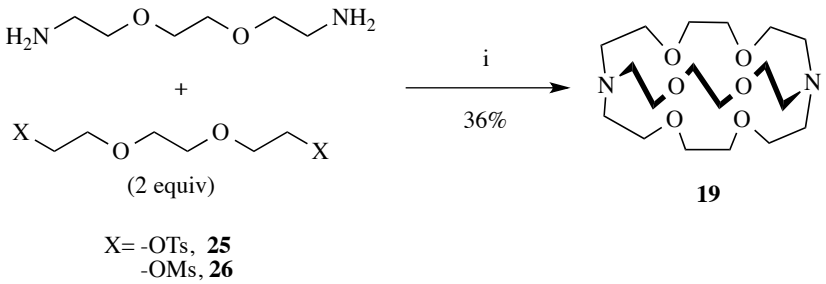

i. Na_2CO_3 (19 equiv), CH_3CN, reflux, 6 d, 36%.

Scheme 22: Reliable one-spot synthesis of Kryptofix [2.2.2] **19**.

The ditosylated triethylene glycol **25** is generally preferred to the dimesylated triehylene glycol **26** as it is commercially available. However, both glycol derivatives generate the Kryptofix [2.2.2] with a similar yield.

In conclusion, this method provided the Kryptofix [2.2.2] **19** in the highest yield (36%). Others advantages were the one step synthesis and the commercially availability of all reagents.

This reaction was performed in the laboratory. Unfortunately no significant product was collected at the end of the purification step (alumina and silica columns). The Kryptofix [2.2.2] synthesis could not be repeated. The requirement of a long reaction time (6 days) favored the purchase by suppliers.

However the ditosylate was synthesised successfully by using two methods (see Scheme 23).

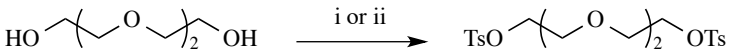

24 **25**

i. TsCl (2 equiv), KOH (4.3 equiv), THF/water (20/7, v/v), 0 °C→r.t., 4 h, 43%; ii. TsCl (3 equiv), TEA (3 equiv), DMAP (5 mol%), CH_2Cl_2, overnight, 87%.

Scheme 23: Preparation of the ditosylate triethylene glycol **25**.

The first method had the advantage of a 4 hour reaction time but suffered from low yield (43%).[91] This route was proposed for the synthesis of ditosylates tetraethylene and pentaethylene glycols and offered 35% and 96% yield, respectively. The second procedure[92] was catalysed by a nucleophilic base (DMAP) and produced the desired product **25** in 87% yield (lit. 88%).

An alternative synthesis of the monocycle **18** was explored to perform the synthesis of Kryptofix [2.2.2] **20**. The procedure started with the condensation of the previous diamine with [2-(2-oxo-ethoxy)-ethoxy]-acetaldehyde **27** with the diamine **15** to form the monocycle **18** after reduction (see Scheme 24).

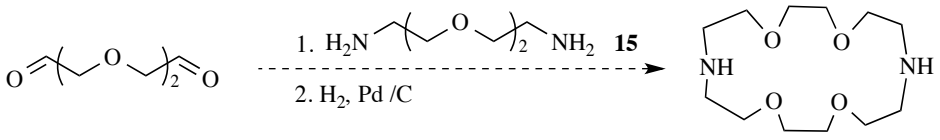

27 **18**

Scheme 24: Route to the aza-crown ether **18** from the dialdehyde **27**.

The triethylene glycol was oxidised[93] with a catalytic amount of 2,2,6,6-tetramethylpiperidine-*N*-oxide **28** (TEMPO) and trichloroisocyanuric acid **29** (TCCA, 2 equiv) as a a co-oxidant following the mechanism shown in Scheme 25[94]. After 20 minutes, the reaction mixture was filtered through Celite and the solvent was removed under *vacuo*. The product was analysed by ^{1}H NMR but no aldehyde signal could be identified. To avoid any polymerisation, the solution must be kept in a solution of water (20 mL) with traces of trifluoroacetic acid. The reaction was repeated and the diamine was added just after the filtration, but no monocycle **18** was observed in ^{1}H NMR.

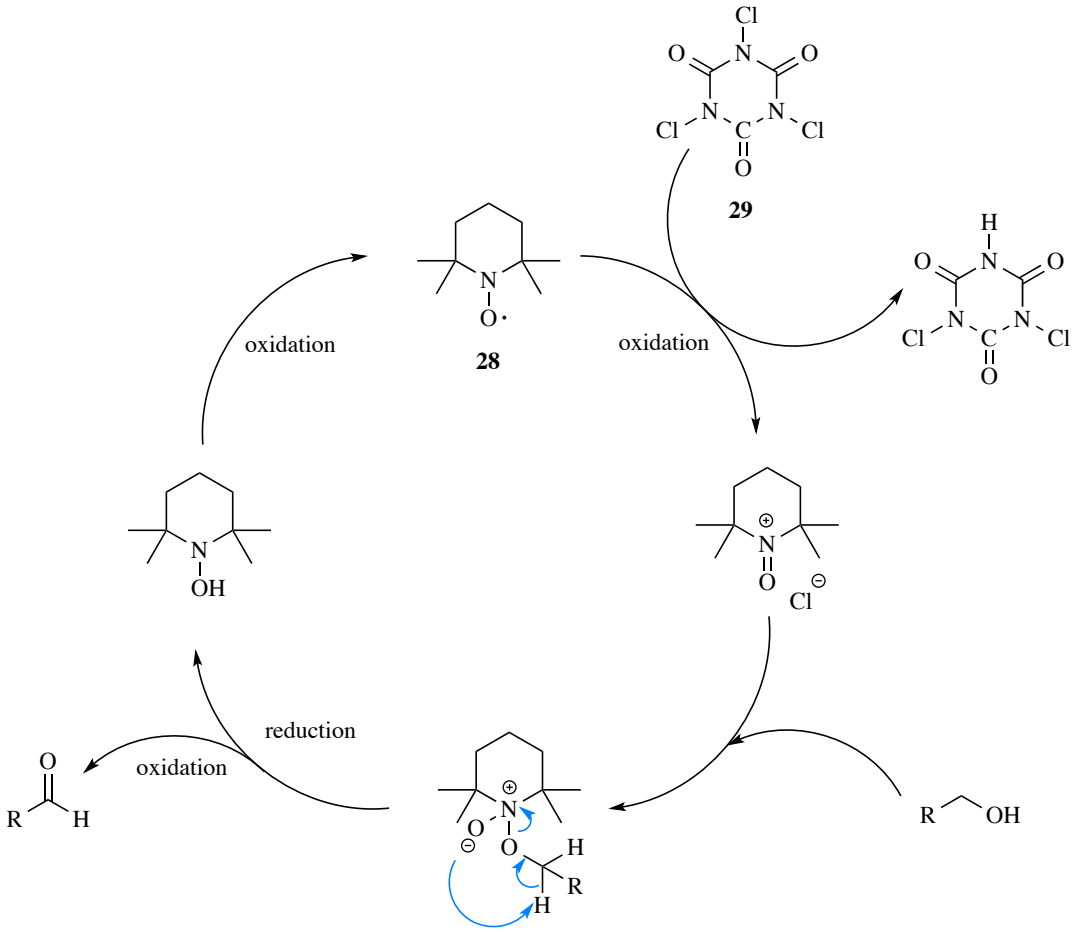

Scheme 25: Proposal mechanism for TEMPO-catalysed alcohol oxidation to corresponding aldehyde.

5.2 Investigation into protection of triethylene glycol

The interest of triethylene glycol derivatives was not limited to the synthesis of the Kryptofix [2.2.2]. The preparation of florbetaben **7** also required the incorporation of a triethylene glycol chain as shown in Scheme 26.

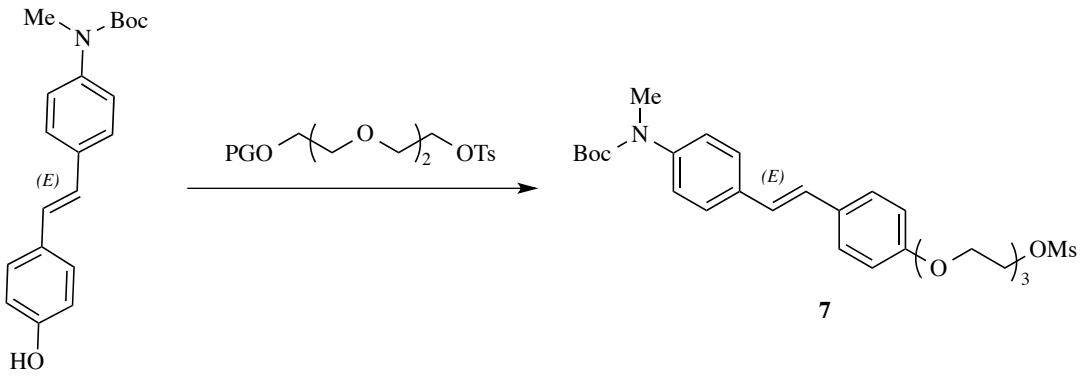

Scheme 26: Incorporation of monotosylated side chain to Florbetaben precursor **7**.

Following the work on Kryptofix [2.2.2], the tosylate group seems to be the most reliable leaving group, more efficient than halogens. The other protecting group (PG) should have some characteristics such as resistance to basic media and, being able to deprotect under mild conditions e. g. a benzyl group.[95]

5.2.1 Preparation of monobenzylated and monotosylated triethylene glycol

The selective protection of only one of the two hydroxyl groups was performed by the addition of benzyl moiety.[91] To a stirred solution of triethylene glycol (4 equiv) in a basic medium (NaOH, 50%, 4 equiv), one equivalent of benzyl chloride was added and the reaction mixture was stirred under reflux for 20 hours (see Scheme 27). The crude mixture was not distillated with Kugelrohr, as mentioned in the reference, but just placed under vacuum to remove the solvents and triethylene glycol. The next step was carried out at 0 °C in the same flask, with addition of TsCl (1.5 equiv) and KOH (3.3 equiv) in 1.6 mL of water. The reaction was heated to room temperature over two hours and quenched with a saturated solution of ammonium chloride. After extraction and dried over Na_2SO_4, the residue was purified by flash chromatography to yield the glycol **31** in 40% yield over two steps (lit. 60%[91]).

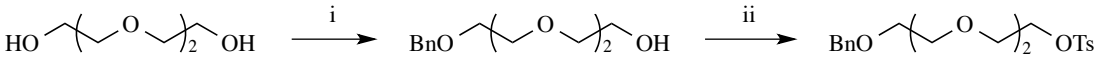

24 **30** **31**

i. BnCl (1 equiv), NaOH (4 equiv), H_2O, reflux, 20 h; **ii.** TsCl (1.5 equiv), KOH (3.3 equiv), H_2O, 0 °C→r.t., 2 h, 40% overall yield.

Scheme 27: Selective protection of the monobenzylated and monotosylated glycol **31**.

Despite an excess of base and triethylene glycol for the first step, the reaction, which was followed by TLC, did not offer significant results, even under reflux (40% overall yield).

5.2.2 Preparation of monosilylated triethylene glycol

Tert-butyldimetylsilyl moiety is a possible protecting group resistant to basic conditions, with a deprotection commonly carried out under mild conditions *via* a fluoride agent such as TBAF.[95, 96] Two relatively similar methods have been described in the literature, one provided by Zhang *et al.*[40] (catalysed) and another one performed by Jose *et al.*[97] (non-catalysed) (see Scheme 28).

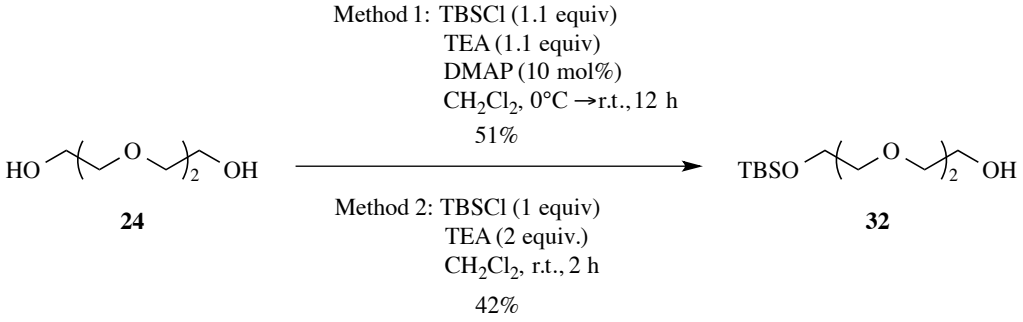

Scheme 28: Reported procedure for monosilylated triethylene glycol **32**.

These two reactions afforded the monosilylated glycol **32** in 51 and 42% yield (see Scheme 28). An alternative synthetic route was found to prepare the monotosylated and silylated glycol in better yield.

5.2.3 Preparation of monotosylated and silylated triethylene glycol

To our knowledge no mechanism was suggested for this reaction, only an intermediate was proposed. [98, 99] The coordination of the triethylene glycol around the silver cation, acting as a Lewis acid, increases the lability of the hydrogen especially the one not involved in the intramolecular bonding (see Scheme 29). The effect is proportionally stronger to the number of oxygen atoms chelating the silver cation. The reaction is not performed under basic conditions but with the use of a catalytic amount of potassium iodide, which accelerates the sulfonylation. Following the reaction,[100] the monotosylated triethylene glycol was prepared in dichloromethane (HPLC grade). The yield dropped significantly to 60% instead of 95% in the literature with distilled dichloromethane. An attempt was performed by

simply degas the dichloromethane (HPLC grade) over 10 minutes before to commence the reaction. It is possible than the molecules of oxygen present inside the dichloromethane might interfere with the silver oxide reagent. The monosulfonylation was afforded in 90% yield.

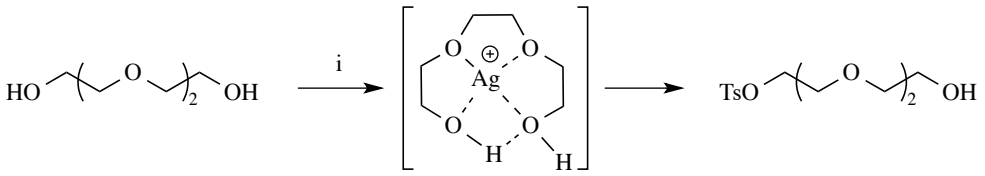

24 **33** **34**

i. KI (0.1 equiv), Ag_2O (1.2 equiv), TsCl (1 equiv), Ar, degassed CH_2Cl_2, r.t., overnight, 90%.

Scheme 29: Selective silver oxide mediated monosulfonylation.

Afterwards, the silylated group was incorporated based on the strategy of Zhang and co-workers[40] (see Scheme 30).

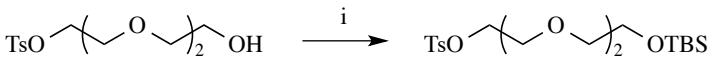

34 **35**

i. TBSCl (1.2 equiv), TEA (1.2 equiv), DMAP (1 mol%), CH_2Cl_2, 0 °C→r.t., overnight, 82%.

Scheme 30: Formation of the side chain for florbetaben precursor **7**.

The tosylated and silylated triethylene glycol **35** was obtained in 74% overall yield. In the literature,[97] the same molecule was synthesised by Jose and co-workers in 48% yield.

5.3 **Conclusion**

The different routes used to provide the Kryptofix [2.2.2] promoted the tosylate moiety as a suitable leaving group for a nucleophilic reaction into triethylene glycol derivative. Two bis-protected triethylene glycol were prepared (**31** and **35**) for the synthesis of the florbetaben precursor **7**. The second (**35**) was obtained in high yield (74%) and will be used in section 7.3.2 with 4-nitro-4'-hydroxystilbene. The benzylated and tosylated glycol **31** will be not used for two reasons. Its formation was performed in lower yield than the tosylated and silylated glycol **35** (40% vs 74% yield). The deprotection of benzyl chloride is

commonly achieved with palladium on charcoal and hydrogen gas, which can reduce the C–C double bond present in the stilbene.

Chapter 6: Synthetic attempts to synthesise the Florbetaben precursor

6 Synthetic attempts to synthesise the Florbetaben precursor

6.1 Florbetaben: a possible β-amyloid PET tracer for Alzheimer desease.

Alzheimer's disease (AD) is a neurodegenrative disease, which gradually worsens over time[101]. Its causative agents have not been yet well estblished. Nevertheless, the abondant number of β-amyloid (Aβ) peptide aggregates and highly phosphorilated tau proteins identified post-mortem in the patient brain could be cytotoxic to the neuronal cells and could indirectly lead to the dementia[102]. An early non-invasive diagnosis of AD could be established by monitoring the progression of theses aggregates. Imaging PET tracers targetting Aβ plaques have been developped based on histological amyloid staining agents such as Congo red, Thioflavin T and on styryl groups[103]. One of the PET tracers is the florbetaben **8**, which can be binding with Aβ aggregates as shown in Figure 25.

.

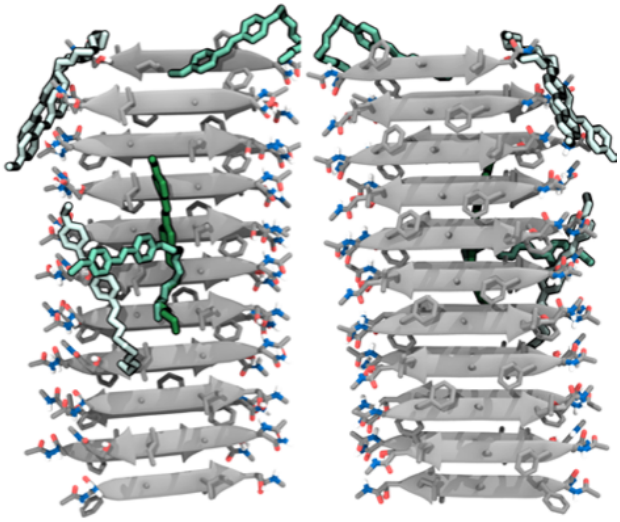

Figure 25: Representative stuctures of the florbetaben cluster binded to the β-amyloid aggregated (grey arrows). The PET tracer has been colored following the free energies calculated for the tracer, light green (lower) and dark green (higher). The left picture is a view of the top layer and the right picture of the bottom layer. The atoms of oxygen, nitrogen and hydrogen at the edge of the β-proteins are shown in red, blue and white, respectively.

6.2 Synthesis of stilbene 7 as precursor for Florbetaben 8, a potential β-amyloid PET tracer

To our knowledge, only a few papers have described the preparation of the polyethylene glycol stilbene **7**. The first steps were reported by Ono and co-workers (see Scheme 31).[104] The nitro stilbene **37** was obtained *via* the Horner-Emmons-Wadsworth (HEW) reaction[105] by coupling the phosphonate **36** with *p*-anisaldehyde. Prior to this coupling, the nitro organophosphorus was synthesised following the Arbuzov reaction.[106] The advantage of using these conditions, compared to the Wittig reaction, was the synthesis of the *E*-isomer without formation of the *Z*-isomer. The nitro moiety was then reduced to the amine by a large excess of tin chloride (6 equiv). The *N*-monomethylation was performed *via* reductive amination of formaldehyde. The last step was the removal of the *O*-methyl group to form the corresponding phenol **40**.

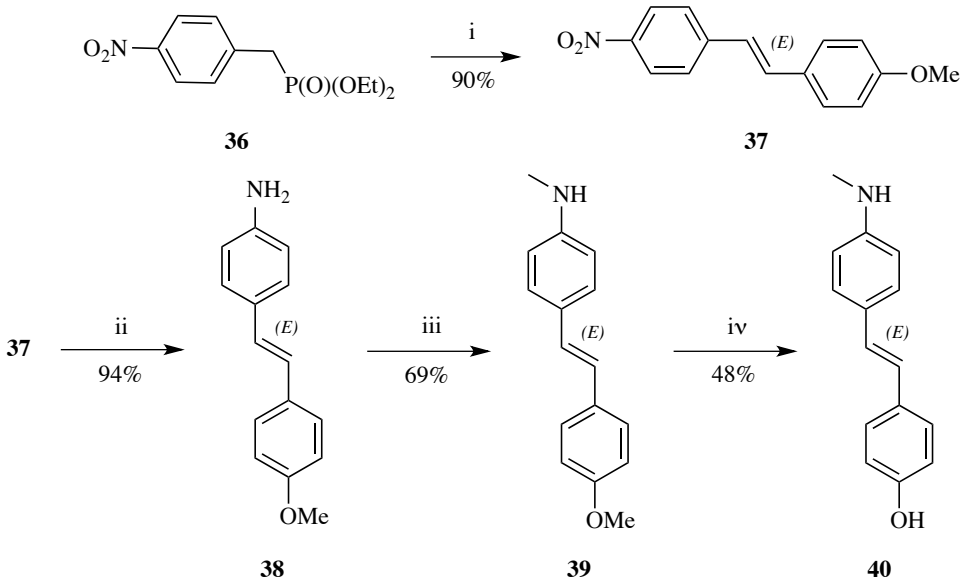

i. *p*-anisaldehyde (1 equiv.), NaOMe (25% w/w in methanol), reflux, 16 h, 90%; **ii.** $SnCl_2$ (6 equiv), EtOH, 70 °C, 2 h, 94%; **iii.** step 1: $(CH_2O)_n$ (1.4 equiv), NaOMe (25% w/w in methanol), MeOH, 0 °C and step 2: $NaBH_4$ (1.5 equiv), reflux, 1 h, 69%; **iv.** BBr_3 (10 equiv), CH_2Cl_2, -78 °C→ r.t., overnight, 48%.

Scheme 31: Synthesis of (*E*)-4-methylamino-4'-hydroxystilbene **40**.

The other route provided the (*E*)-2-(2-(2-(4-(4-((*tert*-butoxycarbonyl)(methyl)amino)styryl)phenoxy)ethoxy)ethoxy)ethyl methanesulfonate **7** by incorporating the triethylene glycol chain and by the replacement of protected groups (see Scheme 32). This sequence was achieved by Zhang and co-workers.[40] To perform the ether linkage, the commercially available 2-(2-(2-chloroethoxy)ethoxy)ethan-1-ol was coupled with stilbene **40** to form stilbene **41**. The hydroxyl moiety was silylated (step ii) and the amine protected with a Boc group (step iii). Fluorine agent (TBAF) allowed the replacement of the TBS group by a mesylate (iv and v). The presence of the mesylate or tosylate will permit an efficient incorporation of the [^{18}F]-fluoride and the absence of silicon atom will not contaminate the labeling by bonding to the fluoride-18.

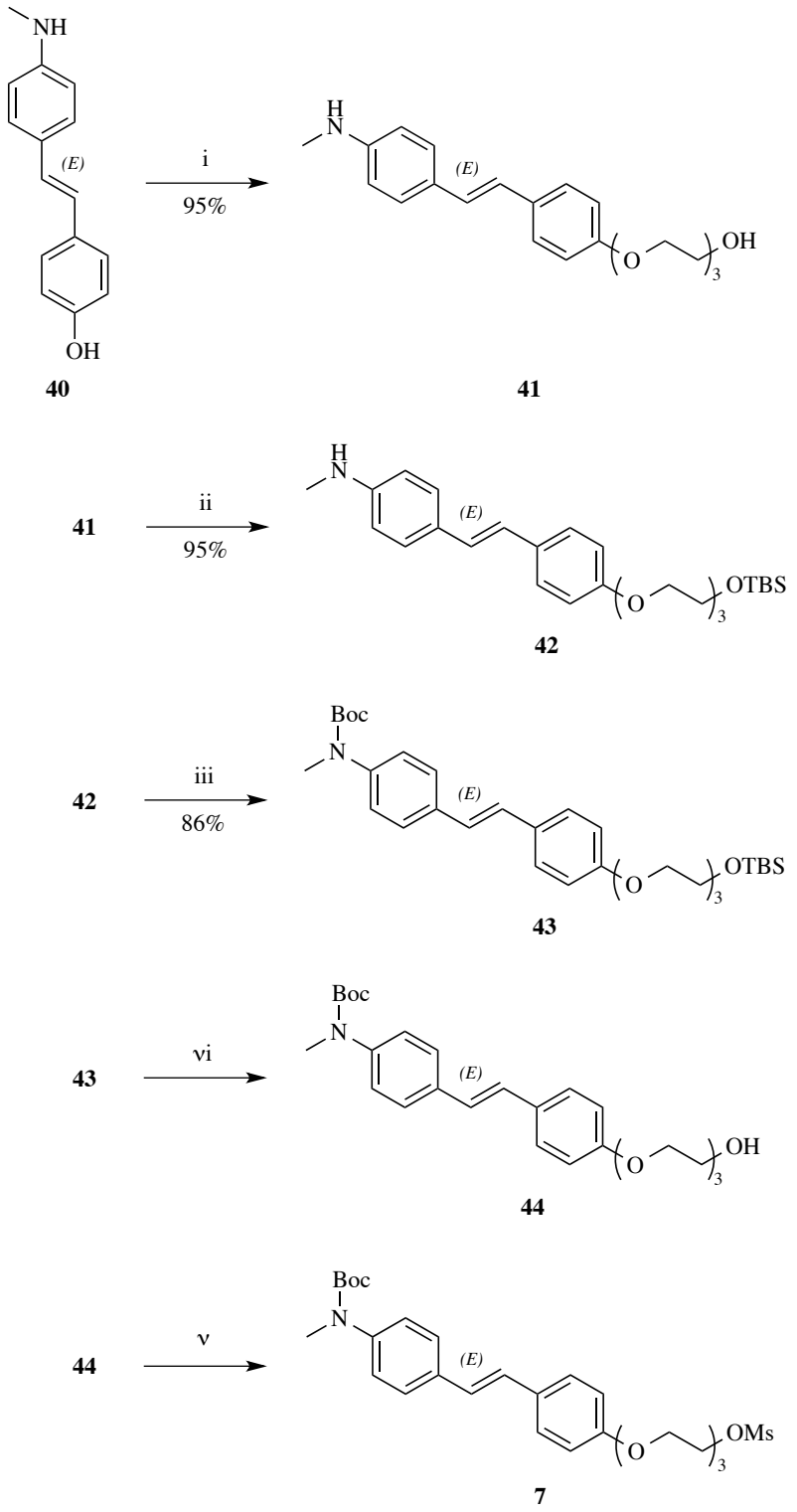

86% over two steps

i. 2-(2-(2-chloroethoxy)ethoxy)ethan-1-ol (1.3 equiv), K_2CO_3 (5 equiv), dry DMF, 100 °C, overnight, 95%; **ii.** TBSCl (1.5 equiv), imidazole (2 equiv), CH_2Cl_2, r.t., 2 h, 95%; **iii.** $(Boc)_2O$ (1.9 equiv), dry THF, N_2, reflux, overnight, 86%; **iv.** TBAF (2 equiv), THF, r.t., 2; **v.** MsCl (3 equiv), TEA (4.9 equiv), CH_2Cl_2, r.t., 4 h, 86% over two steps.

Scheme 32: Synthetic route for preparation of **7** from 4-methylamino-4'-hydroxy stilbene **40**.

To sum up, the stilbene **7** was prepared in 9 steps with an overall yield of 19%. The aim of this chapter will be to identify other routes to perform the desired precursor of Florbetaben **7**. The different key steps were the formation of the stilbene (C-C double bond), the reduction of nitro group, the monomethylation, the deprotection of the *O*-methyl and the incorporation of the polyethoxy chain. The new route should reduce the number of steps and improve the overall yield.

6.3 **Formation of C-C bond for stilbene synthesis**

6.3.1 The Wittig reaction

A well known method for the formation of C-C double bond is the Wittig reaction as shown in Scheme 33. The coupling between a phosphorus ylide and an aldehyde or a ketone generates an olefin and a phosphine oxide (driving force of the reaction). The stereoselectivity of the reaction is dependent of the substituent and can perform *E* and/or *Z* isomers.

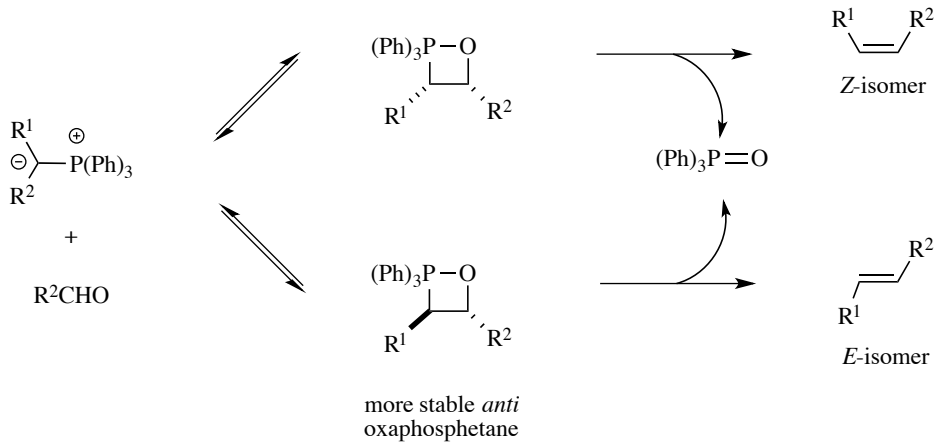

Scheme 33: Basic mechanism of the Wittig reaction.

The phosphorus ylide is generally prepared by using a base and phosphonium salt. The salt is obtained by the nucleophilic attack of a phosphine on an alkyl halide, in this case a benzyl halide. Triphenylphosphine is the most common phosphine used for this reaction.

The (4-nitrobenzyl)triphenylphosphonium bromide, shown in Scheme 34, was isolated in 88% yield after filtration and washing with acetone.[107]

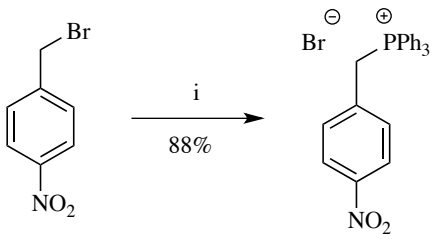

45 **46**

i. PPh_3 (2 equiv), toluene, 40 °C, overnight, 88%.

Scheme 34: Synthesis of (4-nitrobenzyl)triphenylphosphonium bromide **46**.

Various aldehydes were coupled with the phosphonium salt **46**. The first one was prepared as shown in Scheme 35, the others were commercially available such as *p*-anisaldehyde or benzaldehyde. The diversity of these aldehydes permits to determine the reactivity of the nitro phosphonium salt **46** for the Wittig reaction. The acetyl moiety replaced the methyl to ease and increase the yield of the deprotection step.

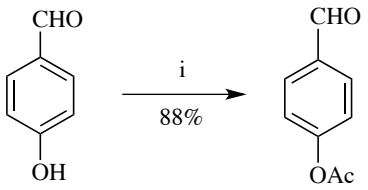

47 **48**

i. AcCl (1.5 equiv), TEA (1.5 equiv), dry CH_2Cl_2, Ar, 1.25 h, 88%.

Scheme 35: Acetylation of 4-hydroxybenzaldehyde **47**.

Despite several conditions the formation of the stilbene in a practical yield failed (see Scheme 36). The crude mixtures were monitored by ^1H NMR to confirm the presence of the stilbene and the aldehyde.

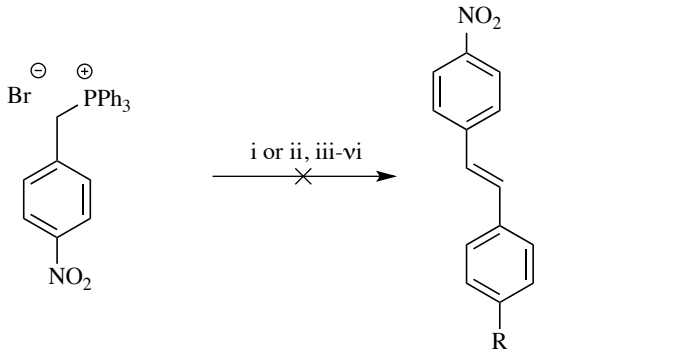

46

i. *n*-BuLi (2.5 M in hexane, 2 equiv), **46** (1 equiv), dry toluene, Ar, r.t.→ 80 °C, overnight; **ii.** *n*-BuLi (2.5 M in hexane, 2 equiv), **46** (1 equiv), dry toluene, Ar, -20 °C→r.t., overnight; **iii.** *n*-BuLi (2.5 M in hexane, 1.1 equiv), benzaldehyde (1.1 equiv), dry THF, -50 °C→r.t., overnight; **iv.** *n*-BuLi (2.5 M in hexane, 2 equiv), *p*-anisaldehyde (1 equiv), dry toluene, Ar, r.t., overnight; **v.** NaOMe (2 equiv), *p*-anisaldehyde (1 equiv), MeOH, r.t.; **vi.** ^{t}BuOK (1.1 equiv), *p*-anisaldehyde (0.8 equiv), dry THF, 0 °C→r.t., overnight.

Scheme 36: The Wittig reactions performed with (4-nitrobenzyl)triphenylphosphonium bromide **46**.

n-BuLi was added dropwise at different temperatures and stirred for 30 minutes before adding the aldehyde. The change of color from yellow to red might be characteristic of the formation of the ylide **49**. Nevertheless, none of the reactions succeeded in synthesising the stilbene. The nitro group placed in *para* position may interfere in the reactivity of the ylide **49** due its conjugate form **50** (see Scheme 37).

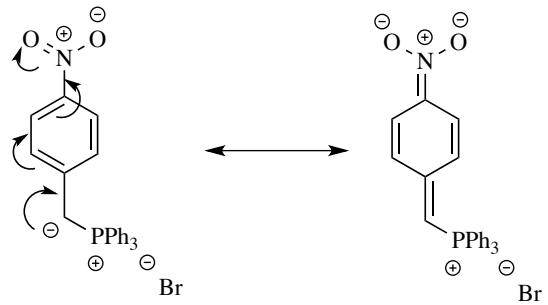

49 **50**

Scheme 37: Possible conjugate form of the ylide made from **46** and the addition of a base.

Therefore, another organophosphorus compound was prepared to form the desired stilbene. It was obtained in three steps in 77% overall yield (see Scheme 38). *p*-Anisaldehyde was reduced with $LiAlH_4$ (94% yield) in dry Et_2O. After workup,

dichloromethane was added in the crude mixture and placed in the dark. The brominating agent (PBr_3) formed the benzyl bromide **52** in 96% yield.[108] The formation of the phosphonium salt **53** with triphenylphosphine occurred quickly after isolation of the halide **52** to avoid any degradation of the starting material due to exposure to the light.

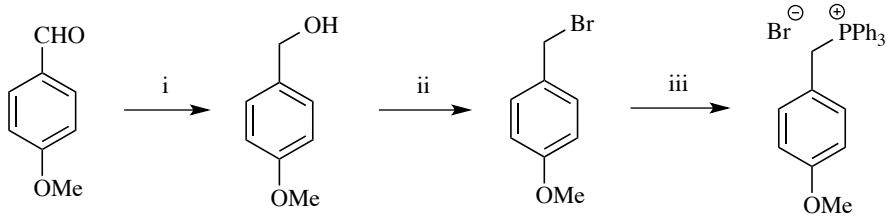

51 **52** **53**

i. $LiAlH_4$ (1 equiv), dry Et_2O, Ar, 0 °C→r.t., 2 h, 94%; **ii.** PBr_3 (1 equiv), CH_2Cl_2, in the dark, r.t., 3 h, 96%; **iii.** PPh_3 (1 equiv), toluene, reflux, overnight, 86%.

Scheme 38: Preparation of (4-methoxybenzyl)triphenylphosphonium bromide **53**.

The triphenylphosphonium salt **53** was then used with 4-nitrobenzaldehyde to form an olefin as shown in Scheme 39.

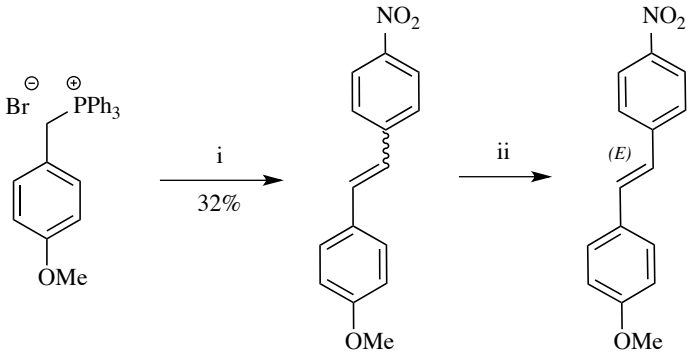

53 **37**

30% over 2 steps

i. ^{t}BuOK (1.3 equiv), *p*-nitrobenzaldehyde (0.9 equiv), dry THF, Ar, r.t., mixture of *E*/*Z* (32%, 14:1); **ii.** I_2 (1 bead), heptane, reflux, 12 h, *E*-isomer (30% over 2 steps).

Scheme 39: Formation of (*E*)-4-nitro-4'-methoxystilbene **37**.

The mixture of *E*/*Z*-isomers was isolated with success after purification by flash chromatography. The pure *E*-isomer was obtained by isomerisation of the *Z*-isomer by using a catalytic amount of iodine in heptane under reflux.[109] After removal of iodine with a saturated aqueous solution of sodium bisulfite the stilbene **37** was collected in 30% yield.

An alternative procedure to form only the *E*-isomer was to reflux the Wittig reaction in CH_2Cl_2. The solution was concentrated under reduced pressure and the residual mixture was purified by filtration in methanol at low temperature (–40 °C). The pure product **37** was obtained as a yellow powder in 16% yield (see Scheme 40).

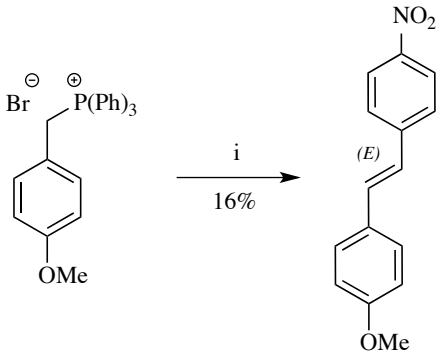

53 **37**

i. *p*-nitrobenzaldehyde (0.9 equiv), K_2CO_3 (2.3 equiv), dry CH_2Cl_2, reflux, overnight, 16%.

Scheme 40: The Wittig reaction under reflux to synthesize the *E*-isomer of the stilbene **37**.

The compound **37** was synthesised but in low yield (16%). However it was the same stilbene than Ono and co-coworkers.[104] A different reaction and/or different substrate should permit the synthesis of a more suitable stilbene.

Therefore, a precursor for the Heck reaction (styrene **54**), shown in section 7.2.2, was prepared from the Wittig reaction to form the C—C double bond (see Scheme 41).

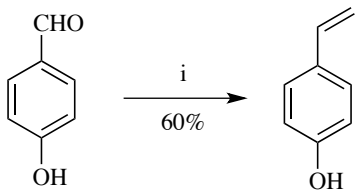

47 **54**

i. ^{t}BuOK (2.5 equiv), $MePPh_3Br$ (1.5 equiv), dry THF, N_2, 0 °C→r.t., 4 h, 60%.

Scheme 41: Synthesis of 4-vinylphenol **54**.

Obtaining a 60% yield for the Wittig reaction with the presence of a labile hydrogen, nitro phosphonium was involved again for the C–C coupling but with 4-hydroxy benzaldehyde. The method[110] was carried out in dry CH_2Cl_2 under reflux with a weak base

(K_2CO_3), instead of strong base such as ^{t}BuOK used previously in Scheme 39. The reaction mixture was purified by flash chromatography to yield the desired *E*-stilbene **55** in 82% yield as shown in Scheme 42.

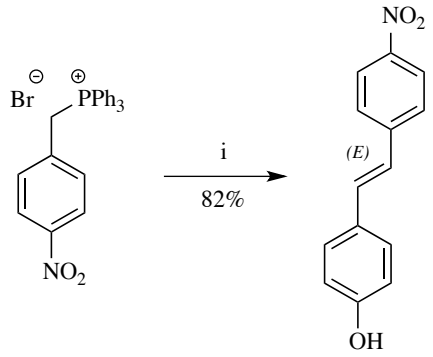

46 **55**

i. 4-hydroxybenzaldehyde (0.8 equiv), K_2CO_3 (4 equiv), dry CH_2Cl_2, Ar, reflux, overnight, 82%.

Scheme 42: Formation of 4-nitro-4'-hydroxystilbene **55**.

In conclusion, after an intensive experimentation to perform a stilbene *via* the Wittig reaction, two stilbenes were synthesised (**37** and **55**). The product **55** formed in high yield (82%) has the advantage of not having a methoxy moiety and so not requiring its deprotection as a further step.

The exploration of phosphonates to perform the HEW reaction was abandoned due to the difficulty to separate the desired phosphonate from the triethyl phosphite. Even though 4-aminobenzylphosphonate was commercially available, its coupling with *p*-anisaldehyde in methanol did not offer the desired stilbene.

6.3.2 Investigation of the stilbene formation *via* the Heck reaction

Based on catalysed C–C bond coupling, Heck, Suzuki and Negishi were awarded the Nobel Prize in 2010.[111] The Heck reaction generates a more highly substituted alkene from an aryl/vinyl halide or triflate coupled with an olefin.

The catalytic cycle occurred by the formation of the Pd^0 by incorporation of monophosphine ligands (L type). The oxidative addition of the aryl halide generates Pd^{II} complex, which can then incorporate the olefin and form the C_{sp3}–C_{sp3} bond. Depending on the orientation of the alkene attached to the palladium complex, the insertion of the aryl group can be achieved at two different positions and so forms two different products (see Scheme 43). After C–C rotation, the *syn* β-hydride elimination occurred and products were

released from the palladium complex. The base, usually TEA, regenerates the Pd^0 and the catalyst can carry on another catalytic cycle. The number of cycles (turn over) performed by the same catalyst can involve more than 150 000 cycles.

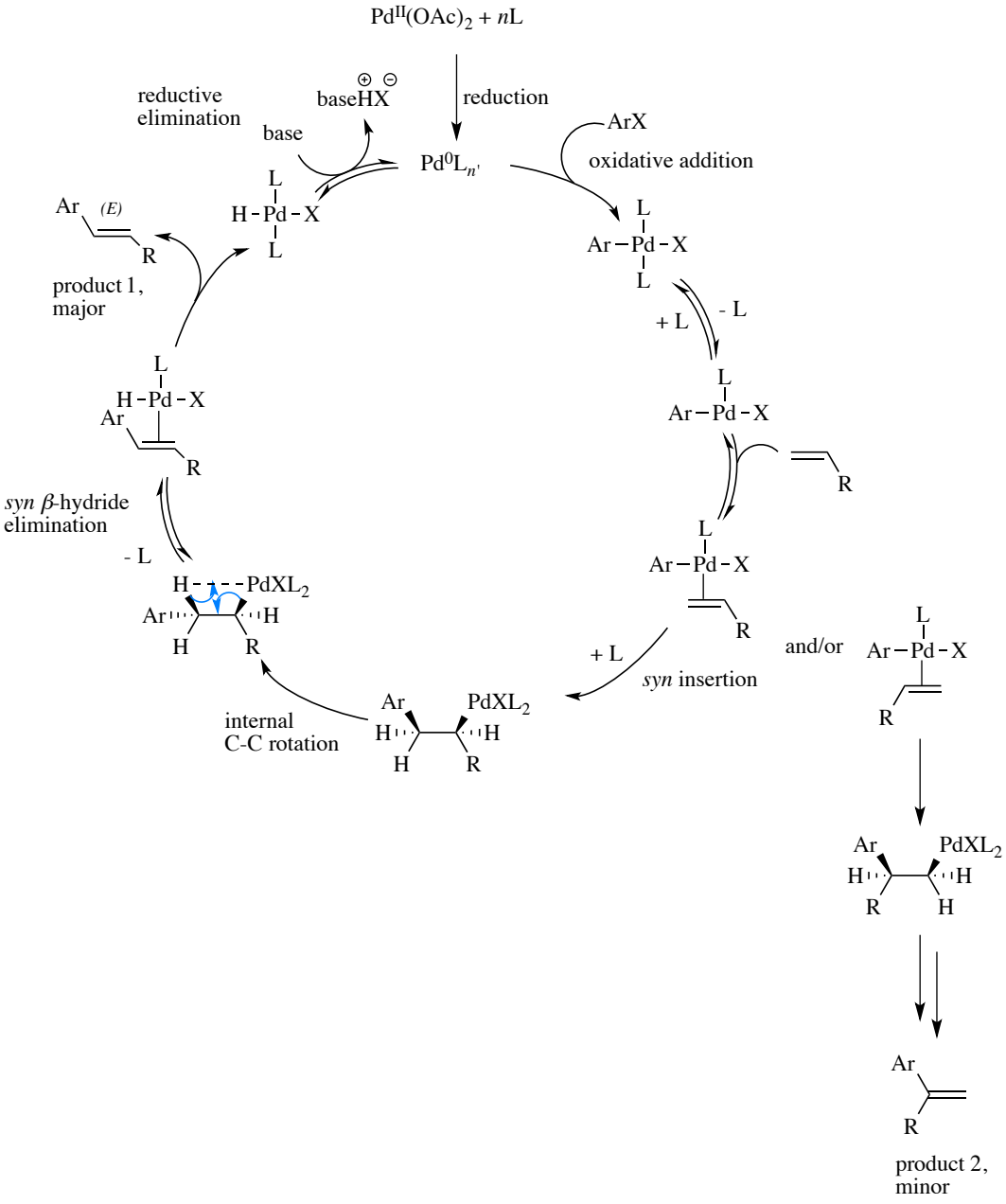

Scheme 43: Mechanism of the Heck reaction performed with monophosphine ligands.[112]

Presented in Scheme 44, the Heck reaction was performed with 4-methoxystyrene and two aryl iodides (4-amino-iodo-benzene and 4-nitro-iodo-benzene). Unfortunately none of the reactions worked, only starting materials were recovered.

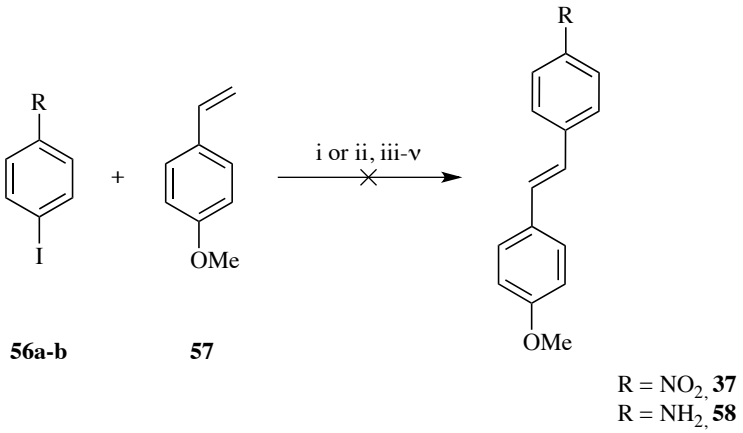

i. (R= NH_2) 4-iodoaniline **56a** (1 equiv), 4-methoxystyrene (2 equiv), $Pd(OAc)_2$ (7 mol%), TEA (63 equiv), PPh_3 (1 equiv), Cu (9 mol%), Ar, dry THF, r.t.→80 °C, overnight; **ii.** same procedure at r.t.; **iii.** (R= NH_2) 4-iodoaniline **56a** (1 equiv), 4-methoxystyrene (2 equiv),), $Pd(OAc)_2$ (7 mol%), K_2CO_3 (2 equiv), TEA (6 equiv PPh_3 (1 equiv), **iv.** (R= NO_2) 1-iodo-4-nitrobenzene **56b** (1 equiv), 4-methoxystyrene (1.3 equiv), $Pd(OAc)_2$ (3 mol%), TEA (2.3 equiv), PPh_3 (7 mol%), **v.** (R= NO_2) 1-iodo-4-nitrobenzene **56b** (1 equiv), 4-methoxystyrene (1.3 equiv), $Pd(OAc)_2$ (3 mol%), TEA (63 equiv), PPh_3 (7 mol%).

Scheme 44: Exploration of the Heck reaction to form amino stilbene **58** or nitro stilbene **37**.

Recently reported, stilbenes can be synthesised *via* a tandem reaction Heck/decarboxylation/Heck (see Scheme 45).[113]

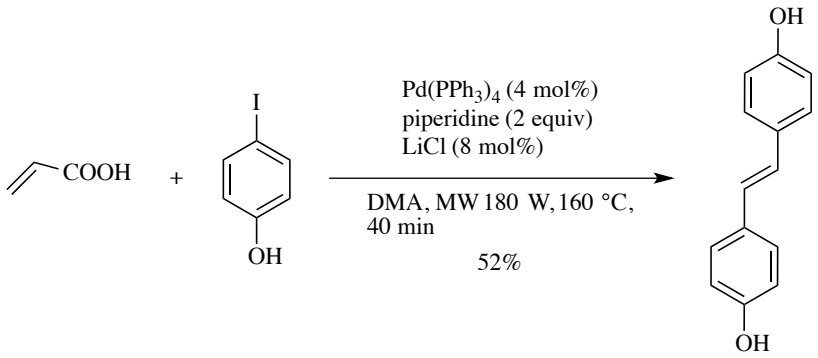

Scheme 45: Formation of stilbenes by using the palladium-catalysed Heck reaction.

To our knowledge, no method was reported to synthesise 4-nitro or 4-amino 4'-hydroxystilbenes by using the Heck reaction, this reaction was abandoned.

6.3.3 Synthesis of the 4-nitro-4'-hydroxystilbene *via* the Knoevenagel reaction

The expansion of scope for stilbene formation continued with the Knoevenagel condensation as shown in Scheme 46. The selectivity of this reaction induced by the *trans*-elimination, forms the *E*-isomer.

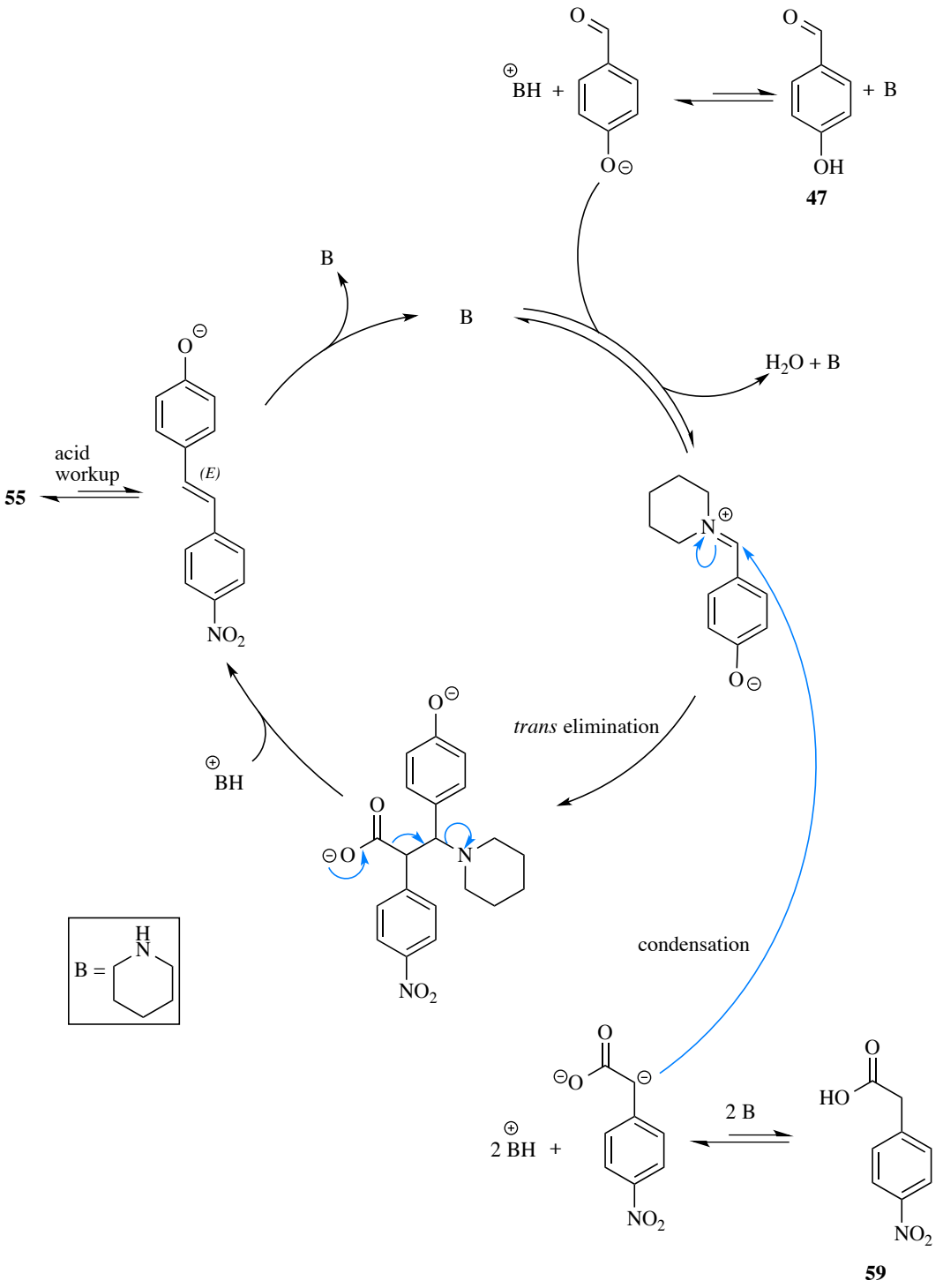

Scheme 46: Mechanism for stilbene **55** synthesis via a Knoevenagel reaction.

The advantages of this method were the use of commercially available reagents (4-hydroxybenzaldehyde and (4-nitrophenyl) acetic acid). Therefore, no preparation of starting materials was required for this procedure. As with the Wittig reaction, the synthesis of 4-nitro-4'hydroxystilbene avoided the deprotection with BBr_3 leading to low yield (48%). The pure stilbene was isolated in reasonable scale (up to 2 grams) after filtration and recrystallisation. Purification by flash chromatography was not required for this synthesis.

4-Nitro-4'-hydroxy stilbene **55** was prepared in 72% yield (lit. 75%) by following the work of Diemer *et al.* (see Scheme 47, step i).[114] The workup involved the addition of H_2O/EtOH (3:1) with glacial acetic acid (0.1 mL) under reflux. The reaction mixture was then filtered and recrystallised in ^{i}PrOH to give the pure product **55**.

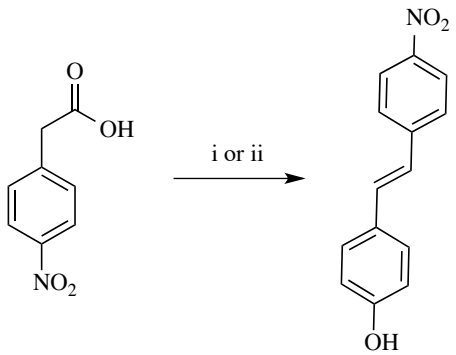

59 **55**

i. 4-hydroxybenzaldehyde (0.7 equiv), piperidine (1 mL), Ar, 140 °C, 1 h, 72%; **ii.** 4-hydroxybenzaldehyde (1 equiv), piperidine (1 equiv), vacuum, 100 →150 °C, 3 h, 85%.

Scheme 47: Formation of 4-nitro-4'-hydroxystilbene **55** following two different methods.

An alternative procedure (see Scheme 47, step ii), proposed by Vangala and co-workers, produced the stilbene **55** in 85% yield (lit. 90%).[115] The reaction was performed under *vacuo* instead of under an inert atmosphere. Heated to 100 °C for 1 hour, the reaction was then heated to higher temperature than the Diemer method for 2 hours (150 °C). The workup was carried out with an aqueous solution of NaOH (6 M) and the mixture heated to 60 °C for 30 minutes. Afterwards a concentrated solution of HCl (36%) was added at room temperature to neutralise the reaction. The pure product **55** was collected after filtration.

The difference between these methods was that the stilbene **55** was obtained in two different colors, brown for Diemer method and yellow for Vangala procedure.

Achieving the stilbene **55** in high yields, this method was expanded to the formation the 4-nitro-4'-methoxystilbene **37**. Described in the literature with low yield

(34%)[116] *via* the Knoevenagel reaction, the synthesis was proceeded following the Vangala's method (see Scheme 44).

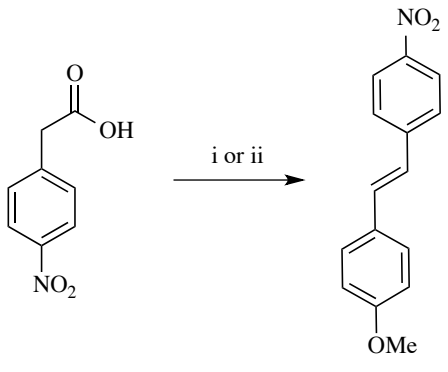

59 **37**

i. *p*-anisaldehyde (1 equiv), piperidine (1 equiv), vacuum, 100 →150 °C, 3 h, 34%; **ii.** *p*-anisaldehyde (1 equiv), piperidine (1 equiv), pyridine (1 equiv), vacuum, 100 →150 °C, 3 h, 52%.

Scheme 48: Formation of the methoxy stilbene **37** by the Knoevenagel reaction.

The first experiment offered the same yield (34%) than the work of Barnwell[116] but the addition of one equivalent of another base, pyridine, increased the yield to 52%. Comparing with the HWE reaction carried out by Ono and co-workers,[104] the experiment in Scheme 48 offered lower yield of 38% difference.

6.3.4 Investigation into 4-hydroxybenzaldehyde

Prior to incorporate the triethylene chain with the 4-nitro-4'-hydroxy-stilbene **55**, commercially available 4-hydroxybenzaldehyde was reacted with the 2-(2-(2-chloroethoxy)ethoxy)ethan-1-ol (see Scheme 49) to develop a suitable method for connecting the three ethoxy glycol derivatives to a phenol.

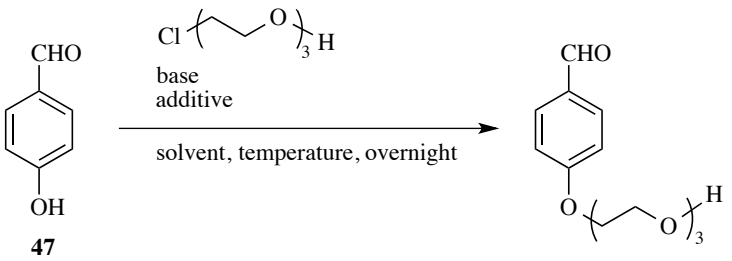

Entry	Ether chain Equivalent	Base (equiv)	Additive (equiv)	Solvent	Temperature (° C)	Presence of product
1[117]	3.5	K_2CO_3 (3.5)	_	DMF	100	yes[a]
2[118]	1	K_2CO_3 (3)	KI (3)	DMF[b]	120	yes[a]
3	1	K_2CO_3 (3)	KI (3)	toluene	100	no
4	1	imidazole (3)	TBAI (3)	MeCN	reflux	no
5	1	DBU (2)	DMAP (2)	toluene	100	no
6	1	K_2CO_3 (2)	MS[c]	acetone	reflux	no
7	1.1	K_2CO_3 (2.2)	KI (cat.)	EtOH	reflux	37%

a. The ^{1}H NMR identified the desired product but the pure product was not obtain after filtration and flash chromatography; b. the reaction was proceeded under inert atmosphere; c. molecular sieves (MS) 4 Å

Scheme 49: Exploration of several condition reactions of a phenol on chloro-triethylene alcohol.

The experiments revealed the need of a potassium base for the nucleophilic attack of the phenol derivative. The use of strong base (DBU) or nucleophilic base such as imidazole and DMAP did not perform S_N2 reaction. The 4-hydroxybenzaldehyde was identified by ^{1}H NMR after each failed reactions without the presence of the desired product. Polar solvents such as DMF or EtOH seemed to promote the reaction. Toluene and acetonitrile, which were used for the Kryptofix [2.2.2] synthesis, did not allow the reaction to take place.

An alternative method for the incorporation of the triethylene glycol was performed by using the Mitsunobu reaction. The synthesis was carried out for 2 days and offered the desired product in 41% yield as shown in Scheme 50.

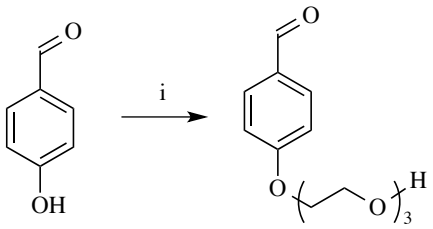

49

i. triethylene glycol (5 equiv), PPh_3 (1 equiv), DIAD (1.1 equiv), CH_2Cl_2, 0 °C→r.t., 2 days, 41%.

Scheme 50: Incorporation of the triethylene chain *via* the Mitsunobu reaction.

6.3.5 Investigation into 4-nitro-4'-hydroxystilbene **55**

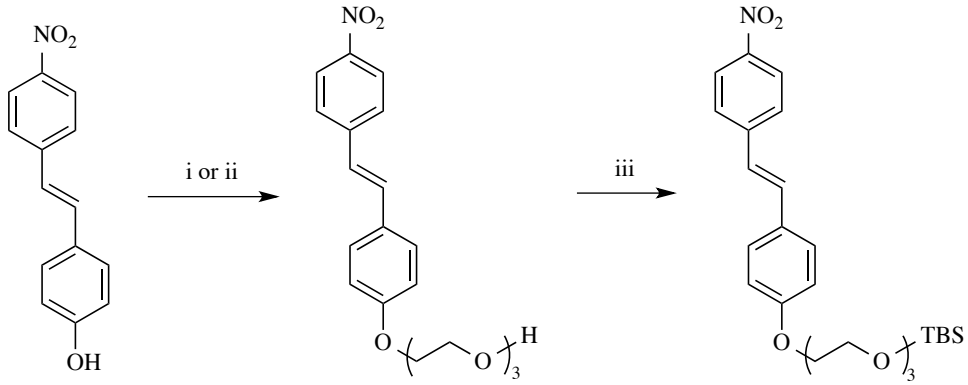

55 **60** **61**

i. 2-(2-(2-chloroethoxy)ethoxy)ethan-1-ol (1.2 equiv), K_2CO_3 (4 equiv), dry DMF, Ar, 90 °C, overnight, 34%; **ii.** 2-(2-(2-chloroethoxy)ethoxy)ethan-1-ol (1 equiv), K_2CO_3 (2 equiv), dry DMSO, Ar, 120 °C, 1.5 h, 71% of *E*/*Z* isomers, ratio 15/1; **iii.** TBSCl (1.2 equiv), imidazole (1.4 equiv), DMAP (3 mol%), CH_2Cl_2, 0 °C →r.t., overnight, 55%.

Scheme 51: Triethylene derivative linked to stilbene **55** *via* nucleophilic attack**.**

The first method (see Scheme 51, step i) was based on Zhang and co-workers.[40] The reaction was performed at 90 °C instead of 100 °C and with one less equivalent of the base (K_2CO_3). The yield dropped significantly to 34% (lit. 95%). The use of anhydrous DMSO instead of dry DMF accelerates the reaction but also forms the *Z*-isomer not initially present. The second method (see Scheme 51, step ii) was performed at 120 °C and followed by TLC monitoring. The enhancement of the nucleophilic attack with a potassium base reagent might be explained by the formation of potassium salt of DMSO which acts as a superbase.[119] However the presence of potassium base with DMSO can create radicals and can explain the formation of the *Z*-isomer.

Even with the use of a catalyst (DMAP), the silyl protection could only be achieved in low yield (55%) compared to the value reported by Zhang and co-workers (95%) for the silyl protection of (*E*)-2-(2-(2-(4-(4-(methylamino)styryl)phenoxy)ethoxy)ethoxy)ethan-1-ol **41**.

As mentioned in section 6.1.1, tosylate group seemed to be a better leaving group and allow a better reactivity to incorporate the triethylene glycol chain. Therefore the chain **35** prepared in section 6.2.3 was linked to the stilbene **55**. This method afforded the protected stilbene with ether chain **61** in one step and in 86% yield (see Scheme 52).

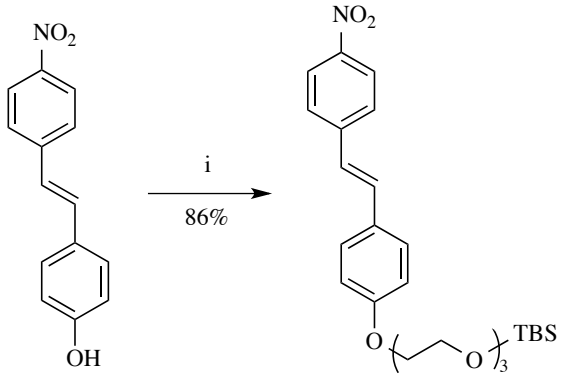

55 **61**

i. 35 (1 equiv), K_2CO_3 (2 equiv), DMF, 90 °C, overnight, 86%.

Scheme 52: Formation of the stilbene **61** in one step.

The 4-nitro-4'-hydroxystilbene **55** was used as limiting reagent (0.9 equiv) and the reaction proceeded at 90 °C. Different from the reaction proposed by Ono and co-workers (see Scheme 32, step i), anhydrous conditions were not required to synthesise the stilbene **61** by using the tosylated silylated glycol **35**.

6.4 Reduction of the nitro moiety to an amine

To form the desired precursor **7**, the nitro group must be reduced to an amine. The most common methods to reduce a nitro moiety to amine are palladium on charcoal (Pd/C) with hydrogen gas or the use of Raney nickel catalyst. The latter method involves the catalyst, a nickel-aluminium alloy, and hydrogen gas or hydrazine. These reactions are also known to reduce C—C double bond of the styrene.[110] Nevertheless these conditions were

performed at low temperature (down to –40 °C) but several side products were formed, so these reactions were not studied further.

6.4.1 Reduction of nitro group *via* Lewis acid

An alternative method for the reduction of nitro group is the use of Lewis acid as reported by Ono and co-workers.[104] Tin chloride or hydrated tin chloride or iron can reduce the nitro moiety in EtOH under reflux with or without additives (brønsted acid). The reduction of the nitro moiety is generally performed with the absence of labile proton.[40, 104, 117, 120] The next experiment confirmed the lack of reactivity with the presence of the phenol. (see Scheme 53).

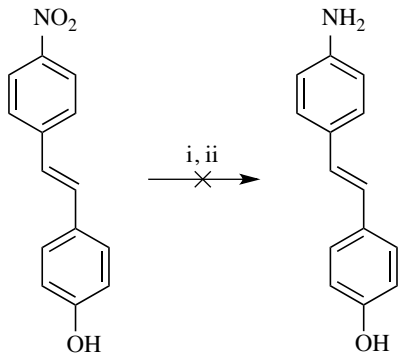

55 **62**

i. Fe (5 equiv), conc. acetic acid (2 drops), EtOH, reflux, overnight; **ii.** $SnCl_2 \bullet H_2O$ (5 equiv), EtOH, reflux 2 h.

Scheme 53: Reduction of the stilbene **55**.

The desired product was identified in both reactions by ^1H NMR but a lot of starting material **55** remained with the presence of side products. This reaction was performed by Vangala and co-workers[115] and afforded the amino stilbene **62** in 17% yield. No explanation was given such as the temperature of the reaction conditions or details about the purification step or the amount of hydrated tin chloride used.

The stilbene **60** was reacted with the same reagent. After purification through silica column the pure product **63** was obtained in 34% yield (see Scheme 54).

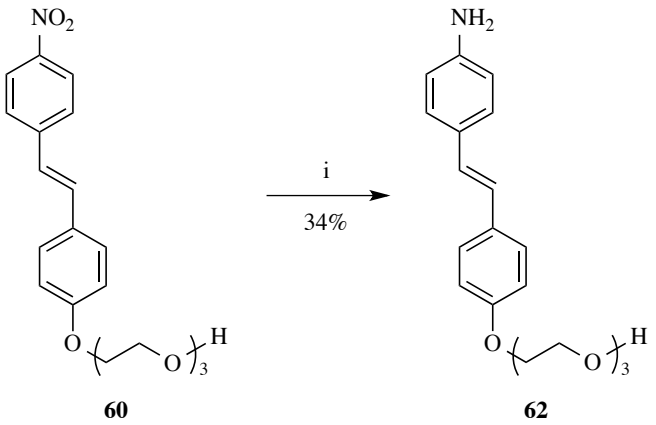

i. $SnCl_2 \bullet H_2O$ (5 equiv), EtOH, reflux overnight, 34%.

Scheme 54: Reduction of the nitro moiety of the stilbene **60**.

The stilbene **61** was also involved by the reduction of the nitro moiety as shown in Scheme 55.

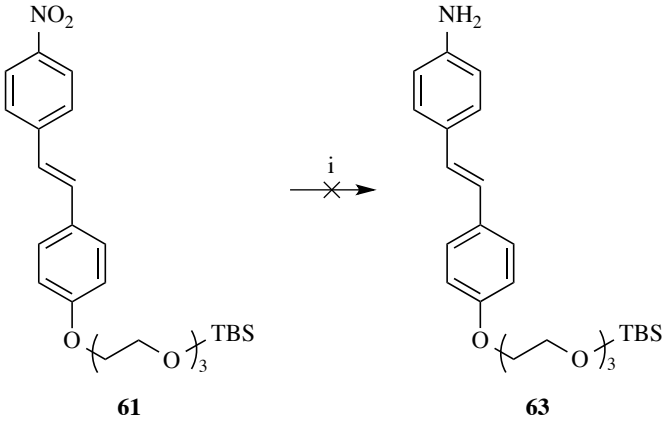

i. $SnCl_2 \bullet H_2O$ (5 equiv), EtOH, reflux overnight.

Scheme 55: Reduction of the stilbene **61**.

However after workup, the ^1H NMR spectroscopy of the crude mixture (see Figure 26) shows the removal of the silyl group. The possible formation of (*E*)-2-(2-(2-(4-(4-aminostyryl)phenoxy)ethoxy)ethoxy)ethan-1-ol was not confirmed due to the absence of data of this molecule. Therefore another method must be found to perform the reduction of the nitro group.

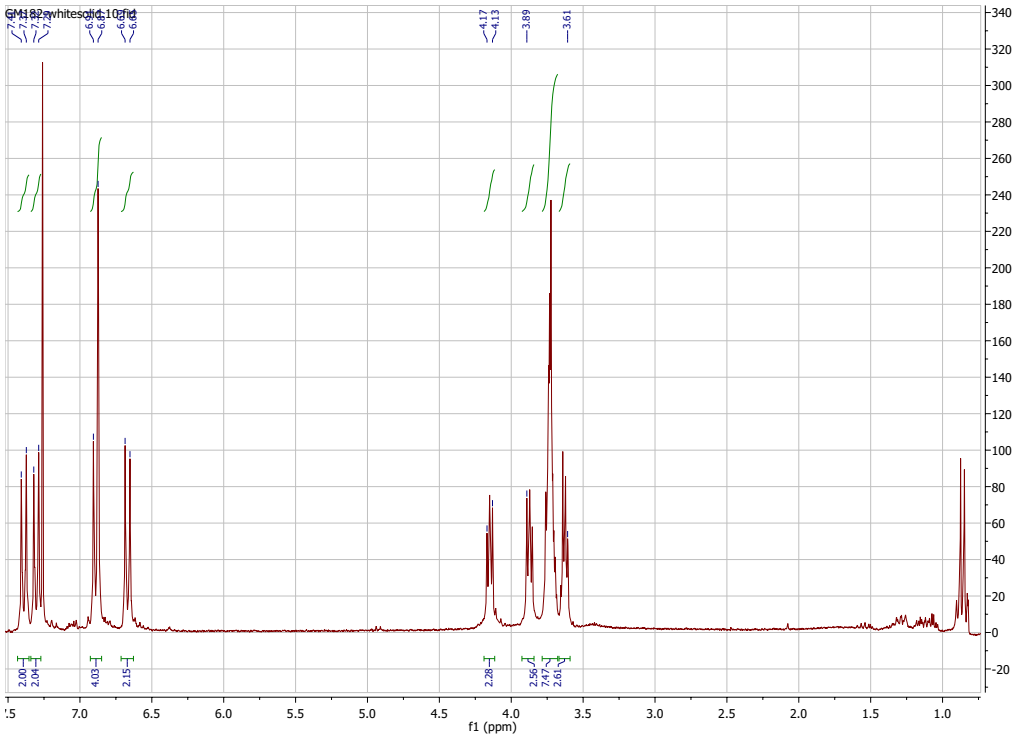

Figure 26: ^{1}H NMR of the crude mixture of the stilbene 61 reacting with tin chloride.

The reduction was performed with palladium on charcoal (10%) and a large excess of $NaBH_4$[121] (see Scheme 56). The reducing agent was added over 30 minutes at –40 °C. The reaction must be kept cold to avoid the formation of side products. The use of two solvents was necessessary for this reaction. The nitro stilbene **61** is solid in methanol at low temperature (below −20 °C) but dissolved in THF at the same temperature. The color of the reaction changed from yellow to colorless, signalling the consumtion of the starting material **61**. After 2 hours the crude mixture was monitored by TLC to confirm the completion of the reaction. Even if some traces of starting material remains, a quick filtration at –20 °C through celite and washing with cold methanol provided the product **63** with $NaBH_4$. The mixture was then put inside a ultrasonic bath to degas the solution and an aqueous solution of KOH (1 M) was added at 0 °C to neutralise the boron salt. After a normal extraction with Et_2O, the pure product **63** was isolated in high yield (82%).

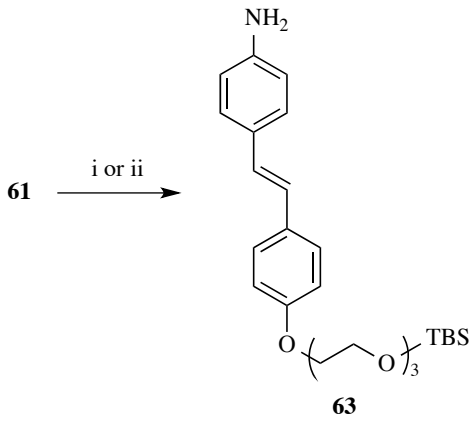

i. Pd/C (20 mg), $NaBH_4$ (26 equiv), EtOH/MeOH, −40 →−20 °C, 3 h, 69%, **ii.** Pd/C (20 mg), $NaBH_4$ (12 equiv), THF/MeOH, −30 →−20 °C, 3 h, 82%.

Scheme 56: Reduction of nitro stilbene **61** by using $NaBH_4$ and Pd/C at low temperature.

No other stilbenes were reduced by this method. The protected alcohol might offer a suitable starting material for the substitution of the aryl amine.

Another mild method was reported by Crump and co-workers as shown in Scheme 57, where the catalyst used was an alloy of 1% platinum with 2% vanadium on charcoal.[122]

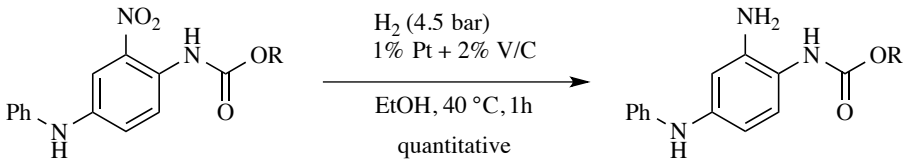

Scheme 57: Nitro reduction by using 1% Pt + 2% V/C.

It was not possible to use this reaction because no supplier was found to buy the vanadium on charcoal or any paper to synthesise it. Nevertheless, the authors mentioned a supposed mechanism for the hydrogenation of the nitro substrate with catalyst.

Indeed within the nitro reduction of **61** with Pd/C and $NaBH_4$, several intermediates were formed and monitored by TLC analysis.

Following this possible mechanism (see Scheme 58),[122, 123] two pathways were described to perform the amine product. For each intermediate formed after hydrogenation, except for the hydrazo compound, one molecule of water was generated.

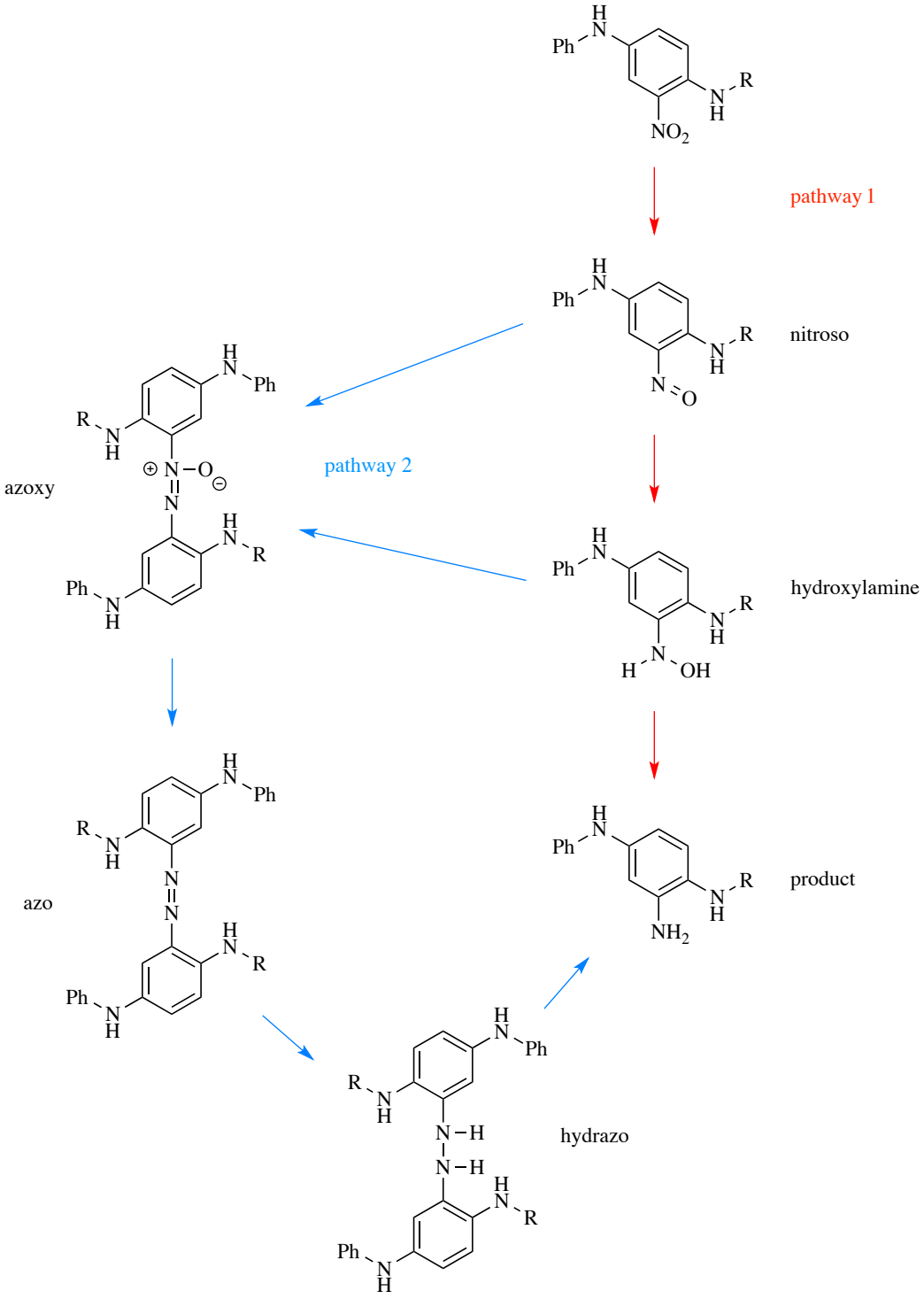

Scheme 58: Potential pathways of the nitro reduction by using H_2 and metal catalyst.

6.4.2 *N*-Monoalkylation of a primary amine

_N_-Monomethylation under basic conditions

Originally performed on 4-amino-4'-methoxystilbene **37** by Ono and co-workers,[104] the *N*-methylation was performed on the (*E*)-2,2,3,3-tetramethyl-12-(4-(4-nitrostyryl)phenoxy)-4,7,10-trioxa-3-siladodecane **63** as shown in Scheme 59. The first step was the formylation of the amine *via* paraformaldehyde in the basic medium under reflux. Instead of waiting to receive a commercial solution of sodium methoxide (25% w/w in MeOH), the reagent was prepared *in situ* with sodium metal and MeOH. After one hour the solution was cooled to room temperature and $NaBH_4$ added. The reaction mixture was stirred for one hour under reflux. The formamide **64** was then reduced to perform the *N*-methylamine **65**.

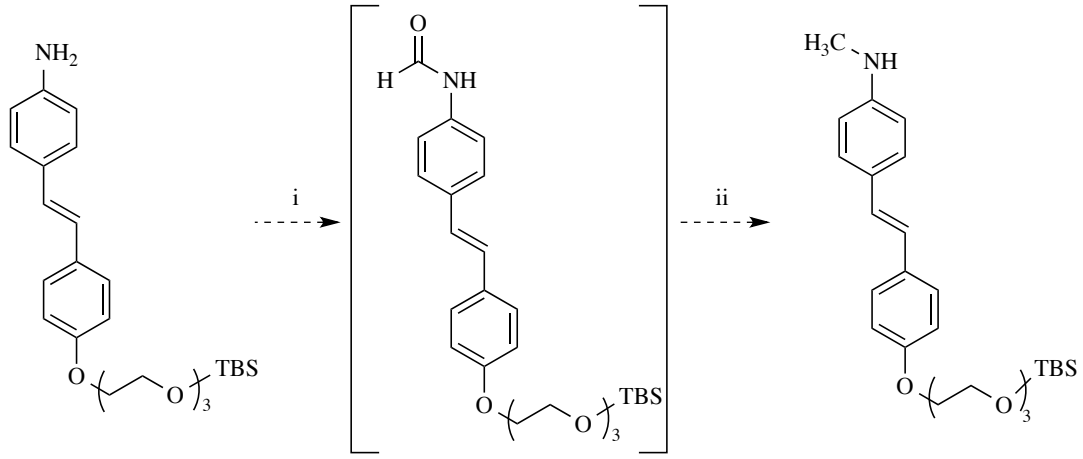

i. Na (4 equiv, 30% w/w in paraffin), paraformaldehyde (1.4 equiv), MeOH, reflux 1 h; **ii.** $NaBH_4$ (1.5 equiv), reflux, 1 h.

Scheme 59: *N*-methylation following the Ono method.[104]

Unfortunately, the experimental ^{1}H NMR of the crude mixture did not match with the NMR data reported by Zhang and co-workers. A doublet at 6.6 ppm was missing. Because of the non-elucidation of this missing peak the method was not repeated and other procedures were used.

***N*-Monomethylation under acidic conditions**

The procedure was reported by Andrews and co-workers[124] in 2012. The first step was the *in situ* formation of the acetic formic anhydride reagent from acetic anhydride and an excess of formic acid (see Scheme 60). The reaction was stirred at 60 °C for two hours and then the amino stilbene **63** was added at 0 °C. After 16 hours the reaction was quenched and the crude mixture analysed by ^{1}H NMR spectroscopy. Unfortunately the proton of the formamide (around 10 ppm) was not observed.

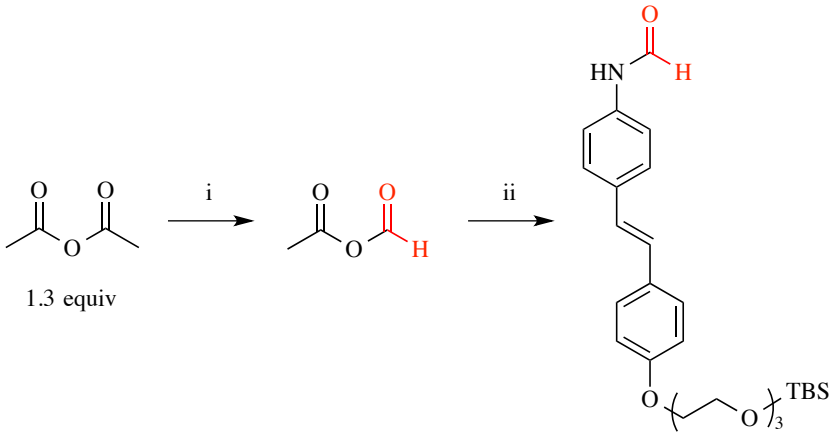

i. formic acid (97%, 1.6 equiv), 60 °C, 2 h; **ii. 63**, 0°C →r.t., 16 h.

Scheme 60: Experimentation of the formylation of an aryl amine under acidic reaction conditions.

6.5 Conclusion and possible other strategy

No reliable methods were found for the *N*-methylation of a stilbene. So the precursor of florbetaben has not been synthesised. Nevertheless the amino stilbene **63** was synthesised in three steps with an overall yield of 60%. A suitable method using Pd/C and $NaBH_4$ allowed the reduction of the nitro moiety with the presence of C–C double bond at low temperature. To reach the precursor the key step remains the monomethylation of the amine.

A new pathway could be to buy a commercially available *N*-methyl substrate to form the 4-methylamino-4-hydroxystilbene over 3 steps. The 4-(methylamino)benzoic acid or

methyl 4-(methylamino) benzoate might facilitate the synthesis to access the desired precursor of florbetaben **7** (see Scheme 61).

The process should be to reduce the 4-(methylamino)benzoic acid to the corresponding alcohol *via* a reducing agent such as DIBAL or borane dimethyl sulfide complex (BMS) or $LiAlH_4$ (step i or ii). The alcohol would be oxidised with MnO_2 to perform the aldehyde, the 4-(methylamino)benzaldehyde (step iii).[125] The key step (iv) would be the formation of the stilbene *via* the Knoevenagel reaction by using this aldehyde and 4-hydroxyphenylacetic acid, which is commercially available. The following steps should be the Boc protection of the amine (step v) and the use of the tosylated, silylated triethylene glycol performed in this work (step v). The next sequences have been already describes by Wang and co-workers[126] to form the precursor **7** in 3 steps (vi to viii, see Scheme 32).

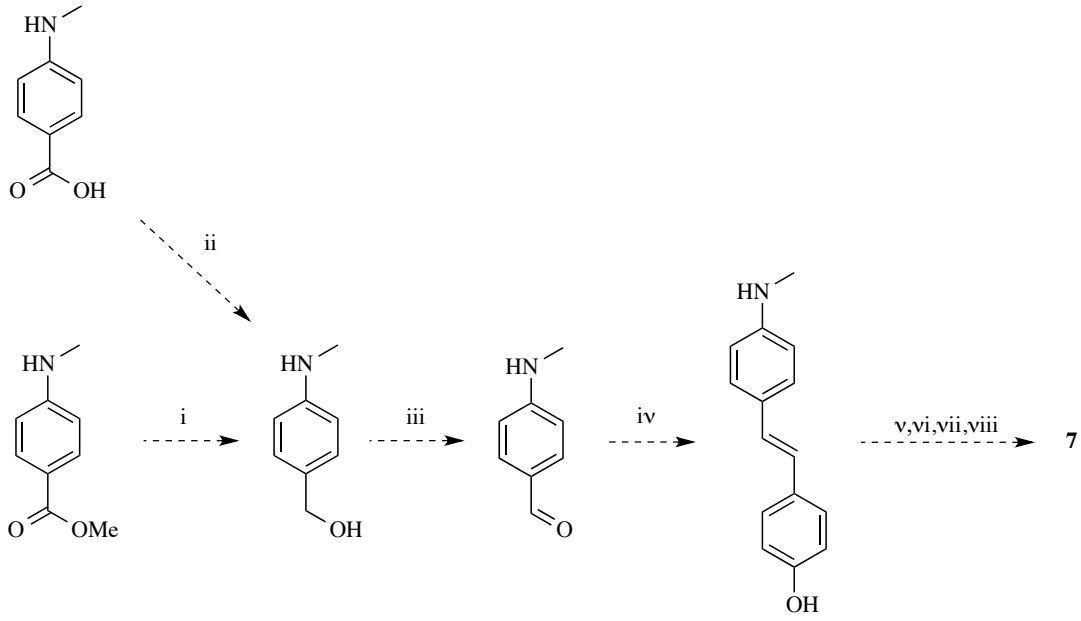

Scheme 61: Possible strategy to perform the N-Boc protected mesylate precursor **7**.

Chapter 7: Experimental

7 General experimental details

Reagents were obtained from Sigma Aldrich, Alfa Aesar, VWR suppliers and ABX (Germany) for the ultra pure mannose triflate and used as received unless otherwise specified. Solvents and reagents were purified according to Perrin, Armarego and Perrin's methods.[127] Dichloromethane were dried by refluxing over, and distilling from, calcium hydride. Anhydrous tetrahydrofuran was performed by refluxing over sodium with sodium benzophenone ketyl as indicator, followed by distillation or directly obtained from an MBRAUN Solvent Purification System like dry diethyl ether and dry toluene. Anhydrous dimethylformamide was purchased to Alfa Aesar in molecular sieves and dry acetonitrile furnished by Sigma Aldrich as well in molecular sieves. "Filtered" designates the removal residues by gravity filtration of organic solutions through filter paper. "Evaporated" points out the distillation of volatiles using a Büchi rotary heated with a water bath between 20 and 80 °C. "Degassed" refers to a ventilated solution placed in an ultrasonic bath.

All reactions using air/moisture sensitive reagents were performed in oven-vacuum-dried apparatus under an Argon atmosphere. Solid carbon dioxide and an acetone/EtOH (1:1) bath (−78 to −20 °C) or an ice-water bath (−5 to 5 °C) were used to obtain low temperatures unless otherwise stated. "m.p." stands for melting point. Heated batch reactions were conducted in a heating block on a magnetically stirred hot plate. Reactions were followed and monitored by TLC, ^{1}H NMR, ^{13}C NMR and ^{19}F NMR. The [^{18}F] syntheses were monitored by radio-TLC and the level of radioactivity of a sample was detected *via* a dose calibrator.

TLC analysis refers to analytical Thin Layer Chromatography, using aluminium-backed plates coated with Merck Kieselgel 60 GF254. Chemical spots were viewed either by UV fluorescence, or stained with a suitable staining agent. Column chromatography designates a flash column chromatography using head pressure by means of compressed air, and using Merck Kiesegel 60 F_{254} silica.

Melting points were recorded using a GallenKamp Melting Point Apparatus and are uncorrected.

Infrared spectra were recorded in the range 4000-700 cm^{-1} using a Iraffinity-1 Shimadzu FTIR-8400S instrument on a zinc selenide crystals. All absorption are quoted in wave numbers (cm^{-1})

8 Organic syntheses

8.1 [^{19}F]-Fluorination of mannose triflate in batch and microtubing

8.1.1 Procedure in batch

1,2,3,4,6-*O*-acetyl-β-D-glucose **13**[128]

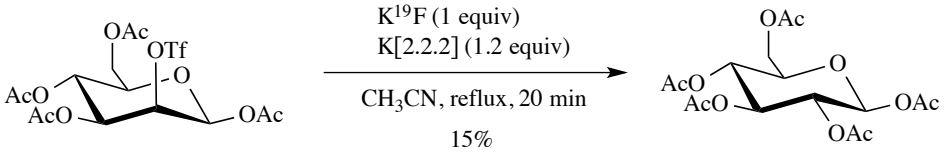

9 **13**

In a 25 mL round-bottomed flask, mannose triflate **9** (25 mg, 52.0 μmol), $K^{19}F$ (3 mg, 52.0 μmol) and Kryptofix [2.2.2] (23.5 mg, 62.4 μmol, 1.2 μmol) were dissolved in CH_3CN (3 mL). After 20 minutes under reflux, the reaction mixture was concentrated and then purified by flash chromatography (Petrol/EtOAc, 3:1). The peracetylated D-glucose **13** was obtained as a colourless solid (3 mg, 7.7 μmol, 15%).

^{1}H NMR (400 MHz, $CDCl_3$): δ = 5.72 (1 H, d, *J* = 8.3 Hz), 5.24 (1 H, dd, *J* = 9.4 Hz), 5.19-5.08 (1 H, m), 4.28 (1 H, dd, *J* = 12.4, 4.4 Hz), 4.11 (1 H, dd, *J* = 12.4 Hz, 2.4 Hz), 3.84 (1 H, ddd, *J* = 10.0, 4.4, 2.2 Hz), 2.11 (3 H, s), 2.09 (3 H, s), 2.04 (3 H, s), 2.02 (3 H, s) ppm.

No additional data due to the low amount of product.

8.2 Mono and bis-protection of triethylene glycol 24[129]

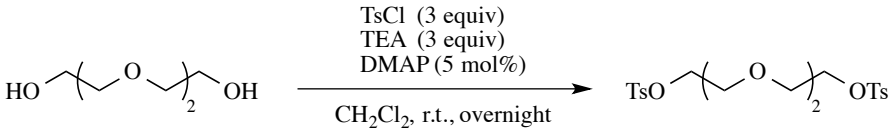

24 **25**

A catalytic amount of DMAP (122 mg, 1 mmol, 5 mol%) and tosyl chloride (11.4 g, 60.0 mmol, 3 equiv) were added in a stirred solution of triethylene glycol **24** (3.0 g, 20.0 mmol) and TEA (8.4 mL, 60.0 mmol, 3 equiv) in CH_2Cl_2 (100 mL). The reaction mixture was stirred overnight at room temperature. After addition of water (100 mL), the aqueous

layer was extracted with CH_2Cl_2 (3 x 50 mL). The combined organic layers were dried over Na_2SO_4, filtered and concentrated under reduced pressure. The crude solid was purified by flash chromatography (Petrol/EtOAc, 1:3) to yield the ditosylate **25** as a white powder (7.56 g, 16.5 mmol, 82%).

m.p. 81-82 °C (lit.[129]: 80-81 °C)

^{1}H NMR (400 MHz, $CDCl_3$): δ = 7.67 (4 H, d, *J* = 8.1 Hz), 7.26 (4 H, d, *J* = 8.0 Hz), 4.04 (4 H, t, *J* = 4.2 Hz), 3.55 (4 H, t, *J* = 8.1 Hz), 3.41 (4 H, t, *J* = 2.3 Hz), 2.34 (6 H, s) ppm.

^{13}C NMR (101 MHz, $CDCl_3$): δ =145.0 (C), 132.9 (C), 129.9 (CH), 127.9 (CH), 70.6 (CH_2), 69.4 (CH_2), 68.7 (CH_2), 21.6 (CH_3) ppm.

IR (ν_{max}) = 3059, 2965, 2872, 1593, 1598, 1451, 1355, 1265, 1190, 1176, 1097, 1097, 920, 886.

2-(2-(2-(Benzyloxy)ethoxy)ethoxy)ethyl 4-methylbenzenesulfonate **31**[130]

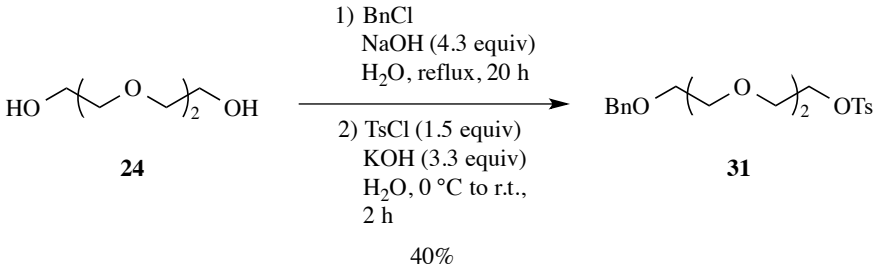

24 **31**

To an aqueous solution of NaOH (516 mg, 12.9 mmol in 2.9 mL of distilled water, 4.3 equiv), triethylene glycol **24** (2 mL, 15.0 mmol, 4 equiv) and benzyl chloride (0.35 mL, 3.0 mmol) were added. The reaction was heated under reflux for 20 hours. The crude mixture was concentrated *in vacuo* and dissolved in THF (20 mL). *p*-Toluenesulfonyl chloride (2.38 g, 12.5 mmol, 1.5 equiv) was added at room temperature followed by an aqueous solution of KOH (1.54 g, 27.4 mmol, 3.3 equiv) in deionised water (1.6 mL) poured dropwise at 0 °C over 15 min. The reaction was kept at 0 °C for 30 min and a white precipitate appeared. After 2 hours at room temperature the mixture was neutralised with a saturated solution of ammonium chloride and extracted with CH_2Cl_2 (3 x 20 mL). The combined organic layers were dried, filtered and concentrated under reduced pressure. The residue was purified by flash chromatography (Petrol/EtOAc, 3:1) to yield the bis-protected glycol **31** (1.79 g, 4.54 mmol, 40%) as a colourless oil.

^{1}H NMR (400 MHz, $CDCl_3$): δ = 7.78 (2 H, *J* = 8.3 Hz, H_{Ar}), 7.50- 7.28 (7 H, m, H_{Ar}), 4.54 (2 H, s, CH_2Ph), 4.20- 4.04 (4 H, m, OCH_2), 3.90- 3.53 (8 H, m, OCH_2), 2.42 (3 H, s, CH_3) ppm.

^{13}C NMR (101 MHz, $CDCl_3$): δ = 144.9 (C), 138.0 (C), 133.1 (C), 129.9 (CH), 128.5 (CH), 128.0 (CH), 127.8 (CH), 127.6 (CH), 73.3 (CH_2), 71.0 (CH_2), 70.7 (CH_2), 70.6 (CH_2), 69.4 (CH_2), 69.3 (CH_2), 68.7 (CH_2), 21.64 (CH_3) ppm.

IR (ν_{max}) = 2917, 2865, 1597, 1496, 1454, 1352, 1189, 1175, 1120, 1096, 1012, 916, 897, 814.

2-(2-(2-Hydroxyethoxy)ethoxy)ethyl 4-methylbenzenesulfonate **34**[100]

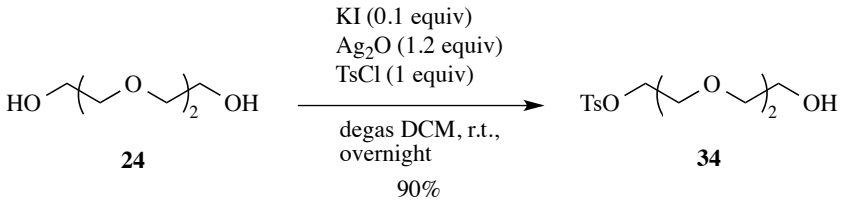

24 **34**

Potassium iodide (276 mg, 1.66 mmol, 0.1 equiv), silver oxide (4.63 g, 16.7 mmol, 1.2 equiv) and *p*-toluenesulfonyl chloride (3.17 g, 16.7 mmol) were added to a solution of triethylene glycol (2.5 g, 16.7 mmol) in degased CH_2Cl_2 (75 mL). The reaction mixture was stirred at room temperature overnight and then filtered through Celite. The filtrate was concentrated and purified by flash chromatography (CH_2Cl_2/acetone, 7:3) to yield the title product **34** (4.33 g, 14.9 mmol, 90%) as a colourless oil.

^{1}H NMR (400 MHz, $CDCl_3$): δ = 7.78 (2 H, d, *J* = 8.3 Hz, H_{Ar}), 7.33 (2 H, d, *J* = 8.4 Hz, H_{Ar}), 4.17- 4.11 (2 H, m, OCH_2), 3.72- 3.65 (4 H, m, OCH_2), 3.60- 3.51 (6 H, m, OCH_2), 2.43 (3 H, s, CH_3), 2.29 (1 H, br, OH) ppm.

^{13}C NMR (101 MHz, $CDCl_3$): δ = 145.2 (C), 133.2 (C), 130.2 (CH), 128.3 (CH), 72.8 (CH_2), 71.1 (CH_2), 70.6 (CH_2), 69.5 (CH_2), 69.0 (CH_2), 62.0 (CH_2), 22.0 (CH_3) ppm.

IR (ν_{max}): 3402, 3060, 2918, 2868, 1596, 1452, 1353, 1176, 1120, 1008, 817, 664.

2,2,3,3-Tetramethyl-4,7,10-trioxa-3-siladodecan-12-yl 4-methylbenzenesulfonate **35**[97]

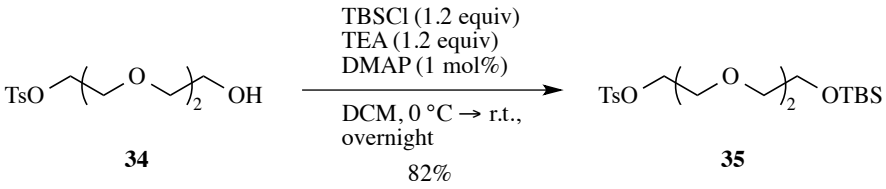

34 **35**

To a solution of mono-protected triethylene glycol **34** (1.61 g, 5.55 mmol), TEA (0.9 mL, 6.65 mmol, 1.2 equiv) and DMAP (10 mg, 81.9 μmol, 1 mol%) in CH_2Cl_2 (20 mL) was added TBSCl (1.0 g, 6.66 mmol, 1.2 equiv) at 0 °C. After 10 min at 0 °C the reaction mixture was allowed to reach room temperature and was stirred overnight. Deionized water was added (10 mL) to the solution and the aqueous layers were extracted with CH_2Cl_2 (3 x 20 mL). The combined extracts were dried over Na_2SO_4 and then filtered off. The product mixture was concentrated and purify by flash chromatography (Petrol/EtOAc, 2:1) to offer the bis-protected triethylene glycol **35** (1.89 g, 4.52 mmol, 90%) as a colourless oil.

^{1}H NMR (400 MHz, $CDCl_3$): δ = 7.83 (2 H, d, *J* = 8.3 Hz, H_{Ar}), 7.36 (2 H, d, *J* = 7.9 Hz, H_{Ar}), 4.18 (2 H, dd, *J* = 5.4, 4.3 Hz, OCH_2), 3.76 (2 H, t, *J* = 5.4 Hz, OCH_2), 3.73- 3.69 (2 H, m, OCH_2), 3.63- 3.57 (4 H, m, OCH_2), 3.54 (2 H, t, *J* = 5.4 Hz, OCH_2), 2.47 (3 H, s, CH_3), 0.90 (9 H, s, ^{t}Bu), 0.07 (6 H, s, $(CH_3)_2$) ppm.

^{13}C NMR (101 MHz, $CDCl_3$): δ = 145.1 (C), 133.3 (C), 130.1 (CH), 128.3 (CH), 73.0 (CH_2), 71.1 (CH_2), 71.0 (CH_2), 69.6 (CH_2), 69.0 (CH_2), 63.0 (CH_2), 26.2 (C), 18.7 (CH_3), –4.9 (CH_3) ppm.

IR (ν_{max}): 2928, 2857, 1738, 1598, 1472, 1463,1359, 1249, 1189 1107, 1097, 1019, 921, 759.

8.3 Precursor syntheses for the formation of stilbene derivatives *via* the Wittig reaction

(4-Nitrobenzyl)triphenylphosphonium bromide **46**[131]

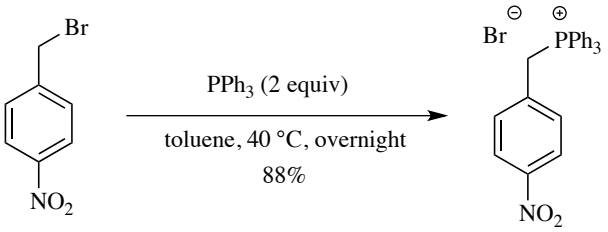

45 **46**

Triphenylphosphine (2.43 g, 9.26 mmol, 2.0 equiv) was added to a stirred solution of 4-nitrobenzyl bromide **45** (1 g, 4.63 mmol) in toluene (50 mL) and heated under reflux overnight. Afterwards the reaction mixture was cooled to room temperature and concentrated under reduced pressure. After addition of acetone (50 mL), the desired solid **46** was filtered using a Büchner funnel and washed with acetone (200 mL). The solid was collected and the solvents were evaporated under reduced pressure to offered (4-nitrobenzyl)triphenylphosphonium bromide **46** as a white powder (1.95 g, 4.08 mmol, 88%).
m.p. 270 °C (lit.[132] 275 °C).
^{1}H NMR (400 MHz, $CDCl_3$): δ = 7.87-7.69 (11 H, m, H_{Ar}), 7.64-7.53 (6 H, m, H_{Ar}), 7.51-7.43 (2 H, m, H_{Ar}), 6.01 (2 H, d, *J* = 15.8 Hz, CH_2P) ppm.
^{13}C NMR (101 MHz, $CDCl_3$): δ = 147.5 (C), 136.0 (C), 135.3 (CH), 134.8 (CH), 134.5 (CH), 134.4 (CH), 132.9 (CH), 132.8 (CH), 130.2 (CH), 130.1 (C), 123.3 (CH), 123.3 (CH), 117.7 (C), 116.9 (C), 29.6 (CH_2) ppm.
IR (ν_{max}): 2990, 2865, 2773, 1593, 1519, 1348, 1105, 871.

4-Acetoxybenzaldehyde **48**[133]

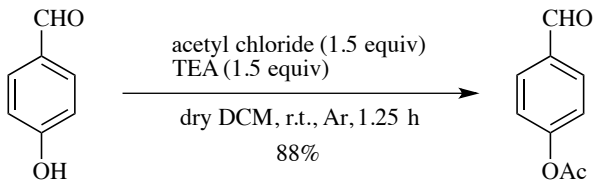

47 **48**

To a solution of 4-hydroxybenzaldehyde **47** (200 mg, 1.64 mmol) and TEA (0.3 mL, 2.5 mmol, 1.5 equiv) in anhydrous CH_2Cl_2 (10 mL), acetyl chloride (0.2 mL, 2.5 mmol, 1.5

equiv) was added dropwise. The reaction mixture was stirred at room temperature and monitored by TLC over 1.25 hours. The aqueous layers were extracted with CH_2Cl_2 (3 x 20 mL) and the combined organic layers were dried over Na_2SO_4 and filtered. The solution was concentrated under reduced pressure and then purified by flash chromatography (Petrol/EtOAc, 3:1). After removal of solvents, the product **48** was obtained as a colourless oil (237 mg, 1.65 mmol, 88%).

^{1}H NMR (400 MHz, $CDCl_3$): δ = 9.94 (1 H, s, CHO), 7.87 (2 H, d, *J* = 8.6 Hz, H_{Ar}), 7.23 (2 H, d, *J* = 8.6 Hz, H_{Ar}), 2.29 (3 H, s, CH_3) ppm.

^{13}C NMR (101 MHz, $CDCl_3$): δ = 191.2 (C), 168.9 (C), 155.5 (C), (134.2 (C), 131.4 (CH), 122.6 (CH), 21.3 (CH_3) ppm.

IR (ν_{max}): 2935, 2862, 1759, 1699, 1594, 1502, 1370, 1201, 1052, 1011, 908, 858.

4-Methoxybenzyl alcohol **51**[134]

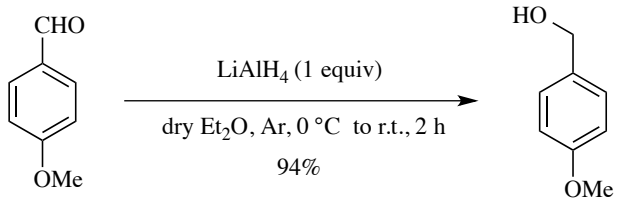

51

In a 50 mL two-neck round-bottomed flask, lithium aluminium hydride (279 mg, 7.34 mmol, 1 equiv) was added in anhydrous Et_2O (10 mL) under an argon atmosphere. Dissolved in dry Et_2O (5 mL), *p*-anisaldehyde (1 g, 7.34 mmol) was added dropwise to the flask at 0 °C. After that the completion of the reaction was observed by TLC analysis (2 hour), the mixture was quenched slowly with ice and an aqueous solution of NaOH (2 M, 2 mL) at 0 °C for 10 minutes. The resulting mixture was filtered through Celite and washed with Et_2O (100 mL). The aqueous layer was extracted by Et_2O (2 x 50 mL) then washed with brine and dried over Na_2SO_4. The resulting mixture was filtered and the solvents were evaporated under reduced pressure. The alcohol **51** was isolated as a colourless oil (943 mg, 6.83 mmol, 94%).

^{1}H NMR (400 MHz, $CDCl_3$): δ = 7.23 (2 H, d, *J* = 8.4 Hz, H_{Ar}), 6.86 (2 H, d, *J* = 8.6 Hz, H_{Ar}), 4.52 (2 H, s, CH_2), 3.77 (3 H, s, CH_3) ppm.

^{13}C NMR (101 MHz, $CDCl_3$): δ = 159.2 (C), 133.4 (C), 128.8 (CH), 114.1 (CH), 64.8 (CH_2), 55.5 (CH_3) ppm.

IR (ν_{max}): 3348, 2940, 2836, 1612, 1511, 1302, 1241, 1173, 1031, 813.

4-Methoxybenzyl bromide **52**[135]

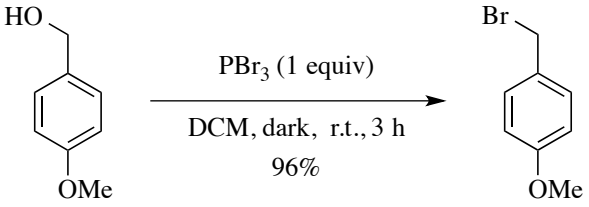

51 **52**

Phosphorus tribromide (0.6 mL, 6.83 mmol) was added in the dark to a solution of 4-methoxybenzyl alcohol **51** (943 mg, 6.83 mmol) in CH_2Cl_2 (7 mL). The reaction was monitored by TLC and after completion (3 hours), the mixture was quenched with a saturated solution of $NaHCO_3$ at 0 °C. The aqueous layer was extracted with CH_2Cl_2 (3 x 10 mL). The combined organic extracts were dried over Na_2SO_4 and filtered. The residue was concentrated *in vacuo* to yield (1.32 g, 6.57 mmol, 96%) as a yellow oil.

^{1}H NMR (400 MHz, $CDCl_3$): δ = 7.36 (2 H, d, *J* = 8.7 Hz, H_{Ar}), 6.90 (2 H, d, *J* = 8.7 Hz, H_{Ar}), 4.54 (2 H, s, CH_2), 3.84 (3 H, s, CH_3) ppm.

^{13}C NMR (63 MHz, $CDCl_3$): δ = 160.0 (C), 130.8 (CH), 130.3(C), 114.5 (CH), 55.7 (CH_3), 34.3 (CH_2) ppm.

IR (ν_{max}): 2959, 2904, 835, 1607, 1511, 1303, 1226, 1111, 1026, 825.

(4-Methoxybenzyl)triphenylphosphonium bromide **53**[136]

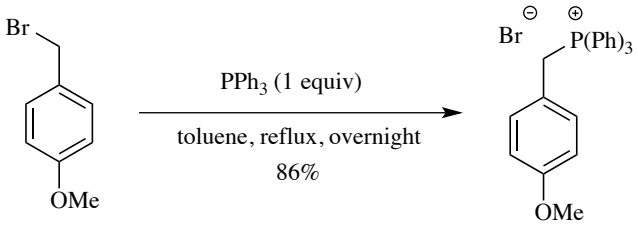

52 **53**

To a solution of 4-methoxybenzyl bromide **52** (1.32 g, 6.57 mmol) in toluene (20 mL), triphenylphosphine (1.72 g, 6.56 mmol) was added. The reaction mixture was stirred overnight under reflux. At room temperature acetone (20 mL) was added and the phosphonium salt precipitated. The mixture was filtered using a Büchner funnel and washed with acetone (40 mL). The solvents were removed *in vacuo* to yield the desired triphenylphosphonium salt **53** (2.62 g, 5.65 mmol, 86%) as a white powder.

m.p. 234 °C (lit.[109] 234-235 °C).

^{1}H NMR (400 MHz, $CDCl_3$): δ = 7.82- 7.71 (9 H, m, H_{Ar}), 7.69- 7.62 (6 H, m, H_{Ar}), 7.04 (2 H, dd, *J* = 8.8, 2.5 Hz, H_{Ar}), 6.66 (2 H, d, *J* = 8.7 Hz, H_{Ar}), 5.33 (2 H, d, *J* = 13.7 Hz, CH_2P), 3.74 (3 H, s) ppm.

^{13}C NMR (126 MHz, $CDCl_3$): δ = 135.2 (C), 135.2 (C), 134.8 (CH), 134.7 (CH), 133.1 (C), 133.0 (C), 130.5 (CH), 130.4 (CH), 118.7 (C), 118.0 (C), 114.6 (C), 114.6 (C), 55.6 (CH_3), 30.7 (CH_2), 30.3 (CH_2) ppm.

IR (ν_{max}): 3052, 2990, 2860, 2774, 1610, 1585, 1513, 1439, 1264, 1180, 1112, 1031, 997, 838.

8.4 Precursor synthesis for the formation of stilbene derivatives *via* the Heck reaction

4-Vinylphenol **54**[137]

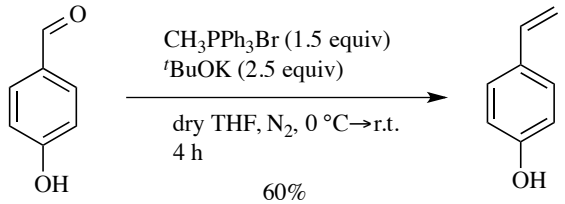

47 **54**

In a two-necked round-bottomed flask under a nitrogen atmosphere, ^{t}BuOK (1.40 g, 12.5 mmol, 2.5 equiv) was added slowly to a stirred solution of methyltriphenylphosphonium bromide (2.68 g, 7.5 mmol, 1.5 equiv) in dry THF (10 mL) at 0 °C for 10 minutes. At room temperature, 4-hydroxybenzaldehyde **47** (610.6 mg, 5.0 mmol) dissolved in dry THF (5 mL) was added dropwise to the above suspension. The resulting mixture was stirring at room temperature and monitored by TLC analysis for 4 hours. The reaction mixture was quenched with a saturated solution of NH_4Cl and concentrated in *vacuo*. The aqueous layer was extracted with CH_2Cl_2 (3 x 20 mL). The organic layers were combined and dried over Na_2SO_4. After filtration, the solvents were evaporated under reduced pressure. The residue was purified by flash chromatography (Petrol/EtOAc 5:1) to obtain the pure product **54** (361 mg, 3.0 mmol, 60%) as a colourless oil.

^{1}H NMR (250 MHz, $CDCl_3$): δ = 7.19 (2 H, d, *J* = 8.5 Hz, H_{Ar}), 6.75 (2 H, d, *J* = 8.5 Hz, H_{Ar}), 6.56 (1 H, dd, *J* = 17.5, 10.9 Hz, H_{vinyl}), 5.49 (1 H, d, *J* = 17.5 Hz, H_{vinyl}), 5.00 (1 H, d, *J* = 10.9 Hz, H_{vinyl}) ppm.

^{13}C NMR (126 MHz, $CDCl_3$): δ = 154.0 (C), 136.4 (CH), 127.0 (CH), 124.9 (C), 115.0 (CH), 110.0 (CH) ppm.

IR (ν_{max}): 3414, 2963, 1670, 1502, 1303, 1173, 1033, 810.

8.5 **Formation of stilbene derivatives**

4-Nitro-4'-methoxystilbene **37**[138]

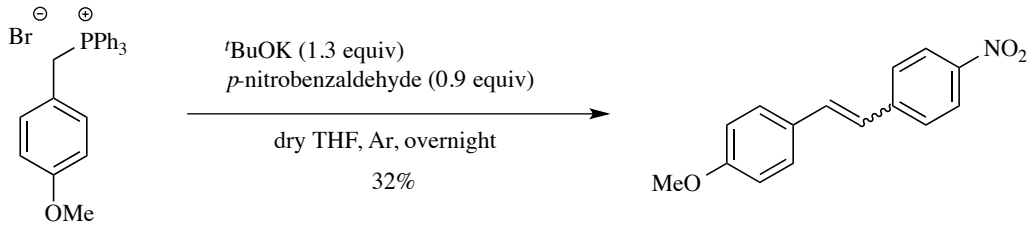

53

In a 50 mL two-necked round-bottomed flask under inert atmosphere, *p*-nitrobenzaldehyde (59 mg, 0.39 mmol, 0.9 equiv) was added at 0 °C to a stirred solution of triphenylphosphonium salt **53** (200 mg, 0.43 mmol) with ^{t}BuOK (62 mg, 1.3 equiv) in anhydrous THF (15 mL) and was stirred for 20 minutes at 0 °C. The reaction mixture was stirred at room temperature overnight and concentrated under reduced pressure. After quenching with deionised water (5 mL) the resulting aqueous layer were extracted with EtOAc (3 x 20 mL). The combined organic layer was washed with brine and dried over Na_2SO_4. After filtration and evaporation of the solvents under reduced pressure, purification by flash chromatography (Petrol/EtOAc, 3:1) offered a mixture of the two isomers of 4-nitro-4'-methoxystilbene (37 mg, 0.14 mmol, 32%, ratio *E*/*Z* = 14:1) as a yellow powder.

^{1}H NMR (400 MHz, $CDCl_3$): <u>*E*-isomer:</u> δ = 8.21 (2 H, d, *J* = 8.8 Hz, H_{Ar}), 7.60 (2 H, d, *J* = 8.8 Hz, H_{Ar}), 7.50 (2 H, *J* = 8.8 Hz, H_{Ar}), 7.49 (1 H, d, *J* = 15 Hz, H_{vinyl}), 7.26 (1 H, d, *J* = 16.4 Hz, H_{vinyl}), 6.98 (2 H, d, H_{Ar}), 3.84 (3 H, s, CH_3) ppm.

<u>*Z*-isomer:</u> δ = 8.0 (2 H, d, *J* = 8.9 Hz, H_{Ar}), 7.32 (2 H, d, *J* = 8.8 Hz, H_{Ar}), 7.07 (2 H, d, *J* = 8.9 Hz, H_{Ar}), 6.70 (2 H, d, *J* = 8.8 Hz, H_{Ar}), 6.65 (1 H, d, *J* = 12.4 Hz, H_{vinyl}), 6.45 (1 H, d, *J* = 12.4 Hz, H_{vinyl}) ppm.

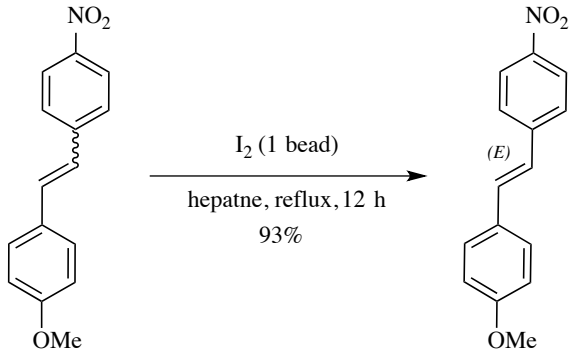

37

In a 50 mL round-bottomed flask fitted with a condenser, the mixture of *E*/*Z* isomer of the 4-nitro-4'-methoxy stilbene (37 mg, 0.14 mmol) and iodine (1 bead) were added in heptane (5 mL). The reaction mixture was heated under reflux for 12 hours. The solution was diluted with Et_2O (10 mL) and washed with an aqueous saturated solution of sodium bisulfite (20 mL). The organic layer was dried over Na_2SO_4 and filtered. The residue was concentrated under reduced pressure to obtain the *E*-isomer **37** (34 mg, 0.13 mmol) as a yellow powder.

m.p. 128 °C (lit.[139] 131-132.5 °C).

^{1}H NMR (400 MHz, d^6-acetone): δ = 8.21 (2 H, d, *J* = 8.8 Hz, H_{Ar}), 7.60 (2 H, d, *J* = 8.8 Hz, H_{Ar}), 7.50 (2 H, *J* = 8.8 Hz, H_{Ar}), 7.49 (1 H, d, *J* = 16.4 Hz, H_{vinyl}), 7.26 (1 H, d, *J* = 16.4 Hz, H_{vinyl}), 6.98 (2 H, d, *J* = 8.8 Hz, H_{Ar}), 3.84 (3 H, s, CH_3) ppm.

^{13}C NMR (101 MHz, d^6-acetone): δ = 162.24 (C), 148.23 (C), 146.56 (C), 134.86 (CH), 131.07 (C), 130.38 (2 CH), 128.58 (CH), 125.81 (CH), 125.73 (CH), 116.06 (2 CH), 56.60 (CH_3) ppm.

IR (ν_{max}): 2957, 2831, 1587, 1509, 1336, 1252, 1174, 1108, 1033, 970, 843, 750.

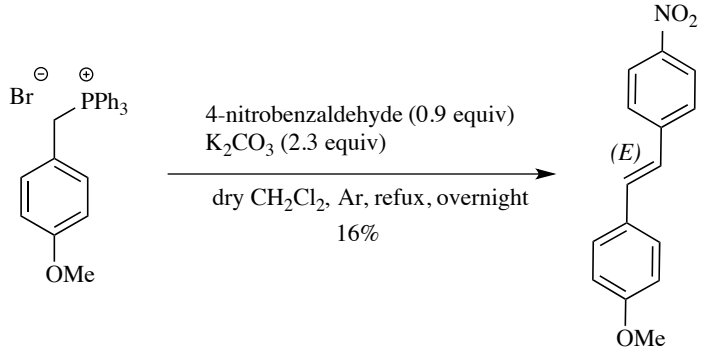

53 **37**

In a 50 mL two-necked round-bottomed flask fitted with a condenser under an argon atmosphere, was added the phosphonium salt **53** (500 mg, 1.08 mmol), 4-nitrobenzaldehyde

(147 mg, 0.97 mmol, 0.9 equiv) and K_2CO_3 (343 mg, 2.48 mmol, 2.3 equiv) in dry CH_2Cl_2 (15 mL). The reaction mixture was heated under reflux overnight. The aqueous phase was extracted with CH_2Cl_2 (3 x 15 mL). The organic phases were combined and dried over Na_2SO_4. The mixture was concentrated under reduced pressure and 20 mL of MeOH was added. The product mixture was then cooled at –40 °C and filtered. The title product **37** was obtained as a yellow solid (40 mg, 0.16 mmol, 16%).

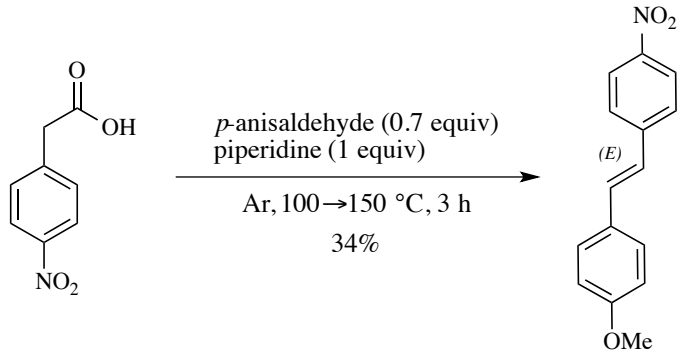

59 **37**

4-Nitrophenylacetic acid **59** (1.81 g, 10.0 mmol), piperidine (1 mL, 10.0 mmol, 1 equiv) and *p*-anisaldehyde (1.36 g, 10.0 mmol, 1 equiv) were mixed in a 25 mL two-necked round-bottomed flask with a condenser. The reaction was heated at 100 °C under vacuum for 1 hour and for an additional 2 hours at 150 °C *in vacuo*. The collected brown solid was was crushed and then heated under reflux in a solution of EtOH/H_2O (3:1, 20 mL) and concentrated AcOH (0.1 mL). At room temperature the yellow solid was filtered an recrystalised in ^{i}PrOH to yield the desired product **37** (868 mg, 3.4 mmol, 34%).

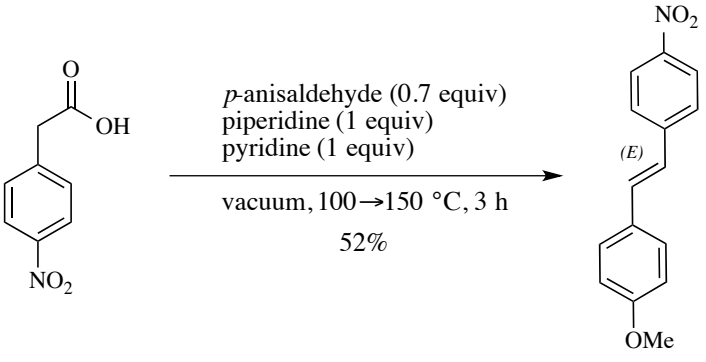

59 **37**

4-Nitrophenylacetic acid **59** (1.81 g, 10.0 mmol), piperidine (1 mL, 10.0 mmol, 1 equiv), pyridne (0.8 mL, 10.0 mmol, 1 equiv) and *p*-anisaldehyde (1.36 g, 10.0 mmol) were mixed in a 25 mL two-necked round-bottomed flask with condenser. The reaction was heated

at 100 °C under vacuum for 1 hour and for an additional 2 hours at 150 °C *in vacuo*. The collected brown solid was crushed and then heated under reflux in a solution of EtOH/H_2O (3:1, 20 mL) with 0.1 mL of glacial AcOH. At room temperature the yellow solid was filtered and recrystalised in ^{i}PrOH to yield the desired product **37** (1.33 g, 5.2 mmol, 52 %).

(*E*)-4-nitro-4'-hydroxystilbene **55**[114]

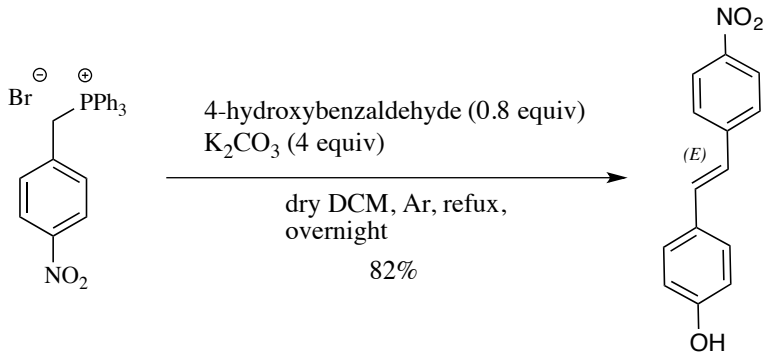

46 **55**

Under inert atmosphere 4-hydroxybenzaldehyde (100 mg, 0.82 mmol, 0.79 equiv), the phosphonium salt **46** (470 mg, 0.98 mmol) and K_2CO_3 (453 mg, 3.28 mmol, 4 equiv) were added to a 50 mL two-necked round-bottomed flask with condenser. After addition of anhydrous CH_2Cl_2 (10 mL) the stirred reaction was heated under reflux overnight. The resulting mixture was filtered using a Büchner funnel and washed with MeOH (20 mL). The corresponding filtrate was concentrated under reduced pressure and purified by flash chromatography (CH_2Cl_2/MeOH, 20:1). After evaporation of the solvents under vacuum, the desired stilbene **55** was isolated as a yellow solid (163 mg, 0.68 mmol, 82%).

^{1}H NMR (500 MHz, CD_3OD): δ = 6.81 (2 H, d, *J* = 8.8 Hz, H_{Ar}), 6.32 (2 H, d, *J* = 8.8 Hz), 6.09 (2 H, d, *J* = 8.6 Hz, H_{Ar}), 5.94 (1 H, *J* = 16.3 Hz, H_{vinyl}), 5.69 (1 H, d, *J* = 16.3 Hz, H_{vinyl}), 5.45 (2 H, *J* = 8.6 Hz, H_{Ar}) ppm.

^{13}C NMR (126 MHz, CD_3OD): δ = 160.4 (C), 148.4 (C), 147.1 (C), 135.4 (CH), 130.6 (CH), 130.4 (C), 128.5 (CH), 125.8 (CH), 125.2 (CH), 117.6 (CH) ppm.

IR (ν_{max}): 3412, 1631, 1583, 1498, 1336, 1315, 1172, 1107, 974, 841, 749.

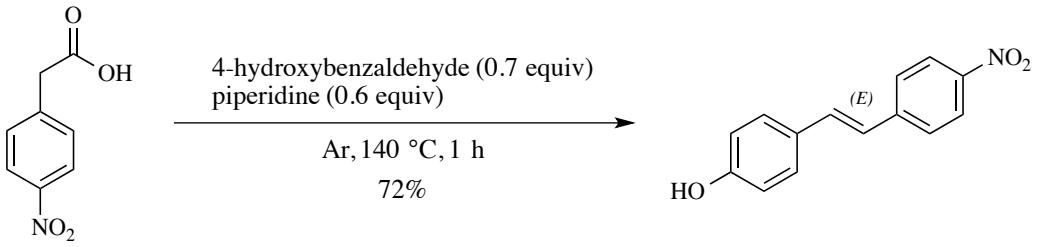

59 **55**

In a 50 mL two-necked round bottomed flask with condenser under inert atmosphere, (4-nitrophenyl)acetic acid **59** (4 g, 22 mmol, 1.3 equiv), 4-hydroxybenzaldehyde (2 g, 16.4 mmol) and piperidine (1 mL, 10.1 mmol, 0.6 equiv) were stirred at 140 °C for 1 hour. The obtained brown solid was crushed and then heated under reflux with a solution of $EtOH/H_2O$ (3:1, 20 mL) and concentrated AcOH (0.1 mL). At room temperature the brown solid was filtered and recrystallized with ^{i}PrOH to yield the desired stilbene **55** (2.86 g, 11.85 mmol, 72%) as a brown powder.

m.p. 203 °C (^{i}PrOH) (lit.[140] 204 °C).

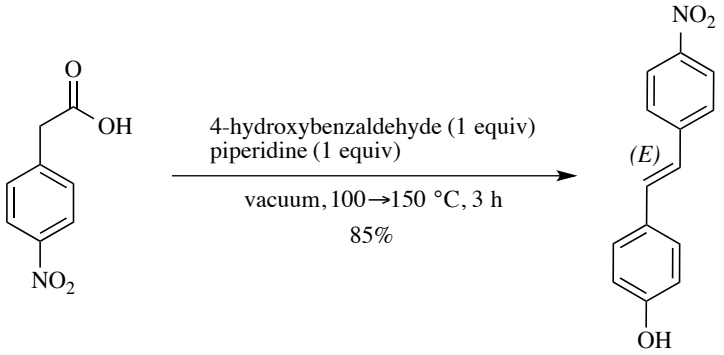

59 **55**

4-Nitrophenylacetic acid **59** (1.81 g, 10.0 mmol), piperidine (1 mL, 10.0 mmol) and 4-hydroxybenzaldehyde (1.22 g, 10.0 mmol) were mixed in a 25 mL two-neck round-bottomed flask with condenser. The reaction was heated at 100 °C under vacuum for 1 hour and for an additional 2 hours at 150 °C. An aqueous solution of NaOH (6 M, 10 mL) was added at room temperature. The mixture was heated at 70 °C for 30 minutes and cooled to 0 °C for the addition of concentrated HCl (36%) to neutralise the pH of the solution. The resulting yellow solid **55** was filtered and dry under reduce pressure (2.05 g, 8.5 mmol, 85 %).

m.p. 199 °C (water).

8.6 Incorporation of derivatives of triethylene glycol into phenols

4-(2-(2-(2-Hydroxyethoxy)ethoxy)ethoxy)benzaldehyde[118]

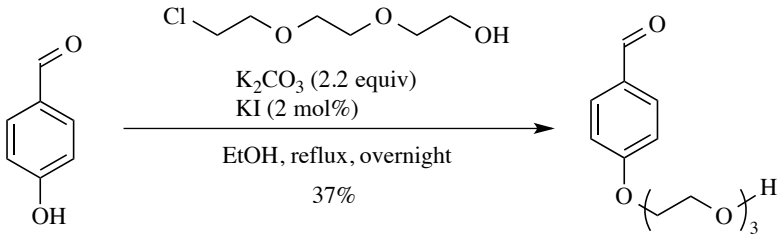

47

To a stirred solution of 4-hydroxybenzaldehyde **47** (398 mg, 3.26 mmol, 1.1 equiv), K_2CO_3 (902 mg, 6.52 mmol, 2.2 equiv) and potassium iodide (10 mg, 60.2 μmol, 2 mol%) in EtOH (5 mL) was added a commercial solution of 2-[2-(2-chloroethoxy)ethoxy]ethanol (0.4 mL, 2.97 mmol). The reaction was heated under reflux overnight and then concentrated under reduced pressure. Deionised water (10 mL) was added to the residual mixture and the aqueous phase was extracted with CH_2Cl_2 (3 x 10 mL). The organic phases were dried over Na_2SO_4 and filtered. The solvents were evaporated under reduced pressure. The mixture was purified by flash chromatography ($CHCl_3$/Petrol, 1:1) to yield the desired compound (276 mg, 1.08 mmol, 37%) as a yellow oil.

^{1}H NMR (400 MHz, $CDCl_3$): δ =9.80 (1 H, s, H_{CHO}), 7.76 (2 H, d, J = 8.7 Hz, H_{Ar}), 6.95 (2 H, d, J = 8.7 Hz, H_{Ar}), 4.23- 4.10 (2 H, m, OCH_2), 3.86- 3.77 (2 H, m, OCH_2), 3.72- 3.50 (8 H, m, OCH_2) ppm.

^{13}C NMR (101 MHz, $CDCl_3$): δ = 191.2 (C), 164.0 (C), 132.3 (CH), 130.3 (CH), 115.1 (CH), 72.8 (CH_2), 71.1 (CH_2), 70.6 (CH_2), 70.0 (CH_2) 67.9 (CH_2), 61.9 (CH_2) ppm.

IR (ν_{max}): 3015, 2930, 2870, 1682, 1600, 1578, 1509, 1427, 1303, 1355, 1217, 1161, 1109, 1058, 909, 833, 729.

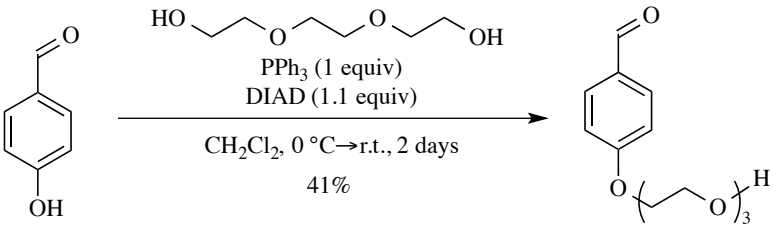

47

To a 1 hour stirred solution of triphenylphosphine (859 mg, 3.28 mmol), 4-hydroxybenzaldehyde **47** (400 mg, 3.28 mmol) and diol (2.38 mL, 20 mmol, 5 equiv) in dry

CH_2Cl_2 (25 mL) was slowly added DIAD (0.71 mL, 3.60 mmol, 1.1 equiv) at 0 °C. After 2 days the solvent was evaporated and the residual mixture was neutralised with a dilute aqueous solution of NaOH (2 M, 10 mL). The aqueous layer was extracted with EtOAc (3 x 20 mL). The combined organic extracts were dried over Na_2SO_4, filtered and evaporated. The resulting mixture was then purified by flash chromatography (EtOAc) to afford the desired aldehyde (341 mg, 1.34 mmol, 41%) as a yellow oil.

(*E*)-2-(2-(2-(4-(4-nitrostyryl)phenoxy)ethoxy)ethoxy)ethanol **60**

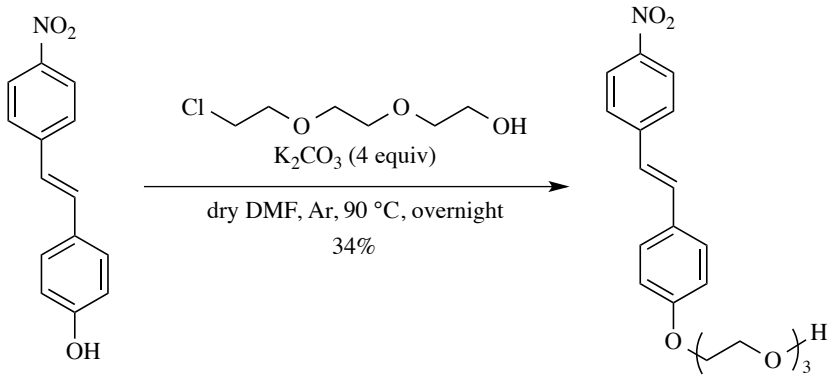

55 **60**

In a 50 mL two-necked round-bottomed flask with condenser under inert atmosphere, was added a commercial solution of 2-[2-(2-chloroethoxy)ethoxy]ethanol (0.15 mL, 3.3 mmol, 1.2 equiv) to a mixture of 4'-hydroxy stilbene **55** (200 mg, 0.83 mmol) with K_2CO_3 (458 mg, 3.3 mmol, 4 equiv) in dry DMF (10 mL). The reaction was stirred at 90 °C overnight and then concentrated *in vacuo*. Deionised water (10 mL) was added to the reaction mixture and the aqueous phase was extracted with CH_2Cl_2 (3 x 15 mL). The combined organic layers were dried over Na_2SO_4 and filtered. The residue was concentrated under reduced pressure and purified by flash chromatography (MeOH/CH_2Cl_2, 1:24). The collected fraction was to obtain the product **60** (104 mg, 0.28 mmol, 34%) as a yellow solid.

m.p. 35 °C.

^{1}H NMR (400 MHz, d^6-acetone): δ = 8.09 (2 H, d, *J* = 8.8 Hz, H_{Ar}), 7.69 (2 H, d, *J* = 8.8 Hz, H_{Ar}), 7.49 (2 H, d, *J* = 8.7 Hz, H_{Ar}), 7.35 (1 H, d, *J* = 16.4 Hz, H_{vinyl}), 7.13 (1 H, d, *J* = 16.4 Hz, H_{vinyl}), 6.88 (2 H, d, *J* = 8.7 Hz, H_{Ar}), 4.10- 3.99 (2 H, m, OCH_2), 3.74- 3.67 (2 H, m, OCH_2), 3.57- 3.37 (6 H, m, OCH_2), 3.18- 3.09 (2 H, m, OCH_2), 2.80 (1 H, br) ppm.

^{13}C NMR (101 MHz, d^6-acetone): δ = 161.3 (C), 148.0 (C), 146.4 (CH), 144.5 (C), 134.7 (CH), 131.0 (C), 130.2 (CH), 128.4 (CH), 125.7 (CH), 116.5 (CH), 74.3 (CH_2), 72.1 (CH_2), 72.0 (CH_2), 71.9 (CH_2), 71.0 (CH_2), 69.2 (CH_2) ppm.

IR (ν_{max}): 2963, 2933, 2876, 1588, 1510, 1456, 1338, 1251, 1176, 1108, 1056, 954, 841, 814, 733.

HRMS (APCI) calculated for $C_{20}H_{23}N_1O_6Na_1$ $[M + Na]^+$ 396.1423 found 396.1421.

(*E*)-2,2,3,3-tetramethyl-12-(4-(4-nitrostyryl)phenoxy)-4,7,10-trioxa-3-siladodecane **61**

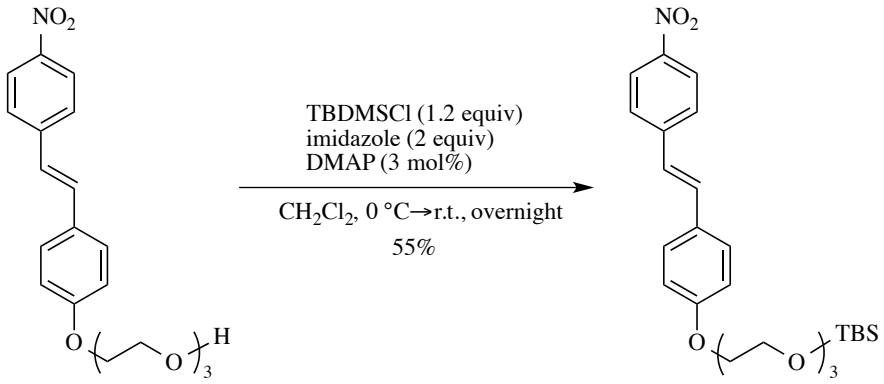

60 **61**

To a stirred solution of stilbene **60** (514 mg, 1.43 mmol), imidazole (132 mg, 1.94 mmol, 1.4 equiv), DMAP (7 mg, 57 μmol, 4 mol%) in CH_2Cl_2 (10 mL), TBSCl (175 mg, 1.16 mmol, 1.2 equiv) was added slowly at 0 °C. The reaction was further stirred at room temperature overnight. The resulting yellow solution was filtered leaving a white solid. After addition of the deionised water (5 mL), the aqueous layer was extracted with CH_2Cl_2 (3 x 10 mL). The combined organic extracts were dried over Na_2SO_4, filtered and concentrated *in vacuo*. The residual mixture was purified by flash chromatography (EtOAc) to yield the title compound **60** (295 mg, 0.79 mmol, 55%) as a yellow solid.

m.p. 35 °C.

^{1}H NMR (500 MHz, $CDCl_3$): δ = 8.20 (2 H, d, *J* = 8.8 Hz, H_{Ar}), 7.59 (2 H, d, *J* = 8.8 Hz, H_{Ar}), 7.48 (2 H, d, *J* = 8.7 Hz, H_{Ar}), 7.21 (1 H, d, *J* = 16.3 Hz, H_{vinyl}), 7.00 (1 H, d, *J* = 16.3 Hz), 6.94 (1 H, d, *J* = 8.7 Hz, H_{Ar}), 4.21- 4.10 (2 H, m, OCH_2), 3.91- 3.86 (2 H, m, OCH_2), 3.77 (2 H, t, *J* = 5.4 Hz, OCH_2), 3.75-3.65 (4 H, m, OCH_2), 3.57 (2 H, t, *J* = 5.4 Hz, OCH_2), 0.89 (9 H, s, ^{t}Bu), 0.06 (6 H, s, $(CH_3)_2$) ppm.

^{13}C NMR (126 MHz, $CDCl_3$): δ = 159.9 (C), 146.8 (C), 144.7 (C), 133.3 (CH), 129.5 (C), 128.7 (CH), 126.9 (CH), 124.5 (CH), 115.4 (CH), 73.1 (CH_2), 71.3 (CH_2), 71.2 (CH_2), 70.0 (CH_2), 67.9 (CH_2), 63.1 (CH_2), 26.3 (CH_3), 18.7 (C), −4.9 (CH_3) ppm.

IR (ν_{max}): 3052, 2953, 2926, 2857, 1607, 1588, 1511, 1338, 1249, 1176, 1108, 954, 836, 814.

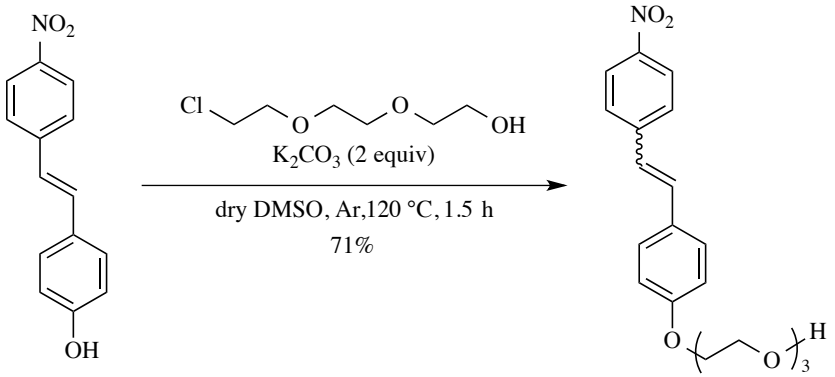

55

The stilbene **55** (115 mg, 4.77 mmol), the ether chain (1.62 mmol, 4.77 mmol) and K_2CO_3 (1.32 g, 9.52 mmol, 2 equiv) were added to a two-necked round-bottomed flask fitted with a condenser under an inert atmosphere. The mixture was stirred in DMSO (5 mL) at 120 °C for 1.5 hours. After addition of an aqueous solution of HCl (2 M, 5 mL) the aqueous layer was extracted with EtOAc (3 x 5 mL). The combined organic layers were dried over Na_2SO_4 and filtered. The solvents were evaporated *in vacuo* to obtain the three ethoxy stilbene as a yellow solid, as an inseparable 15:1 mixture of E/Z isomers.

^{1}H NMR (400 MHz, $CDCl_3$): <u>*E*-isomer:</u> δ = 8.18 (2 H, d, *J* = 8.8 Hz, H_{Ar}), 7.58 (2 H, d, *J* = 8.8 Hz, H_{Ar}), 7.47 (2 H, d, *J* = 8.8 Hz, H_{Ar}), 7.20 (1 H, d, *J* = 16.4 Hz, H_{vinyl}), 6.99 (1 H, d, *J* = 16.4 Hz, H_{vinyl}), 6.93 (2 H, d, *J* = 8.8 Hz, H_{Ar}), 4.19- 4.14 (2 H, m), 3.90- 3.84 (2 H, m), 3.78- 3.58 (8 H, m), 2.96 (1 H, br) ppm.

<u>*Z*-isomer:</u> δ = 7.4 (2 H, d, *J* = 8.8 Hz, H_{Ar}), 7.18 (1 H, d, *J* = 16.4 Hz, H_{vinyl}), 6.85 (2 H, d, *J* = 8.8 Hz, H_{Ar}), 4.27- 4.19 (2 H, m) ppm, only 4 distinct peaks.

(*E*)-2,2,3,3-tetramethyl-12-(4-(4-nitrostyryl)phenoxy)-4,7,10-trioxa-3-siladodecane **61**

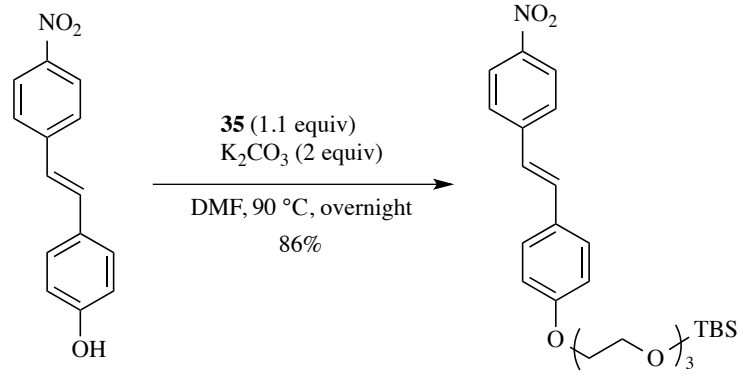

55 **61**

To a solution of stilbene **55** (858 mg, 4.06 mmol) and K_2CO_3 (1.25 g, 9.02 mmol, 2 equiv) in dry DMF (20 mL) was added bis-protected diols **35** (1.89 g, 4.51 mmol, 1.1 equiv).

The reaction was stirred at 90 °C overnight and quenched at room temperature with deionised water (30 mL). The aqueous layer was extracted with EtOAc (3 x 10 mL) and the resulting combined organic phases were dried, filtered and concentrated *in vacuo*. The residual was purified by flash chromatography (Petrol/EtOAc, 2:1) to yield **61** (1.71 g, 3.51 mmol, 86%) as a yellow solid.

^{1}H NMR (500 MHz, d^{6}-acetone): δ = 8.23 (2 H, d, *J* = 8.8 Hz), 7.83 (2 H, d, *J* = 8.8 Hz), 7.63 (2 H, d, *J* = 8.8), 7.49 (1 H, d, *J* = 16.4 Hz), 7.27 (1 H, d, *J* = 16.4 Hz), 7.01 (2 H, d, *J* = 8.8), 4.18 (2 H, t, *J* = 4.8 Hz), 3.84 (2 H, t, *J* = 4.8 Hz), 3.75 (2 H, t, *J* = 5.2 Hz), 3.65 (m, 4 H), 3.52 (2 H, t, *J* = 5.6 Hz), 0.89 (9 H, s), 0.07 (6 H, s) ppm.

^{13}C NMR (126 MHz, d^{6}-acetone): δ = 161.4 (C), 148.1 (C), 146.4 (C), 134.7 (CH), 131.0 (C), 130.2 (CH), 128.5 (CH), 125.7 (CH), 125.6 (CH), 116.6 (CH), 74.2 (CH_2), 72.3 (CH_2), 72.2 (CH_2), 71.1 (CH_2) 69.3 (CH_2), 64.3 (CH_2), 27.1 (CH_3), 19.6 (C), -4.3 (CH_3) ppm.

IR (ν_{max}): 2953, 2926, 2858, 1607, 1588, 1511, 1338, 1249, 1176, 1108, 955, 836, 832

HRMS (APCI) calculated for $C_{26}H_{37}N_1O_6Na_1Si_1$ $[M + Na]^+$ 510.2288 found 510.2275

8.7 **Reduction of the nitro moiety**

General procedure: To a mixture of nitrostilbene **61** in MeOH, a co-solvent was added with a catalytic amount of palladium on charcoal and an excess of $NaBH_4$ at low temperature. The reaction was monitored by TLC analysis. After completion (3 hours), the solution was degased with an ultrasonic bath for 5 minutes. The residual mixture was cooled in liquid nitrogen and filtered through Celite and then concentrated under reduced pressure. After quenching with an aqueous solution of KOH (1 M, 5 mL), the aqueous phase was extracted with Et_2O (3 x 20 mL). The combined organic layers were dried over Na_2SO_4 and filtered. The solvents were evaporated *in vacuo* to obtain the desired aniline derivative **63**.

(*E*)-4-(4-((2,2,3,3-tetramethyl-4,7,10-trioxa-3-siladodecan-12-yl)oxy)styryl)aniline **63**

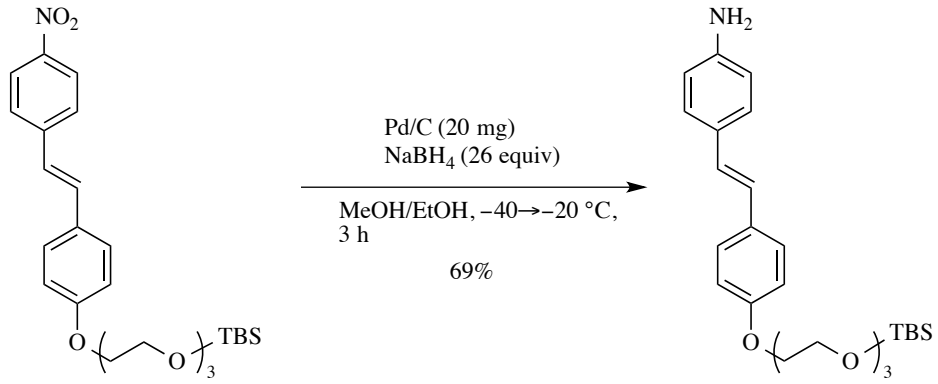

61 **63**

In a 50 mL round-bottomed flask cooled at −40 °C, the stilbene **61** (200 mg, 0.41 mmol) and Pd/C (20 mg) were added to a MeOH/EtOH mixture (25 mL, 4:1). The $NaBH_4$ (400 mg, 10.57 mmol, 26 equiv) was added slowly for 10 minutes at −40 °C. After 2 hours, the reaction mixture was stirred at −20 °C for 1 hour. Following the general procedure the title product was obtained (130 mg, 0.28 mmol, 69%) as a yellow solid.

m.p. 68 °C.

^{1}H NMR (400 MHz, d^6-acetone): δ = 7.48 (2 H, d, *J* = 8.7 Hz, H_{Ar}), 7.32 (2 H, *J* = 8.5 Hz, H_{Ar}), 7.03- 6.89 (4 H, m, H_{Ar} and $(H_{vinyl})_2$), 6.70 (2 H, d, *J* = 8.5 Hz), 4.82 (1 H, br), 4.19-4.14 (2 H, m), 3.88- 3.84 (2 H, m), 3.79 (2 H, t, *J* = 5.2 Hz), 3.72- 3.64 (4 H, m), 3.56 (2 H, t, *J* = 5.2 Hz), 2.91 (1 H, br), 0.93 (9 H, s, ^{t}Bu), 0.11 (6 H, s, $(CH_3)_2$) ppm.

^{13}C NMR (101 MHz, d^6-acetone): δ = 159.7 (C), 149.8 (C), 132.8 (C), 128.9 (CH), 128.6 (CH), 128.1 (CH), 124.8 (C), 116.3 (CH), 116.0 (CH), 74.1 (CH_2), 72.2 (CH_2), 72.2 (CH_2), 71.12 (CH_2), 69.1 (CH_2), 64.3 (CH_2), 27.0 (CH_3), 19.61 (CH_3) ppm.

IR (ν_{max}): 3019, 2930, 2865, 1601, 1511, 1251, 1215, 1161, 1125, 1097, 1036, 935, 834.

HRMS (APCI) calculated for $C_{26}H_{39}N_1O_4Na_1Si_1$ $[M + Na]^+$ 480.246 found 480.246.

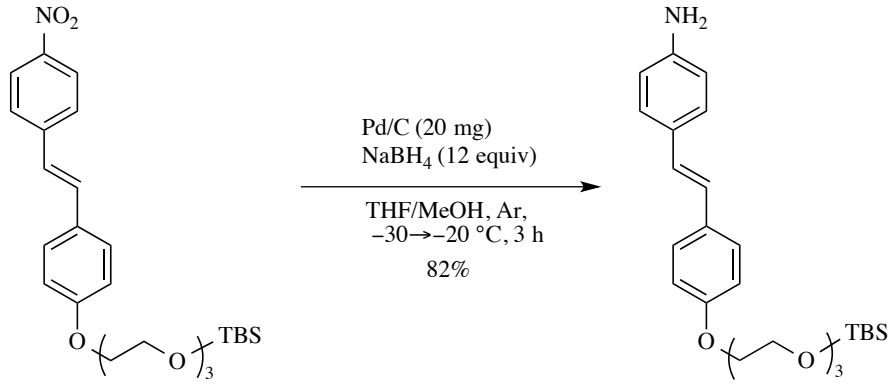

61 **63**

In a 25 mL round-bottomed flask cooled at −30 °C, the stilbene **61** (400 mg, 0.82 mmol) and Pd/C (20 mg) were added to a MeOH/THF mixture (11 mL, 5:6). The $NaBH_4$ (300 mg, 7.9 mmol, 12 equiv) was added slowly for 10 minutes at −40 °C. A balloon of argon was connected to the flask. After 2 hours, the reaction mixture was stirred at −20 °C for 1 hour under an argon atmosphere. Following the general procedure the title product was obtained (130 mg, 0.28 mmol, 69%) as a yellow solid.

9 Radiosyntheses

9.1 Production of [^{18}F]-fluoride with no-carrier-added (nca)

The [^{18}F]-fluoride was produced from an onsite cyclotron (cyclone® 18/9, IBA, Belgium). It was obtained by the bombardment of enriched [^{18}O]-water (>98%, Nukem GmbH, Germany) by following the $^{18}O(p,n)^{18}F$ nuclear reaction.

9.2 General procedure for microfluidic [^{18}F]-fluorination

The QMA cartridge was preconditioned with an aqueous solution of $NaHCO_3$ (1 M, 5 mL, ABX) and washed with deionised water (10 mL). The Kryptofix solution used was purchased from ABX (K[2.2.2] (22.6 mg, 60.0 μmol) and K_2CO_3 (4.2 mg, 30.4 μmol) in acetonitrile (300 μL) and deionised water (300 μL)) or unless otherwise stated. The radiolabeling process was described in several steps. The final step of the synthesis was the measurement of the radioactivity by the dose calibrator and the analysis of the radioactive mixture by radio-TLC. The [^{18}F]-fluorination occurred in a PEEK loop tubing (length = 3 m, ∅ = 0.5 mm, Vici, Switzerland) unless otherwise mentioned. Each reaction was performed by using the same amount of mannose triflate **9** (25 mg, 52 μmol).

9.3 Procedure for formation of peracetylated [^{18}F]-deoxy-glucose 14 using loop system

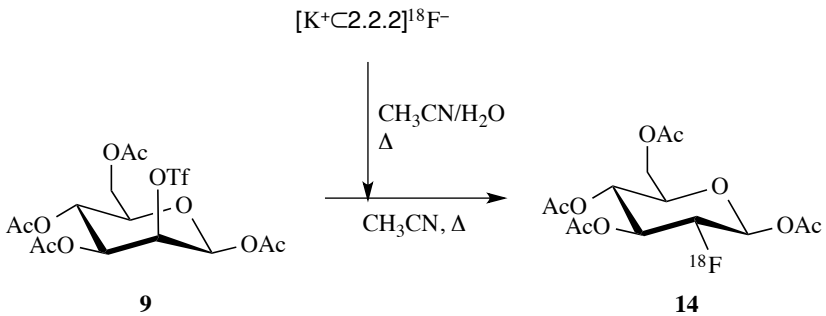

9 **14**

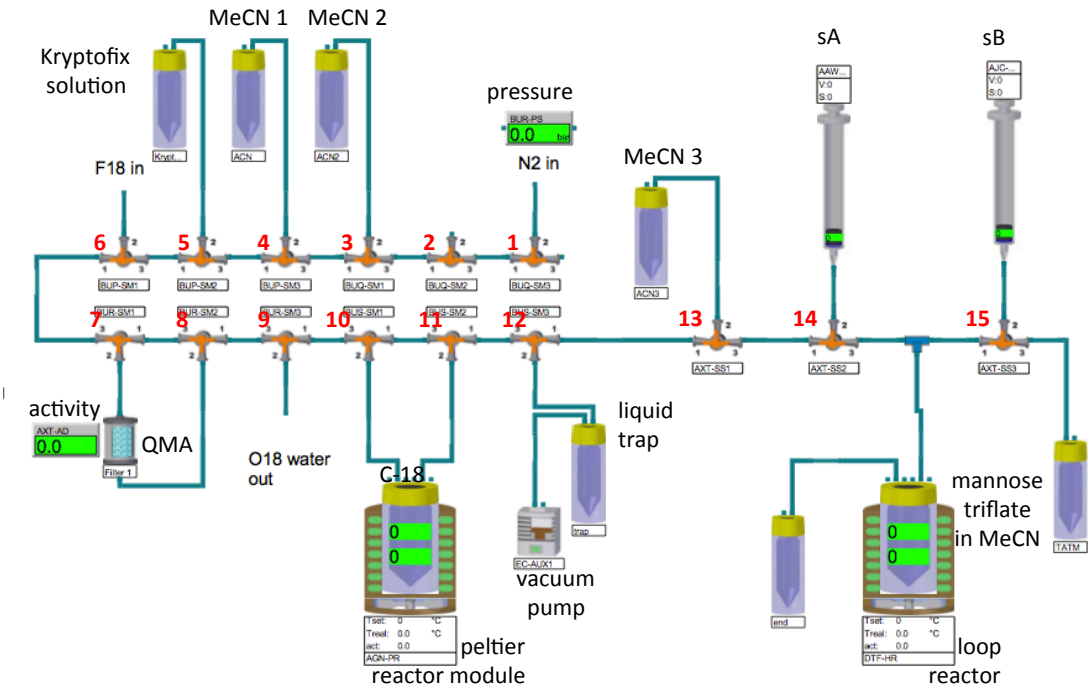

Experiment 1 to 3

Entry	Activity received (GBq)	Process time (min)	Recovery of activity, decay-corrected (%)
1	1.5	34	19
2	1.5	30	27
3	1.5	30	23

Procedure A:

Step 1: The aqueous [^{18}F]-fluoride was delivered from the cyclotron to the synthesiser at the intersection 6 by following the path 6, 7, 8, 9. The aqueous mixture passed through a QMA cartridge to trap the [^{18}F]-fluoride and transferred the [^{18}O]-water to the waste vial (O18 water). A flow of nitrogen from the intersection 1 was applied to dry the [^{18}F]-Fluoride for 80 seconds.

Step 2: The ABX Kryptofix solution passed through the QMA cartridge to form the [$K^+ \subset 2.2.2$]$^{18}F^-$ complex. This complex was then eluted into the V-shape reactor vial for 35 seconds at room temperature (switching valves 5, 7, 8, 10, 11, 12).

Step 3: The drying process occurred at 90 °C for 2 minutes in the Peltier reactor module. The azeotropic distillation was performed with 2 vials of MeCN (2 x 1 mL). One vial of MeCN (MeCN 1) was eluted to the reaction mixture heated at 55 °C. The mixture was maintained at 55 °C for 30 seconds and for an additional 90 seconds at 95 °C under reduced pressure and nitrogen flow. This sequence was repeated once with another 1 mL of acetonitrile (MeCN 2).

Step 4: Syringe A transferred the acetonitrile (2 mL, MeCN 3) to the reactor vial heated at 35 °C. The $[K^+ \subset 2.2.2]^{18}F^-$ complex dissolved in acetonitrile was transferred into syringe A. The mannose triflate **9** in MeCN (2 mL) was transferred to syringe B.

Step 5: Both solutions were mixed together *via* a T-mixer (ETFE). The reaction took place in the loop (double helix, length = 3 m, ∅ = 0.5 mm) heated at 80 °C in the loop reactor. The overall flow rate of the radiolabeling occurred at 14 µL/s (7 µL/s per syringe).

Experiments 4 and 5

Entry	Activity received (GBq)	Process time (min)	Recovery of activity, decay-corrected (%)
4	1.8	34	30
5	1.5	30	37

Procedure B: based on the procedure A, the reactions 4 and 5 were performed with a different Step 3.

Step 3: The drying process occurred at 90 °C for 2 minutes in the Peltier reactor module. The azeotropic distillation was performed with 2 vials of MeCN (2 x 1 mL). One vial of MeCN (MeCN 1) was eluted to the reaction mixture heated at 55 °C. The mixture was heated at 55 °C for 30 seconds and for an additional 90 seconds at 90 °C under reduced pressure and nitrogen flow. This sequence was repeated once with another 1 mL of acetonitrile (MeCN 2).

9.4 Procedure using microfluidic technology for the [^{18}F]-FDG 1 in continuous flow

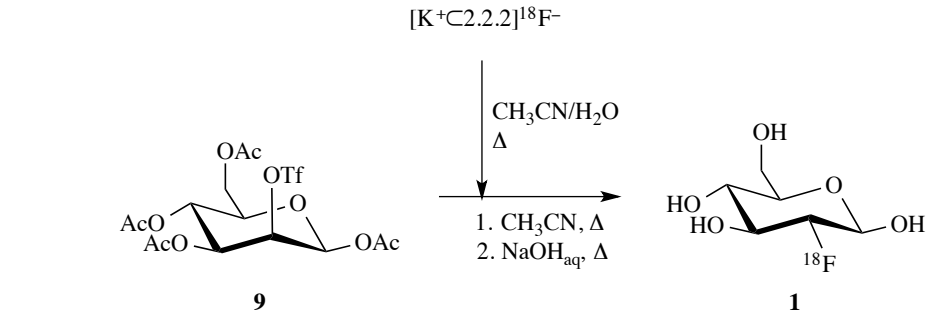

9 **1**

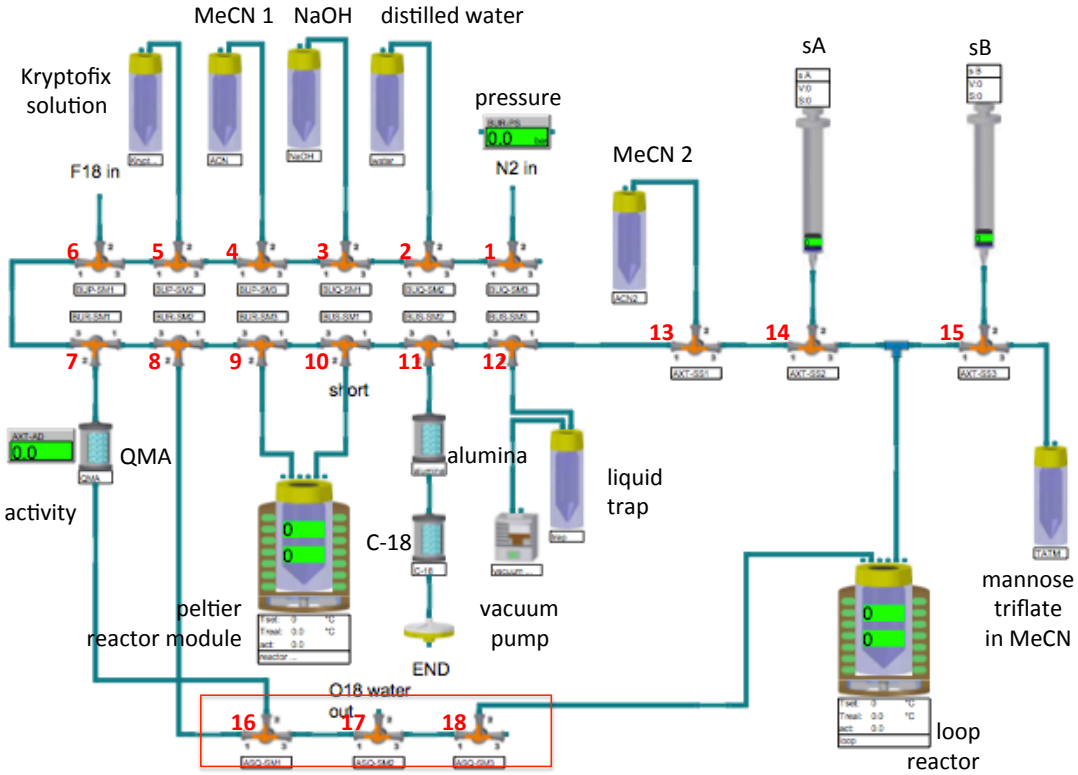

Experiment 6 to 8

Entry	Activity received (GBq)	Process time (min)	Recovery of activity, decay-corrected (%)
6	3.0	38	10
7	2.4	34	18
8	1.5	36	14

Procedure C:

Step 1: The aqueous [^{18}F]-fluoride was delivered from the cyclotron to the QMA cartridge by following the path 6, 7, 16, 17. The [^{18}O]water was collected in a vial at the intersection 17. The [^{18}F]-fluoride was dried for 80 seconds under nitrogen pressure.

Step 2: The commercial Kryptofix solution (ABX) was eluted through the QMA cartridge and then transferred to the Peltier module in a V-shape glass vial at room temperature for 35 seconds under reduced pressure (switching valves 5, 7, 16, 8, 9, 10, 12).

Step 3: The Peltier module heated the reaction mixture at 70 °C for 50 seconds under negative pressure and for an additional 70 seconds under reduced and nitrogen pressure (switching valves 10, 12). The azeotropic distillation occurred at 55 °C with the elution of the dry acetonitrile (MeCN 1) under reduced pressure (switching valve 4, 9, 10, 12). The reaction mixture was heated at 95 °C for 50 seconds under negative pressure and for an additional 20 seconds under reduced pressure and nitrogen flow (switching valves 1, 9, 10, 12).

Step 4: The heated $[K^{+}\subset 2.2.2]^{18}F^{-}$ complex (39 °C) was transferred to syringe A *via* the dry acetonitrile (1.5 mL) present in the MeCN 2 vial (switching valves 13, 14, 9). The mannose triflate dissolved in dry MeCN (1.5 mL) was transferred to syringe B (switching valve 15).

Step 5: Both solutions were mixed together *via* a T-mixer. The reaction took place in the loop heated at 85 °C in the loop reactor. The overall flow rate of the radiolabeling was 14 µL/s (switching valves 14 and 15). The resulting mixture was transported into the reactor vial (switching valves 18, 16, 8, 9, 10, 12).

Step 6: The deprotection step occurred at 50 °C in the Peltier module after the addition of the NaOH solution (1 M, 1 mL) for 50 seconds under reduced pressure (switching valves 3, 9, 10, 12). The addition of distilled water (4 mL) to the crude mixture was performed by syringe A. The purification of this mixture through the alumina and C-18 cartridges was provided by using syringe A (switching valves 2, 9, 14).

Experiment 9 to 11

Entry	Activity received (GBq)	Process time (min)	Recovery of activity, decay-corrected (%)
9	1.1	30	68
10	1.85	33	52
11	1.1	30	64

The 5 mL V-shape vial was replaced by a 7 mL flat PEEK vial.

Procedure D: based on the procedure C, the reactions 9 to 11 were performed with a different Step 2.

Step 2: The commercial Kryptofix solution (ABX) was eluted through the QMA cartridge and then transferred to the Peltier module in a flat bottom PEEK vial at room temperature for 35 seconds under reduced pressure (switching valves 5, 7, 16, 8, 9, 10, 12).

9.5 Procedure for synthesis of peracetylated [^{18}F]-deoxy-glucose 14 in segmented flow with presence of an ionic liquid.

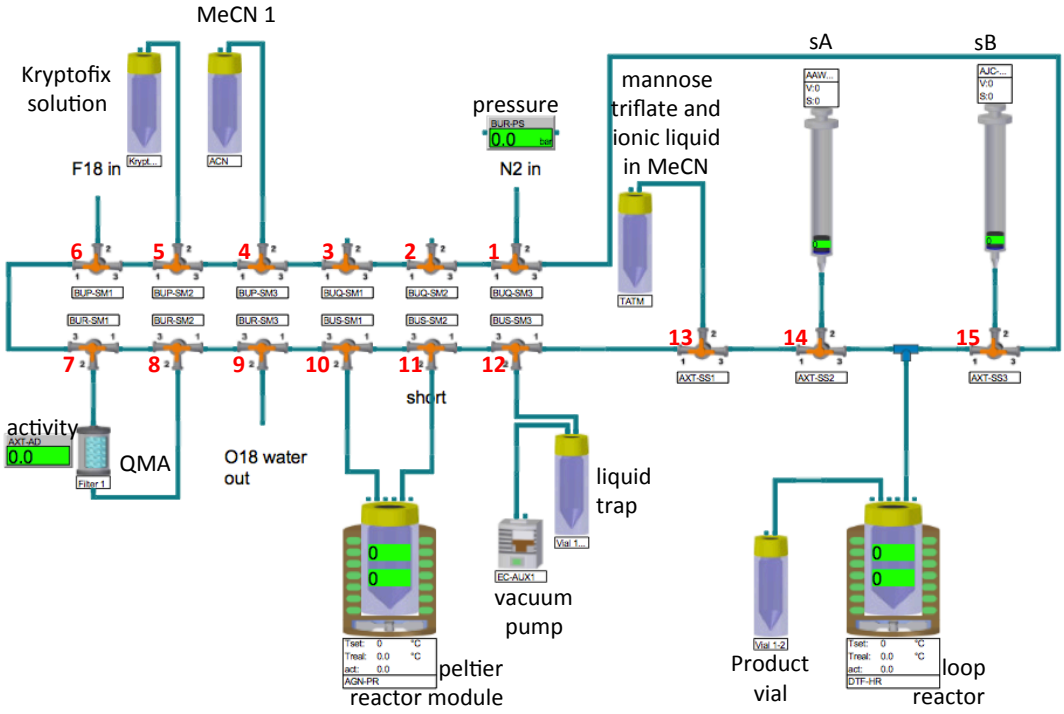

Entry	Activity received (GBq)	Process time (min)	Recovery of activity, decay-corrected (%)	Radiochemical conversion (%)
12	3.3	38	69	5
13	1.3	30	—	54

Experiment 12

Procedure E:

Step 1: The aqueous [^{18}F]-fluoride was introduced to the system *via* the F18 in path to the QMA cartridge (switching valves 6, 7, 8 and 9). At the end of the delivery the cartridge was dried over nitrogen flow for 50 seconds (switching valves 6, 1, 7, 8 and 9).

Step 2: The commercial Kryptofix solution was withdrawn through the QMA cartridge and then to the reactor vessel under reduced pressure for 1 minute (switching valve 5, 7, 8, 10, 11 and 12).

Step 3: The $[K^{+}\subset 2.2.2]^{18}F^{-}$ complex was heated at 100 °C under reduced pressure for 50 seconds (switching valves 11 and 12). The drying process continued with the addition of a nitrogen pressure into the reactor vial for 70 seconds (switching valves 1, 10, 11 and 12).

Step 4: The acetonitrile was driven into the 50 °C reactor vial by using a negative pressure (switching valves 4, 10, 11 and 12). The reaction mixture was then heated at 110 °C under reduced pressure for 80 seconds (switching valves 11 and 12). The temperature was increased to 120 °C for 1 minute. An additional 80 seconds of drying was performed under negative and nitrogen flow (switching valves 1, 10, 11 and 12).

Step 5: The mannose triflate solution in dry acetonitrile (1.5 mL) with BMI(OTf) (300 μL, 1.6 mmol) was added into the reactor vessel heated at 43 °C by syringe A. The reaction mixture was then withdrawn into syringe A (switching valves 13, 14 and 10). Syringe B was filled with nitrogen gas (switching valves 1 and 15).

Step 6: The two phases were injected simultaneously to the loop heated at 95 °C with an overall flow rate of 14 μL/s.

Experiment 13

Procedure F: based on the procedure E, the reaction 13 was performed with a different Step 4.

Step 4: The acetonitrile was driven into the 50 °C reactor vial by using a negative pressure (switching valves 4, 10, 11 and 12). The reaction mixture was then heated at 110 °C under reduced pressure for 80 seconds (switching valves 11 and 12). The temperature was increased to 125 °C for 1 minute. An additional 80 seconds of drying was performed under negative and nitrogen flow (switching valves 1, 10, 11 and 12).

9.6 **Segmented technique used for [^{18}F]-fluorination of mannose triflate 9 performed in different loop sizes.**

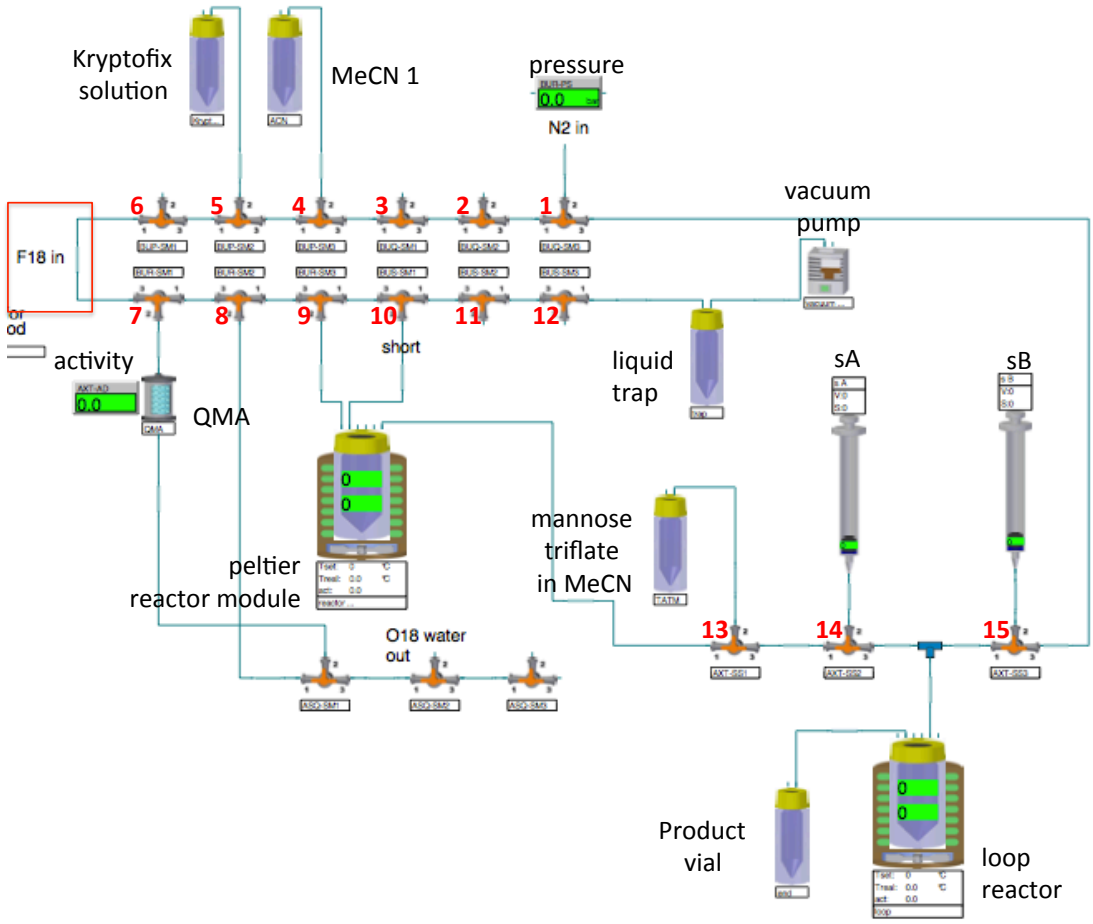

Entry	Activity received (GBq)	Process time (min)	Recovery of activity, decay-corrected (%)	Radiochemical conversion (%)
14	1.2	35	40	54

Procedure F:

Step 1: The aqueous [^{18}F]-fluoride was introduced to the system *via* the "F18 in" path to the QMA cartridge (switching valves 6, 7, 16, and 17). At the end of the delivery, the cartridge was dried over nitrogen flow for 50 seconds (switching valves 6, 1, 7, 16 and 17).

Step 2: The Kryptofix solution was withdrawn through the QMA cartridge and then to the reactor vessel under reduced pressure for 1 minute (switching valve 5, 7, 16, 8, 10, 11 and 12).

Step 3: The $[K^{+}\subset 2.2.2]^{18}F^{-}$ complex was heated at 120 °C under reduced pressure for 50 seconds (switching valves 10 and 12) and for an additional 70 seconds under negative and nitrogen pressure (switching valves 10, 12, 1 and 10). The dry acetonitrile (1 mL, MeCN 1) placed above the intersection 4 was driven into the reactor vial heated at 80 °C for 15 seconds under negative pressure (switching valves 5, 9, 10 and 12). The reaction mixture was heated at 110 °C over 80 seconds and for an additional 1 minute at 130 °C under reduced pressure (switching valves 10 and 12). The azeotropic distillation carried on at the same temperature for 80 seconds under reduced pressure and nitrogen flow (switching valves 1, 9, 10, 11 and 12).

Step 4: The mannose triflate solution in dry acetonitrile (1.5 mL) was added into the reactor vessel heated at 43 °C by syringe A. The reaction mixture was then withdrawn into syringe A (switching valves 13, 14 and 10). Syringe B was filled with nitrogen gas (switching valves 1 and 15).

Step 5: The two phases were injected simultaneously into the PEEK loop (length = 3 m, ∅ = 0.5 mm) heated at 100 °C with an overall flow rate of 14 µL/s.

Experiment 15

Entry	Activity received (GBq)	Process time (min)	Recovery of activity, decay-corrected (%)	Radiochemical conversion (%)
15	1.2	102	21	74

Procedure G: based on the procedure F, the reaction 15 was performed with a different Step 5.

Step 5: The two phases were injected simultaneously into the first PEEK loop (length = 3 m, ∅ = 0.5 mm) heated at 100 °C. Then the reaction mixture passed through the second PEEK loop (length = 3 m, ∅ = 0.5 mm) directly connected at one edge of the first loop and heated at 75 °C in a water bath. The overall flow rate of the reaction was 14 µL/s.

Experiment 16

Entry	Activity received (GBq)	Process time (min)	Recovery of activity, decay-corrected (%)	Radiochemical conversion (%)
16	1.2	36	27	62

Procedure H: based on the procedure G, the reaction 16 was performed with a different Step 5.

Step 5: The two phases were injected simultaneously into a longer and smaller PEEK loop (length = 5 m, ∅ = 0.01 mm) heated at 100 °C. The overall flow rate of the reaction was 14 µL/s.

9.7 Semi-automated radiosynthesis performed with the minimum of check valves

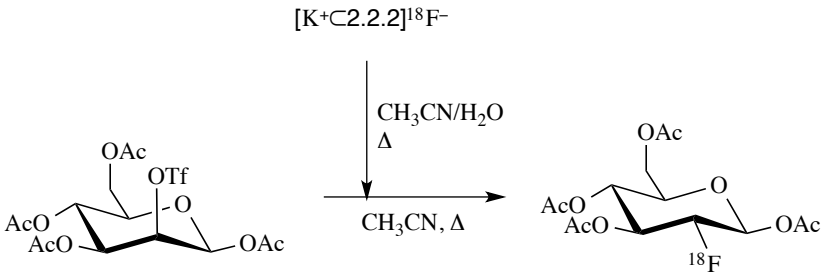

c **9** **14**

The configuration of the synthesiser was modified by using one new module (Hamilton device), check valves (C V) and luer connectors.

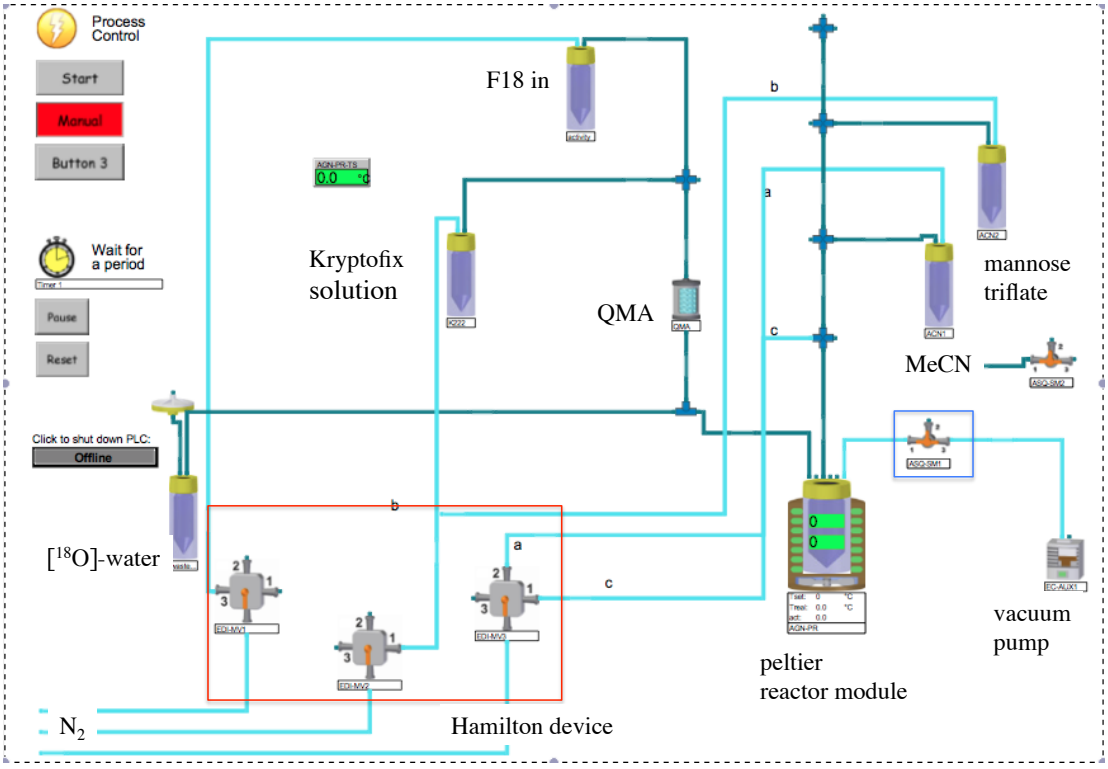

Experiment 17

Entry	Activity received (GBq)	Process time (min)	Recovery of activity, decay-corrected (%)	Radiochemical conversion (%)
17	1.5	36	67	36

Procedure I:

Step 1: The aqueous [^{18}F]-fluoride was eluted through the QMA cartridge *via* a nitrogen stream applied on the top of the vial having the radioactivity (F18 in). The [^{18}O]-water was

driven to the waste vial by using a nitrogen flow (e). This sequence was performed over 105 seconds. The QMA cartridge was dried over a nitrogen (K222 and e) flow for 270 seconds.

Step 2: The Kryptofix solution was driven through the QMA cartridge and into the reactor vial (5 mL, PP) under nitrogen flow and reduced pressure directly applied from the K222 vial and from the reactor vial, respectively. This elution took place for 15 seconds and the reactor vial was heated to 50 °C.

Step 3: The azeotropic distillation started with the addition of 1 mL of dry acetonitrile to the reactor vial under reduced pressure and nitrogen flow (a) for 15 seconds. The reaction mixture was heated to 95 °C over 105 seconds under nitrogen (c) and reduced pressure. Another 1 mL of acetonitrile was added into the reactor vessel still heated at 95 °C. The solvents were evaporated for 150 seconds under reduced pressure and nitrogen (b and c) flow.

Step 4: The mannose triflate solution in dry acetonitrile (1.2 mL) was added into the reactor vessel heated at 85 °C under reduced pressure and nitrogen (d) stream for 20 seconds. The reaction mixture was heated at 90 °C over 180 seconds under both reduced and nitrogen (c) pressure.

Experiments 18 and 19

Some luer connectors were replaced by a 1-way cassette to drive away the [^{18}O]-water and to perform the elution of [K^+⊂2.2.2]$^{18}F^-$ complex into the reactor vial. Two Tefzel® tees were connected to the mannose triflate vial and the aqueous solution of NaOH by replacement of luer connectors.

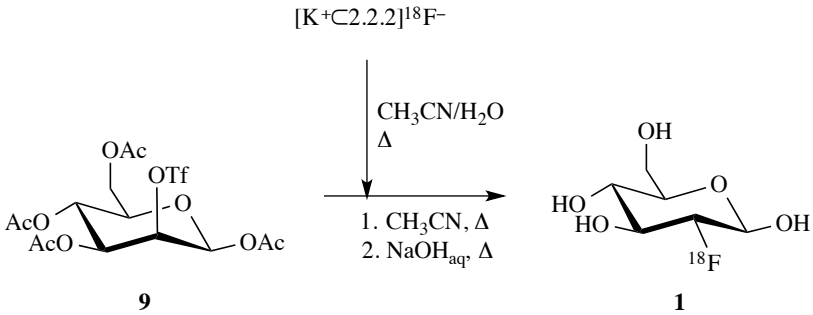

9 **1**

Entry	Activity received (GBq)	Process time (min)	Recovery of activity, decay-corrected (%)	Radiochemical conversion (%)
18	1.5	109	85	19
19	0.9	32	44	91

Procedure J:

Step 1: The aqueous [^{18}F]-fluoride was eluted through the QMA cartridge *via* a nitrogen stream applied on the top of the vial containing the radioactivity (F18 in). The [^{18}O]-water was driven to the waste vial by using a nitrogen flow (e). This sequence was performed over 105 seconds. The QMA cartridge was dried over a nitrogen (K222 and e) flow for 270 seconds.

Step 2: The Kryptofix solution was driven to the QMA cartridge and into the reactor vial (5 mL, glass and flat) under nitrogen flow and reduced pressure directly applied from the K222 vial and from the reactor vial, respectively. This elution took place for 15 seconds and the reactor vial was heated to 50 °C.

Step 3: The azeotropic distillation started with the addition of 1 mL of dry acetonitrile to the reactor vial under reduced pressure and nitrogen flow (a) for 15 seconds. The reaction mixture was heated to 105 °C over 240 seconds under nitrogen (c) and reduced pressure. Another 1 mL of acetonitrile was added into the reactor vessel and the solvents were evaporated for 1 minute under reduced and nitrogen (b and c) flow at 90 °C.

Step 4: The mannose triflate solution in dry acetonitrile (1 mL) was added to the reactor vessel heated at 85 °C under reduced pressure and nitrogen (d) stream for 20 seconds. The reaction mixture was heated at 100 °C for 300 seconds under both reduced and nitrogen (c) pressure.

Experiment 20

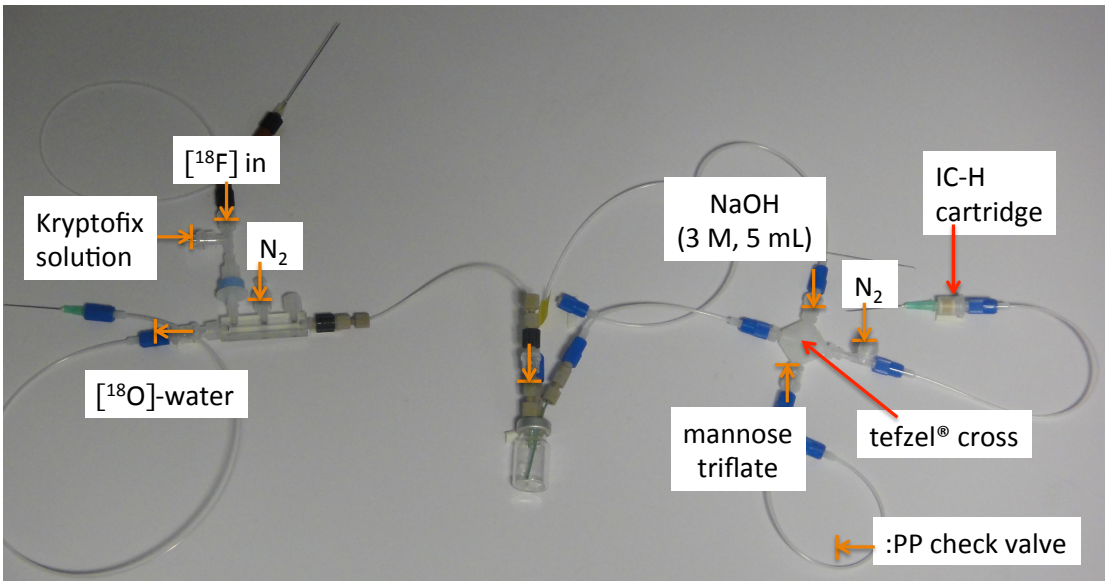

Entry	Activity received (GBq)	Process time (min)	Recovery of activity, decay-corrected (%)	Radiochemical conversion (%)
20	1.4	26	37	74

Procedure K: based on the procedure J, the reaction 20 was performed with a different Step 3.

Step 3: The evaporation of the solvents occured at 105 °C for 390 seconds under reduced and nitrogen (e) flow and for an additional 210 seconds at 110 °C.

Experiment 21

The 5 mL flat glass reactor vial was replaced by a 5 mL flat plastic vial (PP).

Entry	Activity received (GBq)	Process time (min)	Recovery of activity, decay-corrected (%)	Radiochemical conversion (%)
21	1.2	29	20	26

Procedure L: based on the procedure K, the reaction 21 was performed with a 5 mL plastic flat vial (PP) instead of a 5 mL glass vial.

Experiment 22 and 24

Entry	Activity received (GBq)	Process time (min)	Recovery of activity, decay-corrected (%)	Radiochemical conversion (%)
22	1.1	32	59	20
23	1.0	27	57	32
24	1.2	28	35	72

Procedure M: based on the procedure K, the reactions 22 to 24 were performed with the nitrogen input c directly connected through the seal of the reactor vial.

9.8 Radiolabeling syntheses performed with a Kryptofix solution prepared with 100 µL of deionised water

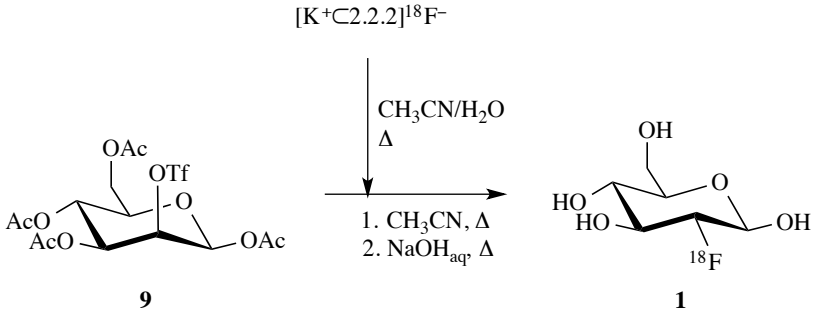

9 **1**

Entry	Activity received (GBq)	Process time (min)	Recovery of activity, decay-corrected (%)	Radiochemical conversion (%)
25	1.1	32	50	66
26	1.5	32	59	70
27	1.6	30	59	79
28	0.9	29	54	50

Experiments 25 to 27

Procedure N:

Step 1: The elution of the aqueous [^{18}F] proceeded at room temperature for 2 minutes. Two flows of nitrogen (g and f) were applied to guide the [^{18}F]-fluoride and the [^{18}O]-water to the QMA cartridge. The [^{18}O]-water continued to the [^{18}O]-water waste vial.

Step 2: The elution of the [^{18}F]-fluoride was performed by the prepared Kryptofix solution to the heated reactor vial (65 °C). A nitrogen flow (K[222]) and negative pressure (vacuum) were used.

Step 3: The azeotropic distillation started with the addition of 500 µL of dry acetonitrile to the reactor vial under reduced pressure and nitrogen flow (a) for 15 seconds. The reaction mixture was heated to 105 °C over 360 seconds under reduced pressure. The [K^+⊂2.2.2]$^{18}F^-$ complex was dried for an additional 240 seconds under both reduced and nitrogen (c) pressure.

Step 4: The radiolabelling occurred at 50 °C with the transfer of the mannose triflate solution in dry MeCN (1.2 mL) to the reactor vessel by flows of nitrogen (d and c). The reactor vessel was then heated at 105 °C for 240 seconds under nitrogen pressure (e). At similar

temperature, the procedure continued with negative (vacuum) and positive (e) pressure for 180 seconds.

Step 5: The aqueous solution of NaOH (3 M, 3 mL) was transported to the reactor vessel heated at 55 °C by nitrogen flow (b and c). The hydrolysis took place over 3 minutes. The elution of the crude mixture to the IC-H cartridge and then to the product vial was performed *via* nitrogen flow (e).

Experiment 28

Procedure O: based on the procedure K, the drying process of the reactions 28 was performed without addition of dry acetonitrile (500 μL).

9.9 Semi-automated E&Z platform using anhydrous Kryptofix solution

The Kryptofix solution was prepared with K[2.2.2] (24 mg, 63.7 μmol), K_2CO_3 (4 mg, 28.9 μmol) in anhydrous MeOH (600 μL). The mannose triflate (25 mg, μmol) in dry CH_3CN (1.1 mL).

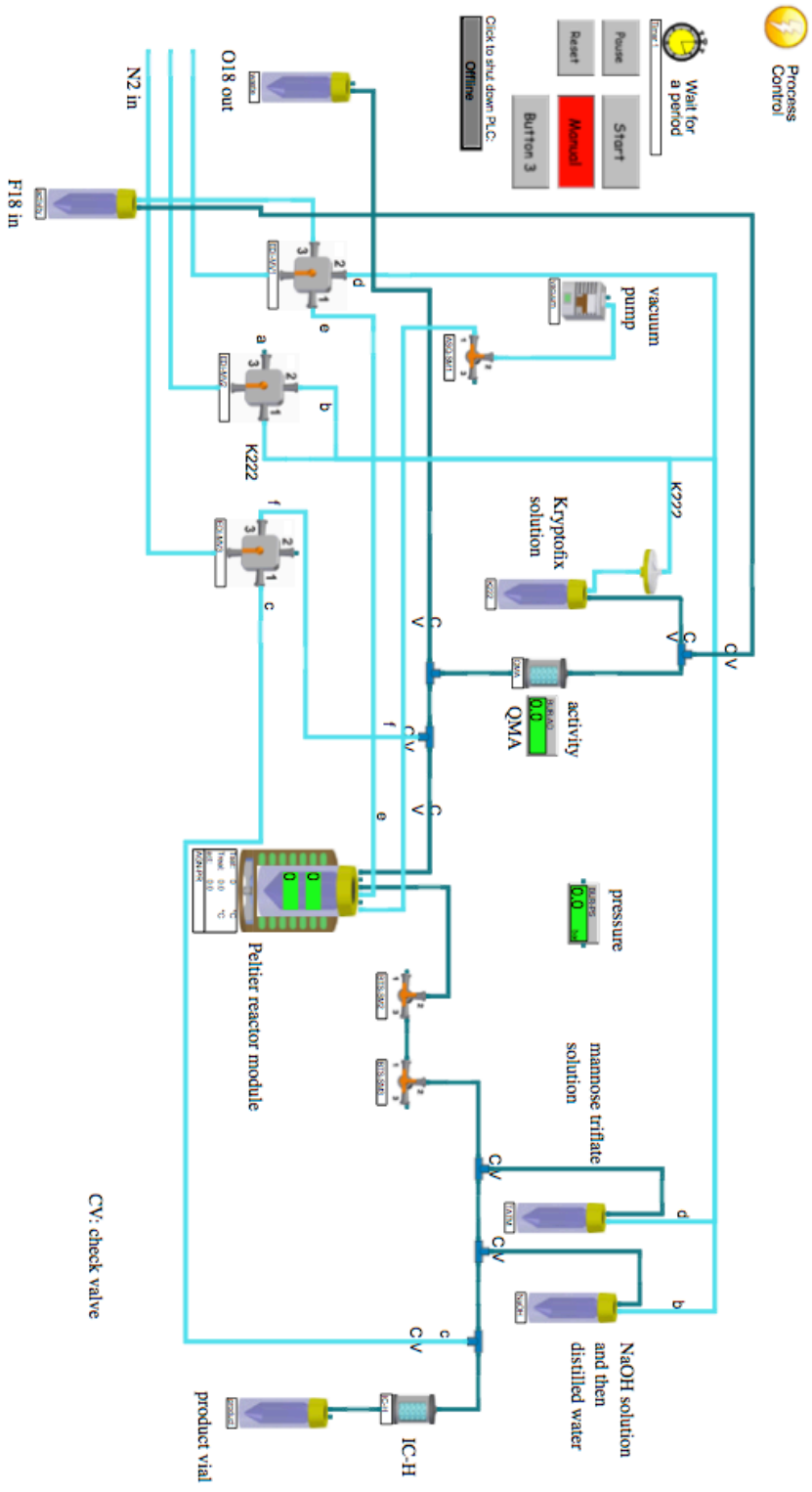

Entry	Activity received (GBq)	Process time (min)	Recovery of activity, decay-corrected (%)	Radiochemical conversion (%)
31	1.6	28	33	73
32	1.2	30	39	50
33	1.6	34	55	32

Experiment 31

Procedure P:

Step 1: The elution of the aqueous [^{18}F] proceeded at room temperature for 2 minutes. Two flows of nitrogen (g and f) were applied to guide the [^{18}F]-fluoride and the [^{18}O]-water to the QMA cartridge. The [^{18}O]-water continued to the to the [^{18}O]-water waste vial.

Step 2: The elution of the [^{18}F]-fluoride was performed by the Kryptofix solution to the heated reactor vial (65 °C). A nitrogen flow (K[222]) and negative pressure (vacuum) were used.

Step 3: The drying process commenced at 105 °C for 200 seconds under flow of nitrogen (e). The sequence carried on at 110 °C under reduced pressure (vacuum) for 90 seconds and finished at 110 °C under flow of nitrogen (e) and reduced pressure (vacuum) for 130 seconds.

Step 4: The radiolabelling occurred at 50 °C with the transfer of the mannose triflate solution in dry MeCN (1 mL) to the reactor vessel by flows of nitrogen (d and c). The reactor vessel was then heated at 105 °C for 100 seconds under nitrogen pressure (e). At similar temperature, the procedure continued with negative (vacuum) and positive (e) pressure for 2 minutes seconds.

Step 5: The aqueous solution of NaOH (3 M, 3 mL) was transported to the reactor vessel heated at 65 °C by nitrogen flows (b and c). The elution of the crude mixture to the IC-H cartridge and then to the product vial was performed *via* nitrogen flow (e).

Experiment 32

Procedure Q: based on the procedure M, the reaction 32 was performed with different steps 3 and 4.

Step 3: The drying process was commenced at 105 °C for 3 minutes under flow of nitrogen (e). The sequence carried on at 110 °C under reduced pressure (vacuum) for 100 seconds and finished at 110 °C under flow of nitrogen (e) and reduced pressure (vacuum) for 100 seconds.

Step 4: The radiolabelling occurred at 50 °C with the transfer of the mannose triflate solution in dry MeCN (1 mL) to the reactor vessel by flows of nitrogen (d and c). The reactor vessel was then heated at 95 °C for 160 seconds under nitrogen pressure (e). At similar temperature, the procedure continued with negative (vacuum) and positive (c) pressure for 100 seconds and the input of nitrogen pressure was replaced by the one placed on the top of the reactor vessel (e) for 2 minutes.

Experiment 33

Procedure R: based on the procedure M, the reaction 33 was performed with different steps 3 and 4.

Step 3: The drying process commenced at 105 °C for 3 minutes under flow of nitrogen (e). The sequence carried on at 110 °C under reduced pressure (vacuum) for 100 seconds and finished at 110 °C under flow of nitrogen (e) and reduced pressure (vacuum) for 2 minutes.

Step 4: The radiolabelling occurred at 50 °C with the transfer of the mannose triflate solution in dry MeCN (1 mL) to the reactor vessel by flows of nitrogen (d and c). The reactor vessel was then heated at 95 °C for 160 seconds under nitrogen pressure (e). At 105 °C, the procedure continued with negative (vacuum) and positive (c) pressure for 2 minutes and the input of nitrogen pressure switched by the one placed on the top of the reactor vessel (e) for 2 minutes.

11 Low concentration of water for Kryptofix solution

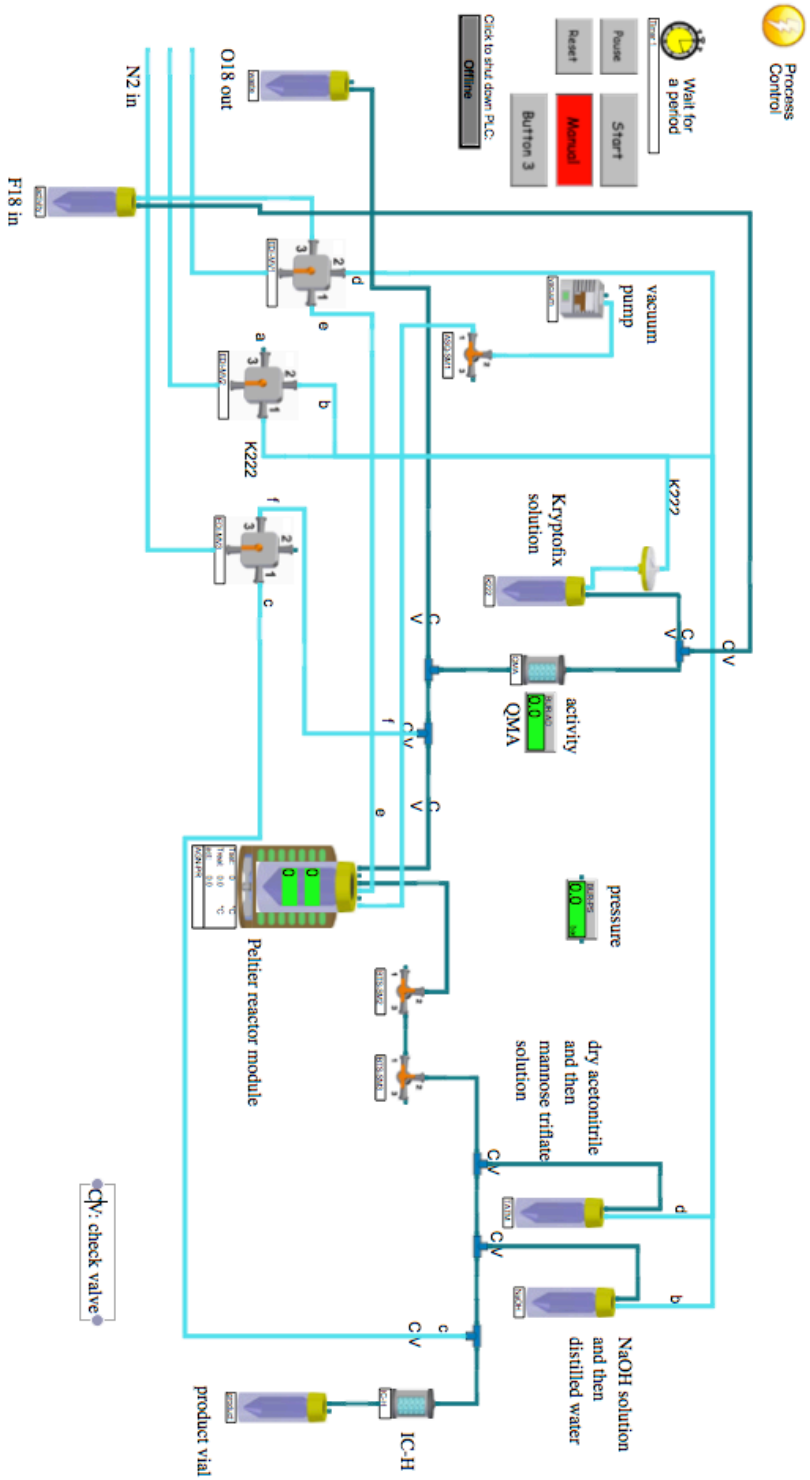

Entry	Activity received (GBq)	Process time (min)	Recovery of activity, decay-corrected (%)	Radiochemical conversion (%)
34	1.6	32	—	82
35	1.5	28	48	8
36	1.7	29	53	67
37	0.4	26	20	84
38	2.0	28	**56**	**77**
39	1.5	33	89	25

Experiment 34

Procedure S:

Step 1: The aqueous [^{18}F-fluoride] was eluted from the "F18 in" vial to the QMA cartridge *via* nitrogen flow applied directly to the "F18 in" vial (activity) for 1 minute. The [^{18}F] was loaded in the QMA cartridge and the [^{18}O]-water was collected in the [^{18}O]-water waste vial by nitrogen pressure (f) for 1 minute.

Step 2: The Kryptofix solution was transferred through the QMA cartridge to unload the [^{18}F]-fluoride and to the reactor vessel heated at 65 °C (30 seconds).

Step 3: The drying process commenced at 105 °C under nitrogen flow (e) for 250 seconds. At 90 °C the dry acetonitrile (500 μL) was transported to the reactor vial for 15 seconds. The reaction mixture was then heated at 105 °C under vacuum for 100 seconds and for an additional 2 minutes under vacuum and nitrogen flow (e).

Step 4: The mannose triflate in 1 mL of acetonitrile replaced the empty acetonitrile vial used in Step 3. The mannose triflate was then transferred to the reactor vial heated at 65 °C. The crude mixture was heated at 95 °C under nitrogen flow (e) for 200 seconds. An additional 140 seconds was performed at 105 °C under negative pressure and nitrogen flow (c).

Step 5: Cooled at 55 °C, the NaOH solution (3 M, 3 mL) was added to the reaction mixture (40 seconds) by an applied nitrogen pressure (d). Afterwards the solution was mixed under nitrogen pressure (e) for 1 minute. The reaction was eluted through the IC-H cartridge and to the product vial *via* nitrogen pressure (e). The empty NaOH vial was replaced by a 4 mL distilled water vial. The water was injected to the reactor vial by using nitrogen pressure (d and c) for 80 seconds. The water was collected to the product vial by an applied nitrogen pressure (e).

Step 6: The product mixture was placed in the sleeve of the dose calibrator to detect the level of radioactivity. The reaction was monitored by radio-TLC to obtain the conversion of the [^{18}F]-FDG **1**.

Experiment 35

Procedure T: based on the procedure P, the reaction 35 was performed with a different step 5.
Step 5: Cooled at 55 °C, the NaOH solution (3 M, 3 mL) was added to the reaction mixture (35 seconds) by an applied nitrogen pressure (d). Afterwards the solution was mixed under nitrogen pressure (e) for 50 seconds. The reaction was eluted through the IC-H cartridge and to the product vial *via* nitrogen pressure (e). The empty NaOH vial was replaced by a 4 mL distilled water vial. The water was injected in the reactor vial by using nitrogen pressure (d and c) for 1 minute. The water was collected to the product vial by using an applied nitrogen pressure (e) for 80 seconds.

Experiment 36

Procedure U: based on the procedure Q, the reaction 36 was performed with different steps 1, 4 and 5.
Step 1: The aqueous [^{18}F-fluoride] was eluted from the "F18 in" vial to the QMA cartridge *via* nitrogen flow applied directly to the "F18 in" vial (activity) for 1 minute. The [^{18}F] was loaded in the QMA cartridge and the [^{18}O]-water was collected in the [^{18}O]-water waste vial by nitrogen pressure (f) for 2 minutes.
Step 4: The mannose triflate solution (1 mL acetonitrile) was connected to the system to be flowed to the reactor vial heated at 65 °C by nitrogen flows (c and d). Once transferred, the mixture was heated at 70 °C for 1 minute under nitrogen pressure (e). An additional 100 seconds at 95 °C was performed under nitrogen flow (e). The solution mixture was then heated at 105 °C with both vacuum and nitrogen pressure (c) for 100 seconds.
Step 5: Cooled at 55 °C, the NaOH solution (3 M, 3 mL) was added to the reaction mixture (35 seconds) *via* a nitrogen pressure (d). Afterwards the solution was mixed under nitrogen pressure (e) for 40 seconds. The reaction was eluted through the IC-H cartridge and to the product vial *via* nitrogen pressure (e). The empty NaOH vial was replaced by a 4 mL distilled water vial. The water was injected to the reactor vial by using nitrogen pressure (d and c) for

40 seconds. Afterwards, the water was collected to the product vial *via* an applied nitrogen pressure (e) for 40 seconds.

Experiment 37:

Procedure V: based on the procedure R, the reaction 37 was performed with a different step 4.

Step 4: The mannose triflate solution (1 mL acetonitrile) was connected to the system to be flowed to the reactor vial heated at 65 °C by nitrogen flows (c and d). Once transferred, the mixture was heated at 90 °C for 1 minute under nitrogen pressure (e). An additional 100 seconds at 95 °C was performed under nitrogen flow (e). The solution mixture was then heated at 105 °C with both vacuum and nitrogen pressure (c) for 100 seconds.

Experiment 38 and 39

Procedure W: based on the procedure S, the reaction 38 and 39 were performed with different steps 1 to 3.

Step 1: The aqueous [^{18}F-fluoride] was eluted from the "F18 in" vial to the QMA cartridge *via* nitrogen flow applied directly to the "F18 in" vial (activity) for 1 minute. The [^{18}F] was loaded in the QMA cartridge and the [^{18}O]-water was collected in the [^{18}O]-water waste vial by nitrogen pressure (f) for 3 minutes.

Step 2: The Kryptofix solution was transferred through the QMA cartridge by using a nitrogen pressure (K222) and vacuum. The nitrogen pressure was stopped after 1 second and the $[K^{+}\subset 2.2.2]^{18}F^{-}$ complex was transported to the heated reactor vial (65 °C) by the applied reduced pressure (vacuum) for 30 seconds.

Step 3: The drying process commenced at 105 °C under nitrogen flow (e) for 250 seconds. The dry acetonitrile (500 µL) was transported to the reactor vial heated at 90 °C for 15 seconds. The reaction mixture was then heated at 105 °C under vacuum for 1 minutes and 40 seconds and for an additional 1 minute and 40 seconds under vacuum and nitrogen flow (e).

References

[1] Beiderwellen, K., Grueneisen, J., Ruhlmann, V., Buderath, P., Aktas, B., Heusch, P., Kraff, O., Forsting, M., Lauenstein, T., Umutlu, L., [^{18}F]FDG PET/MRI vs. PET/CT for whole-body staging in patients with recurrent malignancies of the female pelvis: initial results, *Eur. J. Nucl. Med. Mol.* **2014**, 1-10.

[2] Bailey, D. L., Townsend, D. W., Valk, P. E., Maisey, M. N., *Positron Emission Tomography*, Springer, London, **2005**.

[3] Saha, G. B., *Basics of PET imaging : physics, chemistry, and regulations*, Springer, New York, **2010**.

[4] Plathow, C., Weber, W. A., Tumor cell metabolism imaging, *J. Nucl. Med.* **2008**, *49*, 43S-63S.

[5] Hevesy, G., *Adventures in radioisotope research, Vol. 1*, Pergamon Press, New York, **1962**.

[6] Hevesy, G., Paneth, F. A., *Manual of Radioactivity*, Oxford University Press, London, **1938**.

[7] Wernick, M. N., Aarsvold, J. N., *Emission Tomography: The Fundementals of PET and SPECT*, Elsevier, London, **2004**.

[8] Sharp, P. F., Gemmel, H. G., Murray, A. D., *Practical Nuclear Medecine*, 3rd ed., Oxford University Press, London, **2005**.

[9] Miller, P. W., Long, N. J., Vilar, R., Gee, A. D., Synthesis of C-11, F-18, O-15, and N-13 Radiolabels for Positron Emission Tomography, *Angew. Chem. Int. Ed.* **2008**, *47*, 8998-9033.

[10] Scott, P. J. H., Hockley, B. G., Kilbourn, M. R., *Radiopharmaceuticals for Positron Emission Tomography, Vol. 1*, John Wiley & Sons, New Jersey, **2012**.

[11] Rudin, M., Weissleder, R., Molecular imaging in drug discovery and development, *Nat. Rev. Drug Discov.* **2003**, *2*, 123-131.

[12] Contag, P. R., Whole-animal cellular and molecular imaging to accelerate drug development, *Drug Discov. Today* **2002**, *7*, 555-562.

[13] Chen, K., Conti, P. S., Target-specific delivery of peptide-based probes for PET imaging, *Adv. Drug Delivery Rev.* **2010**, *62*, 1005-1022.

[14] Wängler, C., Kostikov, A., Zhu, J., Chin, J., Wängler, B., Schirrmacher, R., Silicon-[^{18}F]Fluorine Radiochemistry: Basics, Applications and Challenges, *Appl. Sci.* **2012**, *2*, 277-302.

[15] Ache, H. J., Chemistry of the Positron and of Positronium, *Angew. Chem. Int. Ed. Engl.* **1972**, *11*, 179-199.

[16] Anger, H. O., Scintillation Camera, *Rev. Sci. Instrum.* **1958**, *29*, 27-33.

[17] Cherry, S. R., Sorenson, J. A., E., P. M., *Physics in nuclear medicine*, 4th ed., Grune & Stratton, Orlando, **1987**.

[18] Qaim, S. M., Nuclear data relevant to the production and application of diagnostic radionuclides, *Radiochim. Acta* **2001**, *89*, 223-232.

[19] IAEA, *Cyclotron Produced Radionuclides: Principles and Practice*, Technical Reports Series 465, Vienna, 2008.

[20] Powsner, R. A., Powsner, E. R., *Essential Nuclear Medicine Physics*, 2nd ed., Wiley, **2006**.

[21] Ametamey, S. M., Honer, M., Schubiger, P. A., Molecular imaging with PET, *Chem. Rev.* **2008**, *108*, 1501-1516.

[22] Cai, L., Lu, S., Pike, V. W., Chemistry with [^{18}F]Fluoride Ion, *Eur. J. Org. Chem.* **2008**, 2853-2873.

[23] Park, B. K., Kitteringham, N. R., O'neill, P. M., Metabolism of fluorine-containing drugs, *Annu. Rev. Pharmacol. Toxicol.* **2001**, *41*, 443-470.

[24] Bohm, H. J., Banner, D., Bendels, S., Kansy, M., Kuhn, B., Muller, K., Obst-Sander, U., Stahl, M., Fluorine in medicinal chemistry, *ChemBioChem* **2004**, *5*, 637-643.

[25] Isanbor, C., O'hagan, D., Fluorine in medicinal chemistry: A review of anti-cancer agents, *J. Fluorine Chem.* **2006**, *127*, 303-319.

[26] Guillaume, M., Luxen, A., Nebeling, B., Argentini, M., Clark, J. C., Pike, V. W., Recommendations for Fluorine-18 Production, *Appl. Radiat. Isot.* **1991**, *42*, 749-762.

[27] Shiue, C. Y., Salvadori, P. A., Wolf, A. P., Fowler, J. S., Macgregor, R. R., A new improved synthesis of 2-deoxy-2-[^{18}F]fluoro-D-glucose from ^{18}F-labeled acetyl hypofluorite, *J. Nucl. Med.* **1982**, *23*, 899-903.

[28] Chirakal, R., Firnau, G., Schrobilgen, G. J., Mckay, J., Garnett, E. S., The synthesis of [^{18}F]Xenon difluoride from [^{18}F]fluoride gas, *Appl. Radiat. Isot.* **1984**, *35*, 401-404.

[29] Teare, H., Robins, E. G., Arstad, E., Luthra, S. K., Gouverneur, V., Synthesis and reactivity of [^{18}F]-N-fluorobenzenesulfonimide, *Chem. Commun.* **2007**, 2330-2332.

[30] Block, E., Iyer, R., Grisoni, S., Saha, C., Belman, S., Lossing, F. P., Lipoxygenase inhibitors from the essential oil of garlic - Markonikov addition of the allydithio radical to olefins, *J. Am. Chem. Soc.* **1988**, *110*, 7813-7827.

[31] Teare, H., Robins, E. G., Kirjavainen, A., Forsback, S., Sandford, G., Solin, O., Luthra, S. K., Gouverneur, V., Radiosynthesis and Evaluation of [^{18}F]Selectfluor bis(triflate), *Angew. Chem. Int. Ed.* **2010**, *49*, 6821-6824.

[32] Lee, E., Kamlet, A. S., Powers, D. C., Neumann, C. N., Boursalian, G. B., Furuya, T., Choi, D. C., Hooker, J. M., Ritter, T., A Fluoride-Derived Electrophilic Late-Stage Fluorination Reagent for PET Imaging, *Science* **2011**, *334*, 639-642.

[33] Ido, T., Wan, C. N., Casella, V., Fowler, J. S., Wolf, A. P., Reivich, M., Kuhl, D. E., Labeled 2-deoxy-D-glucose analogs. ^{18}F-labeled 2-deoxy-2-fluoro-D-glucose, 2-deoxy-2-fluoro-D-mannose and ^{14}C-2-deoxy-2-fluoro-D-glucose, *J. Label. Compd. Radiopharm.* **1978**, *14*, 175-183.

[34] Ehrenkaufer, R. E., Potocki, J. F., Jewett, D. M., Simple Synthesis of F-18-Labeled 2-Fluoro-2-Deoxy-D-Glucose, *J. Nucl. Med.* **1984**, *25*, 333-337.

[35] Dolbier Jr, W. R., Li, A.-R., Koch, C. J., Shiue, C.-Y., Kachur, A. V., [^{18}F]-EF5, a marker for PET detection of hypoxia: synthesis of precursor and a new fluorination procedure, *Appl. Radiat. Isot.* **2001**, *54*, 73-80.

[36] Namavari, M., Bishop, A., Satyamurthy, N., Bida, G., Barrio, J. R., Regioselective radiofluorodestannylation with F-18 F_2 and F-18 CH_3COOF - A high-yield synthesis of 6-F-fluoro-L-dopa, *Appl. Radiat. Isot.* **1992**, *43*, 989-996.

[37] Hess, E., Blessing, G., Coenen, H. H., Qaim, S. M., Improved target system for production of high purity [^{18}F]fluorine via the ^{18}O(p,n)^{18}F reaction, *Appl. Radiat. Isot.* **2000**, *52*, 1431-1440.

[38] Füchtner, F., Preusche, S., Mäding, P., Zessin, J., Steinbach, J., Factors affecting the specific activity of [^{18}F]fluoride from a [^{18}O]water target, *Nuklearmedizin* **2008**, *47*, 116-119.

[39] Mason, N. S., Mathis, C. A., Klunk, W. E., Positron emission tomography radioligands for in vivo imaging of Aβ plaques, *J. Label. Compd. Radiopharm.* **2013**, *56*, 89-95.

[40] Zhang, W., Oya, S., Kung, M.-P., Hou, C., Maier, D. L., Kung, H. F., F-18 Polyethyleneglycol stilbenes as PET imaging agents targeting Aβ aggregates in the brain, *Nucl. Med. Biol.* **2005**, *32*, 799-809.

[41] Wang, H., Guo, X., Jiang, S., Tang, G., Automated synthesis of [^{18}F]Florbetaben as Alzheimer's disease imaging agent based on a synthesis module system, *Appl. Radiat. Isot.* **2013**, *71*, 41-46.

[42] Burnett, J. F., Zahler, R. E., Aromatic Nucleophilic Substitution Reactions, *Chem. Rev.* **1951**, *49*, 273-412.

[43] Chun, J.-H., Morse, C. L., Chin, F. T., Pike, V. W., No-carrier-added [^{18}F]fluoroarenes from the radiofluorination of diaryl sulfoxides, *Chem. Commun.* **2013**, *49*, 2151-2153.

[44] Hjelstuen, O. K., Svadberg, A., Olberg, D. E., Rosser, M., Standardization of fluorine-18 manufacturing processes: New scientific challenges for PET, *Eur. J. Pharm. Biopharm.* **2011**, *78*, 307-313.

[45] Schlyer, D. J., Bastos, M. a. V., Alexoff, D., Wolf, A. P., Separation of [^{18}F]fluoride from [^{18}O]water using anion exchange resin, *Appl. Radiat. Isot.* **1990**, *41*, 531-533.

[46] Brichard, L., Aigbirhio, F. I., An Efficient Method for Enhancing the Reactivity and Flexibility of [^{18}F]Fluoride Towards Nucleophilic Substitution Using Tetraethylammonium Bicarbonate, *Eur. J. Org. Chem.* **2014**, *2014*, 6145-6149.

[47] Yang, B. Y., Jeong, J. M., Lee, Y.-S., Lee, D. S., Chung, J.-K., Lee, M. C., Facile calculation of specific rate constants and activation energies of ^{18}F-fluorination reaction using combined processes of coat-capture–elution and microfluidics, *Tetrahedron* **2011**, *67*, 2427-2433.

[48] Wessmann, S. H., Henriksen, G., Wester, H. J., Cryptate mediated nucleophilic F-18-fluorination without azeotropic drying, *Nuklearmedizin* **2012**, *51*, 1-8.

[49] Gomzina, N. A., Zaitsev, V. V., Krasikova, R. N., Optimization of nucleophilic fluorination step in the synthesis of various compounds labelled with fluorine-18 for their use as PET radiotracers, *J. Label. Compd. Radiopharm.* **2001**, *44*, S895-S897.

[50] Lemaire, C. F., Aerts, J. J., Voccia, S., Libert, L. C., Mercier, F., Goblet, D., Plenevaux, A. R., Luxen, A. J., Fast Production of Highly Reactive No-Carrier-Added [^{18}F]Fluoride for the Labeling of Radiopharmaceuticals, *Angew. Chem. Int. Ed.* **2010**, *49*, 3161-3164.

[51] He, P., Haswell, S. J., Pamme, N., Archibald, S. J., Advances in processes for PET radiotracer synthesis: Separation of [^{18}F]fluoride from enriched [^{18}O]water, *Appl. Radiat. Isot.* **2014**, *91*, 64-70.

[52] Wong, R., Iwata, R., Saiki, H., Furumoto, S., Ishikawa, Y., Ozeki, E., Reactivity of electrochemically concentrated anhydrous F-18 fluoride for microfluidic radiosynthesis of F-18-labeled compounds, *Appl. Radiat. Isot.* **2012**, *70*, 193-199.

[53] Sadeghi, S., Liang, V., Cheung, S., Woo, S., Wu, C., Ly, J., Deng, Y., Eddings, M., Van Dam, R. M., Reusable electrochemical cell for rapid separation of [^{18}F]fluoride from [^{18}O]water for flow-through synthesis of ^{18}F-labeled tracers, *Appl. Radiat. Isot.* **2013**, *75*, 85-94.

[54] Pascali, G., Del Carlo, S., Rocchiccioli, S., Signore, G., Saccomanni, G., Manera, C., Macchia, M., Salvadori, P., Identification of chemical byproducts in the radiofluorination of structurally complex aryliodonium salts, *J. Radioanal. Nucl. Chem.* **2014**, 1-7.

[55] Lee, S. J., Oh, S. J., Chi, D. Y., Moon, D. H., Ryu, J. S., High Yielding F-18 Fluorination Method by Fine Control of the Base, *Bull. Korean Chem. Soc.* **2012**, *33*, 2177-2180.

[56] Seo, J. W., Lee, B. S., Lee, S. J., Oh, S. J., Chi, D. Y., Fast and Easy Drying Method for the Preparation of Activated F-18 Fluoride Using Polymer Cartridge, *Bull. Korean Chem. Soc.* **2011**, *32*, 71-76.

[57] Kim, D. W., Ahn, D.-S., Oh, Y.-H., Lee, S., Kil, H. S., Oh, S. J., Lee, S. J., Kim, J. S., Ryu, J. S., Moon, D. H., Chi, D. Y., A New Class of S_N2 Reactions Catalyzed by Protic Solvents: Facile Fluorination for Isotopic Labeling of Diagnostic Molecules, *J. Am. Chem. Soc.* **2006**, *128*, 16394-16397.

[58] Kim, H. W., Jeong, J. M., Lee, Y.-S., Chi, D. Y., Chung, K.-H., Lee, D. S., Chung, J.-K., Lee, M. C., Rapid synthesis of [^{18}F]FDG without an evaporation step using an ionic liquid, *Appl. Radiat. Isot.* **2004**, *61*, 1241-1246.

[59] Hamacher, K., Coenen, H. H., Stocklin, G., Efficient Stereospecific Synthesis of No-Carrier-Added 2- F-18 -Fluoro-2-Deoxy-D-Glucose using AminopolyetherSupported Nucleophilic Substitution, *J. Nucl. Med.* **1986**, *27*, 235-238.

[60] Krasikova, R., PET Radiochemistry Automation: State of the Art and Future Trends in F-18-nucleophilic Fluorination, *Curr. Org. Chem.* **2013**, *17*, 2097-2107.

[61] Mason, B. P., Price, K. E., Steinbacher, J. L., Bogdan, A. R., Mcquade, D. T., Greener Approaches to Organic Synthesis Using Microreactor Technology, *Chem. Rev.* **2007**, *107*, 2300-2318.

[62] Wiles, C., Watts, P., *Micro Reaction Technology in Organic Synthesis*, CRC Press, **2011**.

[63] Elizarov, A. M., Microreactors for radiopharmaceutical synthesis, *Lab Chip* **2009**, *9*, 1326-1333.

[64] Arima, V., Pascali, G., Lade, O., Kretschmer, H. R., Bernsdorf, I., Hammond, V., Watts, P., De Leonardis, F., Tarn, M. D., Pamme, N., Cvetkovic, B. Z., Dittrich, P. S., Vasovic, N., Duane, R., Jaksic, A., Zacheo, A., Zizzari, A., Marra, L., Perrone, E., Salvadori, P. A., Rinaldi, R., Radiochemistry on chip: towards dose-on-demand synthesis of PET radiopharmaceuticals, *Lab Chip* **2013**, *13*, 2328-2336.

[65] Lee, C. C., Sui, G. D., Elizarov, A., Shu, C. Y. J., Shin, Y. S., Dooley, A. N., Huang, J., Daridon, A., Wyatt, P., Stout, D., Kolb, H. C., Witte, O. N., Satyamurthy, N., Heath, J. R., Phelps, M. E., Quake, S. R., Tseng, H. R., Multistep synthesis of a radiolabeled imaging probe using integrated microfluidics, *Science* **2005**, *310*, 1793-1796.

[66] Steel, C. J., O'brien, A. T., Luthra, S. K., Brady, F., Automated PET radiosyntheses using microfluidic devices, *J. Labelled Compd. Radiopharm.* **2007**, *50*, 308-311.

[67] Watts, P., Pascali, G., Salvadori, P. A., Positron emission tomography radiosynthesis in microreactors, *J. Flow Chem.* **2012**, *2*, 37-42.

[68] Lin, W.-Y., Wang, Y., Wang, S., Tseng, H.-R., Integrated microfluidic reactors, *Nano Today* **2009**, *4*, 470-481.

[69] Gillies, J. M., Prenant, C., Chimon, G. N., Smethurst, G. J., Dekker, B. A., Zweit, J., Microfluidic technology for PET radiochemistry, *Appl. Radiat. Isot.* **2006**, *64*, 333-336.

[70] Koag, M. C., Kim, H.-K., Kim, A. S., Efficient microscale synthesis of [^{18}F]-2-fluoro-2-deoxy-D-glucose, *Chem. Eng. J.* **2014**, *258*, 62-68.

[71] Chun, J.-H., Telu, S., Lu, S., Pike, V. W., Radiofluorination of diaryliodonium tosylates under aqueous-organic and cryptand-free conditions, *Org. Biomol. Chem.* **2013**, *11*, 5094-5099.

[72] Ren, H., Wey, H.-Y., Strebl, M., Neelamegam, R., Ritter, T., Hooker, J. M., Synthesis and Imaging Validation of [^{18}F]MDL100907 Enabled by Ni-Mediated Fluorination, *ACS Chem. Neurosci.* **2014**, *5*, 611-615.

[73] Mcbride, W. J., Sharkey, R. M., Goldenberg, D. M., Radiofluorination using aluminum-fluoride (Al^{18}F), *EJNMMI Res.* **2013**, *3*, 36/01-36/11.

[74] Gao, Z., Lim, Y. H., Tredwell, M., Li, L., Verhoog, S., Hopkinson, M., Kaluza, W., Collier, T. L., Passchier, J., Huiban, M., Gouverneur, V., Metal-Free Oxidative Fluorination of Phenols with [^{18}F]Fluoride, *Angew. Chem. Int. Ed.* **2012**, *51*, 6733-6737.

[75] Ichiishi, N., Brooks, A. F., Topczewski, J. J., Rodnick, M. E., Sanford, M. S., Scott, P. J. H., Copper-Catalyzed [^{18}F]Fluorination of (Mesityl)(aryl)iodonium Salts, *Org. Lett.* **2014**, *16*, 3224-3227.

[76] Tredwell, M., Preshlock, S. M., Taylor, N. J., Gruber, S., Huiban, M., Passchier, J., Mercier, J., Génicot, C., Gouverneur, V., A General Copper-Mediated Nucleophilic ^{18}F Fluorination of Arenes, *Angew. Chem. Int. Ed.* **2014**, *53*, 7751-7755.

[77] Amaraesekera, B., Marchis, P. D., Bobinski, K. P., Radu, C. G., Czernin, J., Barrio, J. R., Michael Van Dam, R., High-pressure, compact, modular radiosynthesizer for production of positron emitting biomarkers, *Appl. Radiat. Isot.* **2013**, *78*, 88-101.

[78] Herman, H., Flores, G., Quinn, K., Eddings, M., Olma, S., Moore, M. D., Ding, H., Bobinski, K. P., Wang, M., Williams, D., Wiliams, D., Shen, C. K.-F., Phelps, M. E., Van Dam, R. M., Plug-and-play modules for flexible radiosynthesis, *Appl. Radiat. Isot.* **2013**, *78*, 113-124.

[79] Catala-Lopez, F., Crespo-Facorro, B., Vieta, E., Valderas, J. M., Valencia, A., Tabares-Seisdedos, R., Alzheimer's Disease and Cancer: Current Epidemiological Evidence for a Mutual Protection, *Neuroepidemiology* **2014**, *42*, 121-122.

[80] http://medicine.cf.ac.uk/petic/

[81] Brown, L. J., Ma, N., Bouvet, D. R., Champion, S., Gibson, A. M., Hu, Y., Jackson, A., Khan, I., Millot, N., Topley, A. C., Wadsworth, H., Wynn, D., Brown, R. C. D., Synthesis of the positron-emitting radiotracer [^{18}F]-2-fluoro-2-deoxy-D-glucose from resin-bound perfluoroalkylsulfonates, *Org. Biomol. Chem.* **2009**, *7*, 564-575.

[82] Ahmed, B., Barrow, D., Wirth, T., Enhancement of Reaction Rates by Segmented Fluid Flow in Capillary Scale Reactors, *Adv. Synth. Catal.* **2006**, *348*, 1043-1048.

[83] Wirth, T., *Microreactors in Organic synthesis and Catalysis*, Wiley, **2007**.

[84] Latala, A., Nedzi, M., Stepnowski, P., Toxicity of imidazolium and pyridinium based ionic liquids towards algae. Chlorella vulgaris, Oocystis submarina (green algae) and Cyclotella meneghiniana, Skeletonema marinoi (diatoms), *Green Chem.* **2009**, *11*, 580-588.

[85] Walker, R., Toxicology of sorbic acid and sorbates, *Food Additives and Contaminants* **1990**, *7*, 671-676.

[86] Dietrich, B., Lehn, J. M., Sauvage, J. P., Diaza-polyoxa-macrocycles et macrobicycles, *Tetrahedron Lett.* **1969**, *10*, 2885-2888.

[87] Parker, D., *Macrocycle Synthesis: A Practical Approach*, Oxford Univ. Press, **1996**.

[88] Kulstad, S., Malmsten, L. A., Diaza-crown ethers. VIII. Alkali metal ion promoted formation of 4,7,13,16,21,24-hexaoxa-1,10-diazabicyclo-[8,8,8]-hexacosane, *Tetrahedron Lett.* **1980**, *21*, 643-646.

[89] Krakowiak, K. E., Bradshaw, J. S., An, H. Y., Izatt, R. M., Simple methods for the preparation of cryptands, *Pure Appl. Chem.* **1993**, *65*, 511-514.

[90] Krakowiak, K. E., Krakowiak, P. A., Bradshaw, J. S., The most convenient method for the preparation of aliphatic cryptands, *Tetrahedron Lett.* **1993**, *34*, 777-778.

[91] Shan, M., Bujotzek, A., Abendroth, F., Wellner, A., Gust, R., Seitz, O., Weber, M., Haag, R., Conformational Analysis of Bivalent Estrogen Receptor Ligands: From Intramolecular to Intermolecular Binding, *ChemBioChem* **2011**, *12*, 2587-2598.

[92] Budin , G., Dimala , M. M., Lamour, V., Oudet, P., Mioskowski, C., Meunier, S., Brino, L., Wagner, A., A Chemical Labeling Strategy for Proteomics under Nondenaturing Conditions, *ChemBioChem* **2010**, *11*, 79-82.

[93] Lehn, J.-M., Skene, W. G., Polyhydrazones and polyimines exhibiting reversible formation and component exchange. Patent WO2004003044A2, 2004.

[94] De Luca, L., Giacomelli, G., Masala, S., Porcheddu, A., Trichloroisocyanuric/TEMPO Oxidation of Alcohols under Mild Conditions: A Close Investigation, *J. Org. Chem.* **2003**, *68*, 4999-5001.

[95] Greene, T. W., Wuts, P. G. M., *Protective groups in organuc synthesis*, 3rd ed., Wiley-Blackwell, **1998**.

[96] Crouch, R. D., Selective deprotection of silyl ethers, *Tetrahedron* **2013**, *69*, 2383-2417.

[97] Jose, J., Ueno, Y., Burgess, K., Water-Soluble Nile Blue Derivatives: Syntheses and Photophysical Properties, *Chem. Eur. J.* **2009**, *15*, 418-423.

[98] Bouzide, A., Sauvé, G., Highly selective silver(I) oxide mediated monoprotection of symmetrical diols, *Tetrahedron Lett.* **1997**, *38*, 5945-5948.

[99] Carey, F. A., Sundberg, R. J., *Chimie Organique avancée*, 3ème ed., Deboeck Université, **1996**.

[100] Moreau, J., Marchand-Brynaert, J., Modular Synthesis of Bifunctional Linkers for Materials Science, *Eur. J. Org. Chem.* **2011**, 1641-1644.

[101] Vallabhajosula, S., Positron Emission Tomography Radiopharmaceuticals for Imaging Brain Beta-Amyloid, *Semin. Nucl. Med.* **2011**, *41*, 283-299.

[102] Kung, H. F., The β-Amyloid Hypothesis in Alzheimer's Disease: Seeing Is Believing, *ACS Med. Chem. Lett.* **2012**, *3*, 265-267.

[103] Skeby, K. K., Sørensen, J., Schiøtt, B., Identification of a Common Binding Mode for Imaging Agents to Amyloid Fibrils from Molecular Dynamics Simulations, *J. Am. Chem. Soc.* **2013**, *135*, 15114-15128.

[104] Ono, M., Wilson, A., Nobrega, J., Westaway, D., Verhoeff, P., Zhuang, Z. P., Kung, M. P., Kung, H. F., C-11-labeled stilbene derivatives as A beta-aggregate-specific PET imaging agents for Alzheimer's disease, *Nucl. Med. Biol.* **2003**, *30*, 565-571.

[105] Wadsworth, W. S., Emmons, W. D., The Utility of Phosphonate Carbanions in Olefin Synthesis, *J. Am. Chem. Soc.* **1961**, *83*, 1733-1738.

[106] Gester, S., Pietzsch, J., Wuest, F. R., Synthesis of ^{18}F-labelled stilbenes from 4-[^{18}F]fluorobenz-aldehyde using the Horner–Wadsworth–Emmons reaction, *J. Label. Compd. Radiopharm.* **2007**, *50*, 105-113.

[107] Motoshima, K., Ishikawa, M., Hashimoto, Y., Sugita, K., Peroxisome proliferator-activated receptor agonists with phenethylphenylphthalimide skeleton derived from thalidomide-related liver X receptor antagonists: Relationship between absolute configuration and subtype selectivity, *Bioorg. Med. Chem.* **2011**, *19*, 3156-3172.

[108] Wang, M., Gao, M., Miller, K. D., Zheng, Q.-H., Synthesis of C-11 PBR06 and F-18 PBR06 as agents for positron emission tomographic (PET) imaging of the translocator protein (TSPO), *Steroids* **2011**, *76*, 1331-1340.

[109] Zhang, W., Go, M. L., Quinone reductase induction activity of methoxylated analogues of resveratrol, *Eur. J. Med. Chem.* **2007**, *42*, 841-850.

[110] Motoshima, K., Noguchi-Yachide, T., Sugita, K., Hashimoto, Y., Ishikawa, M., Separation of α-glucosidase-inhibitory and liver X receptor-antagonistic activities of phenethylphenyl phthalimide analogs and generation of LXR α-selective antagonists, *Bioorg. Med. Chem.* **2009**, *17*, 5001-5014.

[111] Johansson Seechurn, C. C. C., Kitching, M. O., Colacot, T. J., Snieckus, V., Palladium-Catalyzed Cross-Coupling: A Historical Contextual Perspective to the 2010 Nobel Prize, *Angew. Chem. Int. Ed.* **2012**, *51*, 5062-5085.

[112] Oestreich, M., Editor, *The Mizoroki-Heck Reaction*, John Wiley & Sons Ltd., **2009**.

[113] Shard, A., Sharma, N., Bharti, R., Dadhwal, S., Kumar, R., Sinha, A. K., Tandem Heck/Decarboxylation/Heck Strategy: Protecting-Group-Free Synthesis of Symmetric and Unsymmetric Hydroxylated Stilbenoids, *Angew. Chem. Int. Ed.* **2012**, *51*, 12250-12253.

[114] Diemer, V., Chaumeil, H., Defoin, A., Carre, C., Synthesis of alkoxynitrostilbenes as chromophores for nonlinear optical materials, *Synthesis* **2007**, 3333-3338.

[115] Vangala, V. R., Bhogala, B. R., Dey, A., Desiraju, G. R., Broder, C. K., Smith, P. S., Mondal, R., Howard, J. a. K., Wilson, C. C., Correspondence between Molecular Functionality and Crystal Structures. Supramolecular Chemistry of a Family of Homologated Aminophenols, *J. Am. Chem. Soc.* **2003**, *125*, 14495-14509.

[116] Barnwell, N., Indole and Indolenine Chemistry; Synthetic Approaches to Hinckdentine A (MSc Thesis), **1991**.

[117] Ono, M., Cheng, Y., Kimura, H., Cui, M., Kagawa, S., Nishii, R., Saji, H., Novel ^{18}F-Labeled Benzofuran Derivatives with Improved Properties for Positron Emission Tomography (PET) Imaging of β-Amyloid Plaques in Alzheimer's Brains, *J. Med. Chem.* **2011**, *54*, 2971-2979.

[118] Wang, W., Li, A. D. Q., Design and Synthesis of Efficient Fluorescent Dyes for Incorporation into DNA Backbone and Biomolecule Detection, *Bioconjugate Chem.* **2007**, *18*, 1036-1052.

[119] Øpstad, C. L., Melø, T.-B., Sliwka, H.-R., Partali, V., Formation of DMSO and DMF radicals with minute amounts of base, *Tetrahedron* **2009**, *65*, 7616-7619.

[120] Hirayama, T., Iyoshi, S., Taki, M., Maeda, Y., Yamamoto, Y., Synthesis of a new bifunctionalised fluorescent label and physical properties of the bound form on model peptide of troponin C, *Org. Biomol. Chem.* **2007**, *5*, 2040-2045.

[121] Beccalli, E., Contini, A., Trimarco, P., 3-Nitrocoumarin Amidines: A New Synthetic Strategy for Substituted [1]Benzopyrano[3,4-d]imidazol-4(3*H*)-ones, *Eur. J. Org. Chem.* **2003**, 3976-3984.

[122] Crump, B. R., Goss, C., Lovelace, T., Lewis, R., Peterson, J., Influence of Reaction Parameters on the First Principles Reaction Rate Modeling of a Platinum and Vanadium Catalyzed Nitro Reduction, *Org. Process Res. Dev.* **2013**, *17*, 1277-1286.

[123] Visentin, F., Puxty, G., Kut, O. M., Hungerbühler, K., Study of the Hydrogenation of Selected Nitro Compounds by Simultaneous Measurements of Calorimetric, FT-IR, and Gas-Uptake Signals, *Ind. Eng. Chem. Res.* **2006**, *45*, 4544-4553.

[124] Andrews, M. D., Bagal, S. K., Gibson, K. R., Omoto, K., Ryckmans, T., Skerratt, S. E., Stupple, P. A., Pyrrolo[2,3-d]pyrimidine derivatives as inhibitors of tropomyosin-related kinases and their preparation and use in the treatment of pain. Patent WO2012137089A1, 2012.

[125] Niimi, T., Orita, M., Okazawa-Igarashi, M., Sakashita, H., Kikuchi, K., Ball, E., Ichikawa, A., Yamagiwa, Y., Sakamoto, S., Tanaka, A., Tsukamoto, S., Fujita, S., Tatsuta, K., Maeda, Y., Chikauchi, K., Design and Synthesis of Non-peptidic Inhibitors for the Syk C-Terminal SH2 Domain Based on Structure-Based In-Silico Screening, *J. Med. Chem.* **2001**, *44*, 4737-4740.

[126] Wang, H., Shi, H., Yu, H., Jiang, S., Tang, G., Facile and rapid one-step radiosynthesis of F-18 BAY94-9172 with a new precursor, *Nucl. Med. Biol.* **2011**, *38*, 121-127.

[127] Perrin, D. D., Armarego, W. L. F., Perrin, D. R., *Purification of laboratory chemicals*, 2nd ed., Pergamon Press, **1980**.

[128] Débieux, J.-L., Cosandey, A., Helgen, C., Bochet, C. G., Photoacylation of Alcohols in Neutral Medium, *Eur. J. Org. Chem.* **2007**, 2073-2077.

[129] Chen, Y., Baker, G. L., Synthesis and Properties of ABA Amphiphiles, *J. Org. Chem.* **1999**, *64*, 6870-6873.

[130] Percec, V., Wilson, D. A., Leowanawat, P., Wilson, C. J., Hughes, A. D., Kaucher, M. S., Hammer, D. A., Levine, D. H., Kim, A. J., Bates, F. S., Davis, K. P., Lodge, T. P., Klein, M. L., De Vane, R. H., Aqad, E., Rosen, B. M., Argintaru, A. O., Sienkowska, M. J., Rissanen, K., Nummelin, S., Ropponen, J., Self-Assembly of Janus Dendrimers into Uniform Dendrimersomes and Other Complex Architectures, *Science* **2010**, *328*, 1009-1014.

[131] Miljanić, S., Frkanec, L., Meić, Z., Žinić, M., Gelation Ability of Novel Oxamide-Based Derivatives Bearing a Stilbene as a Photo-Responsive Unit, *Eur. J. Org. Chem.* **2006**, 1323-1334.

[132] Mcdonald, R. N., Campbell, T. W., Synthesis of Hydrocarbon Derivatives by the Wittig Reaction II. Diarylbutadienes and Quinquephenyls[1], *J. Org. Chem.* **1959**, *24*, 1969-1975.

[133] Schiaffo, C. E., Dussault, P. H., Ozonolysis in Solvent/Water Mixtures: Direct Conversion of Alkenes to Aldehydes and Ketones, *J. Org. Chem.* **2008**, *73*, 4688-4690.

[134] Quiroz-Florentino, H., Hernández-Benitez, R. I., Aviña, J. A., Burgueño-Tapia, E., Tamariz, J., Total Synthesis of Naturally Occurring Furan Compounds 5-{[(4-Hydroxybenzyl)oxy]methyl}-2-furaldehyde and Pichiafuran C, *Synthesis* **2011**, *2011*, 1106-1112.

[135] Khartulyari, A. S., Kapur, M., Maier, M. E., Concise Strategy to the Core Structure of the Macrolide Queenslandon, *Org. Lett.* **2006**, *8*, 5833-5836.

[136] Motoshima, K., Noguchi-Yachide, T., Sugita, K., Hashimoto, Y., Ishikawa, M., Separation of α-glucosidase-inhibitory and liver X receptor-antagonistic activities of phenethylphenyl phthalimide analogs and generation of LXRα-selective antagonists, *Bioorg. Med. Chem.* **2009**, *17*, 5001-5014.

[137] Rosengren-Holmberg, J. P., Karlsson, J. G., Svenson, J., Andersson, H. S., Nicholls, I. A., Synthesis and ligand recognition of paracetamol selective polymers: semi-covalent versus non-covalent molecular imprinting, *Org. Biomol. Chem.* **2009**, *7*, 3148-3155.

[138] Wang, Z., Ding, Q., He, X., Wu, J., Palladium-catalyzed decarboxylative cross-coupling reaction of cinnamic acid with aryl iodide, *Org. Biomol. Chem.* **2009**, *7*, 863-865.

[139] Dale, W. J., Hennis, H. E., Substituted styrenes. IV. Reaction of the vinylanisoles with *p*-nitrobenzenediazonium chloride in pyridine, *J. Am. Chem. Soc.* **1959**, *81*, 2143-2146.

[140] Güsten, H., Salzwedel, M., Die kernmagnetischen Resonanzspektren substituierter trans-Stilbene, *Tetrahedron* **1967**, *23*, 173-185.